Reponses to reviewer(s) comments

Dear Editor,

Thank you for your efforts for handling our manuscript. We appreciate to receive the useful comments from all reviewers. These comments are very constructive, and we have now further revised our manuscript in light of all reviewers' comments. Based on the helpful suggestions from all reviewers, we believe that we should have addressed questions and concerns from all reviewers appropriately, and adequately. Please find our point-by-point responses below.

Anonymous Referee #1:

It is appreciated that the authors took great efforts to elucidate the complex relationship between WPSH and air pollution in China during summer, which is interesting. However, the manuscript was not well organized (synoptic characteristics and their influences on pollution are better given in a section), and most analyses were superficial without observational evidence. The manuscript needs better organization and careful English editing.

RESPONSE: Thank you for your valuable time to review this manuscript. We totally agree with your comments. Therefore, we have reorganized our writing structure thoughtfully in the current version. Particularly, we have carefully provided more information regard to the descriptions associated with synoptic weather characteristics and their influences on pollution. We have also added more information in order to provide in-depth results with observational evidences as suggested.

1. Only four types were identified, which tends to oversimplify the complex synoptic situations during summer in eastern China. By contrast, six types were identified by Han et al. (2020) to understand the influence of synoptic weather on the summertime O3 pollution in eastern China; nine types were classified by Ye et al. (2016) for the aerosol pollution in the North China Plain. The region selected for the classification should be consistent with the studied region (eastern China in Fig. 1). Why use the region shown by the black squares in Fig. 4? And present it in a larger domain in Fig.4? The classified region cannot resolve the processes needed? The selection of the classified region can significantly influence the classification results.

RESPONSE: Many thanks for your kind suggestions. The classification results can be largely influenced by the selected region, seasonal effects, and temporal length (time-series) of samples. We have read through the suggested references from reviewer. We found that Han et al. (2020) objectively identified six predominant synoptic weather patterns (SWPs) at 850 hPa level over eastern China (i.e., 20-40°N, 110-130°E) in the summer during 2013–2018. Ye et al. (2016) applied statistical analyses to identify nine types of synoptic flow based on sea level pressure over the North China Plain during autumn and winter (2004–2014). The settings are quite different from our study. Particularly, we chose a relatively large spatial extent as our classified region (0-60°N, 65-150°E) to capture the characteristics of the West Pacific Subtropical High (WPSH) at 500 hPa, as this can modulate the weather conditions and resultant co-occurring pollution events over eastern China. In this study, the number of SWP is determined by explained cluster variances (ECV) (Hoffmann & SchlüNzen, 2013; Philipp et al., 2014). The number of synoptic patterns (k) is optimized when the ΔECV is at the highest value, which suggests that the performance of classification has been improved substantially and with stability (Ning et al., 2019).

In order to further address the comments, we have now included a Fig. S1 to present the

changes of ΔECV against different numbers of classified synoptic patterns, including how we have optimized four SWPs. We have also marked the location of our classified region on the revised Fig. 4. Furthermore, we have revised our title as "Large-scale synoptic drivers of co-occurring summertime ozone and $PM_{2.5}$ pollution in eastern China".

Reference:

Han, H., Liu, J., Shu, L., Wang, T. and Yuan, H.: Local and synoptic meteorological influences on daily variability in summertime surface ozone in eastern China, Atmos. Chem. Phys., 20(1), 203–222, doi:10.5194/acp-20-203-2020, 2020.

Hoffmann, P. and Heinke SchlüNzen, K.: Weather pattern classification to represent the urban heat island in present and future climate, J. Appl. Meteorol. Climatol., 52(12), 2699–2714, doi:10.1175/JAMC-D-12-065.1, 2013.

Ning, G., Yim, S. H. L., Wang, S., Duan, B., Nie, C., Yang, X., Wang, J. and Shang, K.: Synergistic effects of synoptic weather patterns and topography on air quality: a case of the Sichuan Basin of China, Clim. Dyn., 53(11), 6729–6744, doi:10.1007/s00382-019-04954-3, 2019.

Philipp, A., Beck, C., Esteban, P., Krennert, T., Lochbihler, K., Spyros, P., Pianko-kluczynska, K., Post, P., Alvarez, R., Spekat, A. and Streicher, F.: Cost733 user guide., 2014.

Ye, X., Song, Y., Cai, X. and Zhang, H.: Study on the synoptic flow patterns and boundary layer process of the severe haze events over the North China Plain in January 2013, Atmos. Environ., 124(January 2013), 129–145, doi:10.1016/j.atmosenv.2015.06.011, 2016.

2. The classification results are odd. For example, in July of 2016, it quickly turned form Type 2 to Type 4, and then became Type 1 during a few days (Fig. 5). The WPSH cannot jump like that (e.g., from Type 2 to Type 4 in 24 hours). Besides, almost the whole June of 2016 was identified as Type 1 ("South BTH-North YRD O_3-$PM_{2.5}$ compound pollution"), while the South BTH and North YRD often experience clean and pollution situations during a few days (https://www.aqistudy.cn/historydata/daydata.php?city=%E5%8D%97%E4%BA%AC&month=201606). The synoptic pattern of Type 1 cannot explain the formation and evolution of pollution in South BTH and North YRD. The variations of pollution level may be primarily controlled by other synoptic weather systems at 900/850-hPa, rather than the 500-hPa WPSH. The same problems also existed in other Types/regions. The classification results and their relationships with pollution are suspicious and unreliable.

RESPONSE: Thank you for pointing out the "odd" results. In our study, the movement of the WPSH is generally affected by the weather phenomenon of its surrounding climatic systems (such as typhoons, the Tibetan high, etc.) (Ge et al., 2019; Liu and You, 2020; Shu et al., 2016). In order to address this comment, we have now included a Fig. R1 to show the synoptic weather patterns at 500hPa between July 05, 2016 and July 08, 2016. Our results showed that the weather pattern has first quickly changed from Type 2 to Type 4, then finally became a Type 1 pattern under the influence of Super Typhoon Nepartak (Fig. R2). Particularly, our statistical analyses showed that Type 1 pattern can represent the conditions of compound pollution events. Under the influence of this large-scale synoptic pattern, there is a relatively high probability of the occurrence of compound pollution in the BTH-NYRD region, with the maximum occurrence probability reaching to 55.09%. These variations of air pollution level may be primarily controlled by other synoptic weather systems at 900/850-hPa closely related to the movement of WPSH. Additionally, moisture driven by the WPSH could create

inconducive condition for the O_3 formation across South China(Zhao and Wang, 2017). Furthermore, the amount of water vapor is largely reduced as it has been transported to North China through airflow trajectories, resulting in a moderation of RH and high temperature over North China which enhance the formation of O_3-$PM_{2.5}$ co-occurring event.

More importantly, one aim of our study was to examine the effect on O_3-$PM_{2.5}$ co-occurring event caused by the large-scale WPSH related synoptic pattern. As WPSH at 500-hPa is easily identified based on 5880 gpm contour line, we applied the following condition (500 hPa GH) as our dependent variable for classification. In order to further address this comment, our revised Fig.R3 has shown the synoptic weather pattern at 850 hPa corresponding to the classification. This figure can represent matching characteristics of the WPSH at 850 hPa and 500 hPa (Fig.4 and Fig. R3). Based on the comparison, using 500hPa GH for classification should be accurate and reliable in this study.

Reference

Ge, J., You, Q. and Zhang, Y.: Effect of Tibetan Plateau heating on summer extreme precipitation in eastern China, Atmos. Res., 218, 364–371, doi:10.1016/j.atmosres.2018.12.018, 2019.

Hoffmann, P. and Heinke SchlüNzen, K.: Weather pattern classification to represent the urban heat island in present and future climate, J. Appl. Meteorol. Climatol., 52(12), 2699–2714, doi:10.1175/JAMC-D-12-065.1, 2013.

Huth, R.: An intercomparison of computer-assisted circulation classification methods, Int. J. Climatol., 16(8), 893–922, doi:10.1002/(SICI)1097-0088(199608)16:8<893::AID-JOC51>3.0.CO;2-Q, 1996.

Liu, J. and You, Q.: A diagnosis of the interannual variation of the summer hydrometeor based on ERA-interim over Eastern China, Atmos. Res., 231(October 2018), 104654, doi:10.1016/j.atmosres.2019.104654, 2020.

Philipp, A., Beck, C., Esteban, P., Krennert, T., Lochbihler, K., Spyros, P., Pianko-kluczynska, K., Post, P., Alvarez, R., Spekat, A. and Streicher, F.: Cost733 user guide., 2014.

Shu, L., Xie, M., Wang, T., Gao, D., Chen, P., Han, Y., Li, S., Zhuang, B. and Li, M.: Integrated studies of a regional ozone pollution synthetically affected by subtropical high and typhoon system in the Yangtze River Delta region, China, Atmos. Chem. Phys., 16(24), 15801–15819, doi:10.5194/acp-16-15801-2016, 2016.

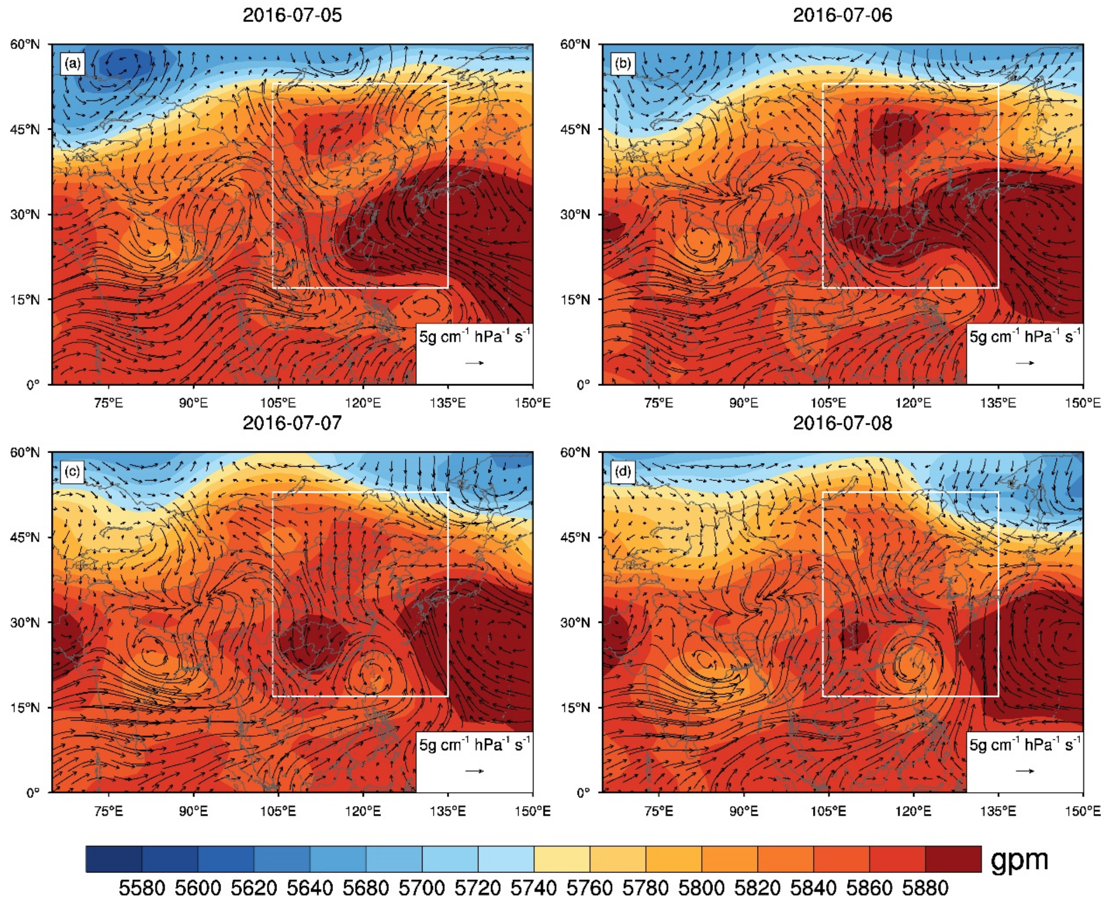

Fig. R1. the case during July 5-8,2016

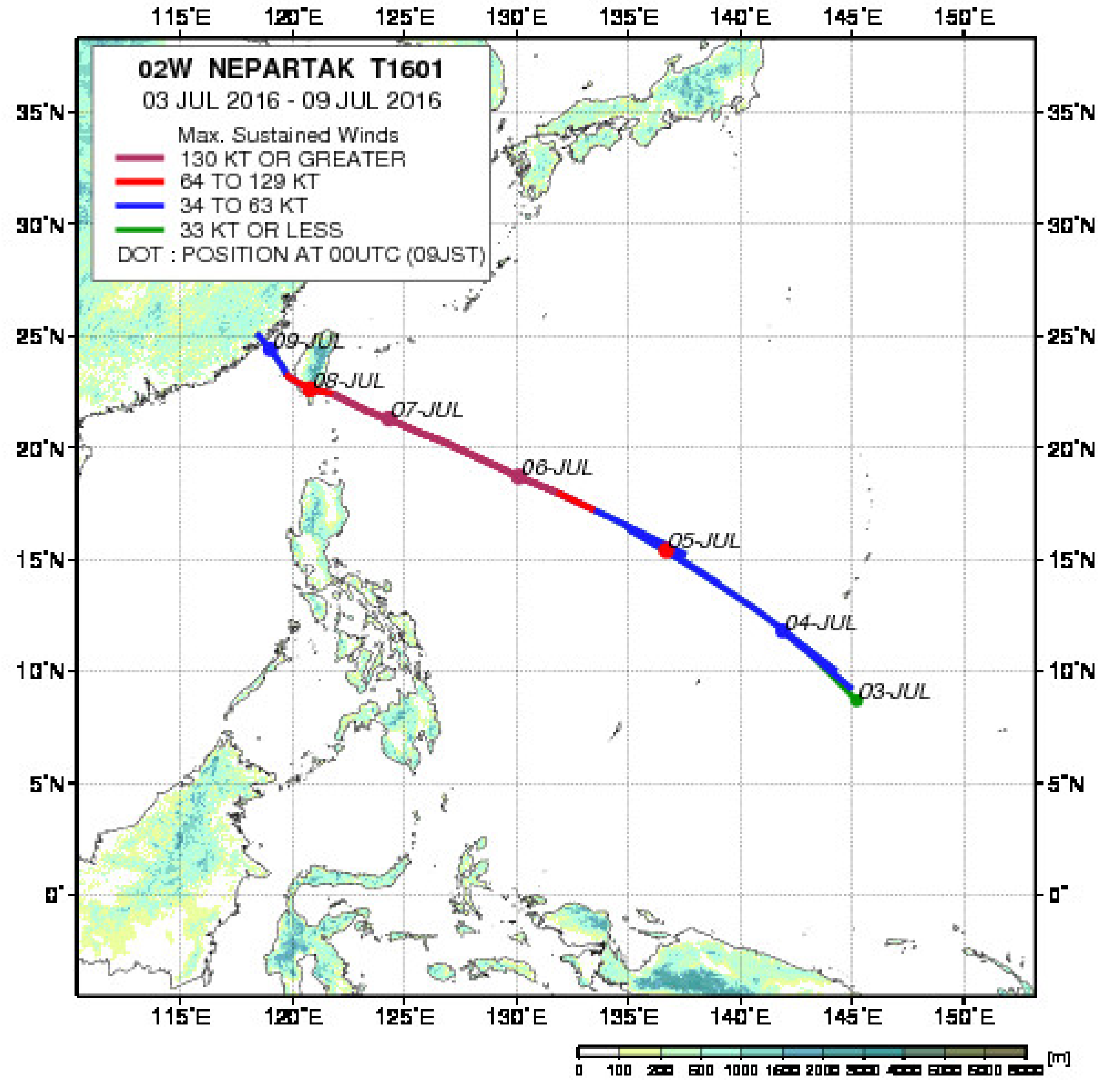

Fig. R2 Track of Super Typhoon Nepartak. This figure can be downloaded on the website (https://sharaku.eorc.jaxa.jp/TYP_DB/data/TYP_DB_COMMON/track/bst_2016s.02W.NEPARTAK.jpg).

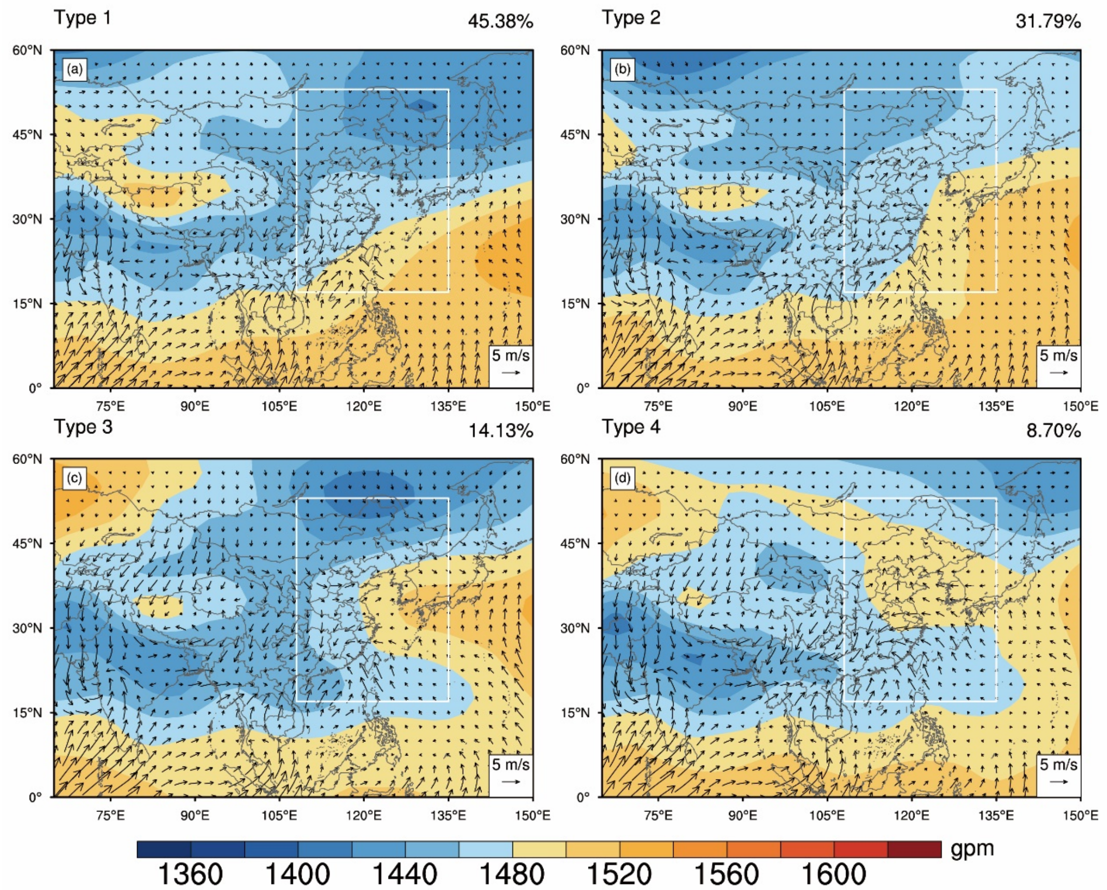

Fig. R3. The 10-m wind (vectors; see scale arrow at the bottom right in units of 5 m/s) and 850-hPa GH (contours; see scale bar at bottom in units of gpm) patterns based on objective classification

3. Physically, the synoptic weather patterns influence the pollutions via PBL structure (e.g., large-scale subsidence), regional-scale transport of pollutants (e.g. PM2.5 and VOCs), and occurrence of precipitations. All these physical processes underlying were not well analyzed. The authors cannot just use simple correlation analysis to explain the mechanisms, which makes the conclusion unreliable and inconvincible. At least, typical pollution episodes of each synoptic weather type should be analyzed in-deep with observational evidence to validate the hypothesis given.

RESPONSE: Based on your suggestions, this study has now considered the role of boundary layer structure in modulating the pollution. Particularly, we conducted an in-depth analysis of the compound pollution under Type 1 and Type 2 patterns. The underlying physical mechanism would be explained by our investigation regarding the characteristics of boundary layer structure, precipitation and ground-level wind flow over the polluted regions. More descriptions have now been noted on lines 410-424. Please also find the information below.

"Furthermore, we summarized boundary layer structure, precipitation, and ground-level wind flow across the BTH region. Based on the characteristics, we separately defined Type 1 and Type 2 into clean (both concentrations of the O_3 and $PM_{2.5}$ are less than polluted level) and compound pollution periods (Figs. 11 and S10-S11). Particularly, Type1 has a significantly warmer temperature over the boundary layer during the compound pollution period of BTH region than that of the clean period. The daytime BLH under compound pollution condition was also higher than that of the clean condition. In addition, there were different directions of

prevailing during the two periods, which prevailing winds during the compound pollution period were usually southward and could be driven by air pollutants transported from the southern plains (Fig. 11; see also Miao et al., 2019b, 2020). Co-influencing by the topographical effect of the northern mountainous areas, air pollutants could be trapped in the BTH region. In comparison, although there was southward wind prevailing in the BTH region (Figs. 11 and S11), the rain belt also located in the southern area of BTH might lead to the potential removal of $PM_{2.5}$ (Fig. 9j). Therefore, compound pollution across the BTH region might mainly be due to local emissions of air pollutants."

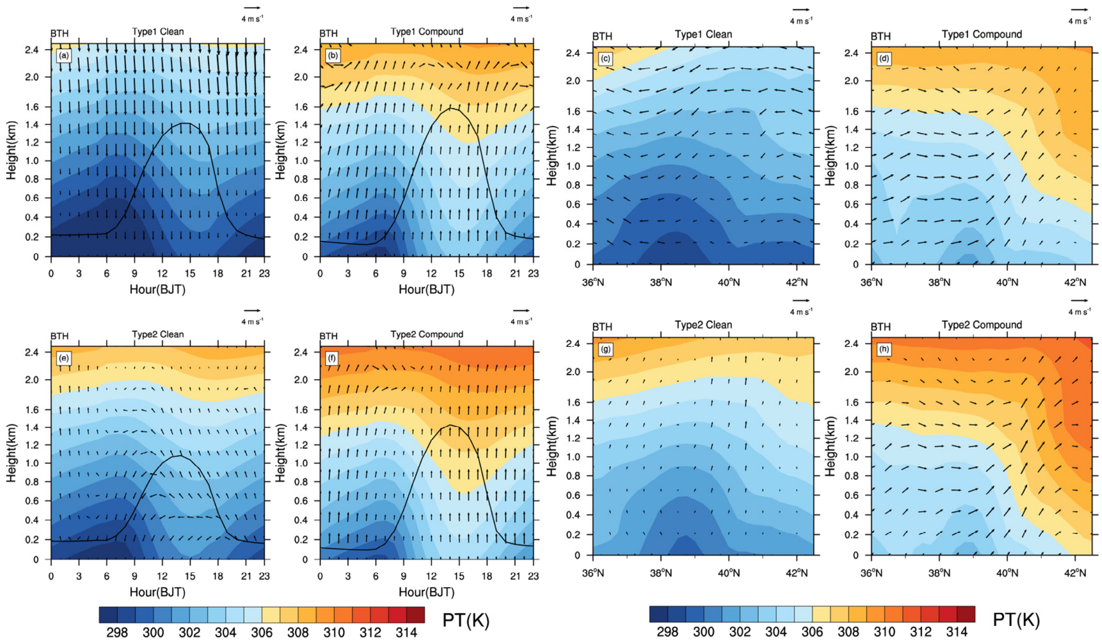

Fig. 11. The daily variation of horizontal wind, potential temperature (PT) and BLH of boundary layer in the BTH under clean and compound pollution period of Type 1 and Type 2 (a, b, e, f). The vertical cross-section of u-wind, w-wind and PT for the same situation of BTH (c, d, g, h). The w-wind is multiplied by 100 when used. The data has been derived from ERA5 reanalysis data.

4."The BLH was calculated according to the method given by Guo et al. (2016, 2019), and the FLWD [frequency of light wind (< 2 m s−1) days], precipitation frequency (PF), and MDA8 O3 were also counted." The detailed information about BLH should be directly given. At present, only a few cities have afternoon soundings during summer. Only 08:00 and 20:00 LT soundings were used to calculate the BLH, which is inappropriate for this study. How to calculate the FLWD and PF? Why only choose these specific parameters? Are they significantly correlated to the pollution levels in all the studied regions (e.g., BTH, YRD, GZP)? How about the precipitation intensity and amount, and its lasting time? How about the wind directions and wind shear, and associated transport of pollutants (PM2.5 and VOCs)?

RESPONSE: Thanks for the comments. More information regarding BLH has now been added in supplementary materials. Please find the details as follows:

"The bulk Richardson number (*Ri*) was applied to calculate the BLH.

Ri can be expressed as:

$$R(i) = \frac{(g/\theta_{vs})(\theta_{vz}-\theta_{vs})(z-z_s)}{(u_z-u_s)^2+(v_z-u_s)^2+(bu_*^2)} \quad (1)$$

where z is height above ground, s is the surface, g is the acceleration due to gravity, θ_v is virtual potential temperature, u and v are the component of wind speed, and u_* is the surface friction velocity. Due to a much smaller magnitude in compared with bulk wind shear term in the denominator, this study does not need to consider the influence of u_* (Seidel et al., 2012).". Furthermore, our revised study has now applied 14:00 LT soundings to estimate the BLH, while the results of BLH at 08:00 and 20:00 LT soundings (calculated in original version) were reported in supplementary materials as references (Fig. S13). Specifically, we have added the following variables for calculation: FLWD and PF. Specifically, FLWD is the frequency of light wind (< 2 m s^{-1}) days, which can be defined as the ratio between the number of the days with average daily WS lower than 2 m s^{-1} and the total days of each synoptic pattern; PF is precipitation frequency, which can be defined as the ratio of the number of the rainy days to the total days associated with each synoptic pattern). The above definitions were due to an unfavorable condition for transporting air pollutants during low WS days as well as low possibility of forming O_3-$PM_{2.5}$ co-occurring pollution during low PH conditions. We also applied specific meteorological parameters associated with air pollution levels in this study, such as Tmax, RH and BLH. Based on our results, we also found that Tmax can exceed 27°C during high O_3 events across five urban clusters of the study area, and moderate RH can be associated with O_3-$PM_{2.5}$ compound pollution in the BTH region and North YRD area. Furthermore, high BLH can enhance the environmental capacity of atmospheric pollutants resulting in a reduction of air pollutant concentration. Additionally, there was not a significant difference of the average daily precipitation among the four types of synoptic weather patterns (Fig. R4). However, we have found a significant difference of precipitation level during clean and compound pollution period under the same SWP (see Figure S10 and S11). Due to a lack of hourly precipitation data, this study cannot show the intensity and lasting time. Therefore, we have now added more information regarding this in the limitation section, as well as a suggestion regarding the future improvement with high-temporal-resolution data.

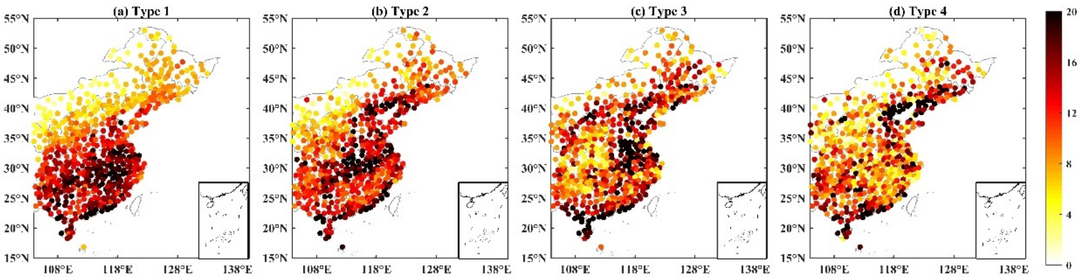

Fig. R4. The daily mean amount of precipitation under each SWPs.

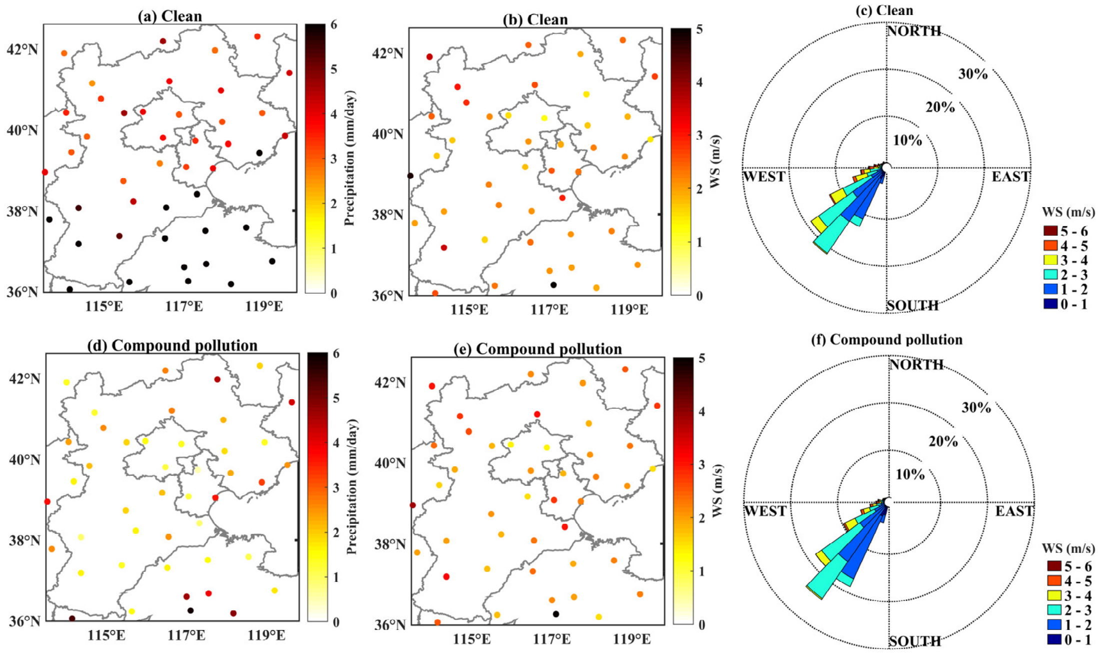

Fig. S10. Precipitation, WS, and WD during clean and compound pollution period under Type 1 over BTH.

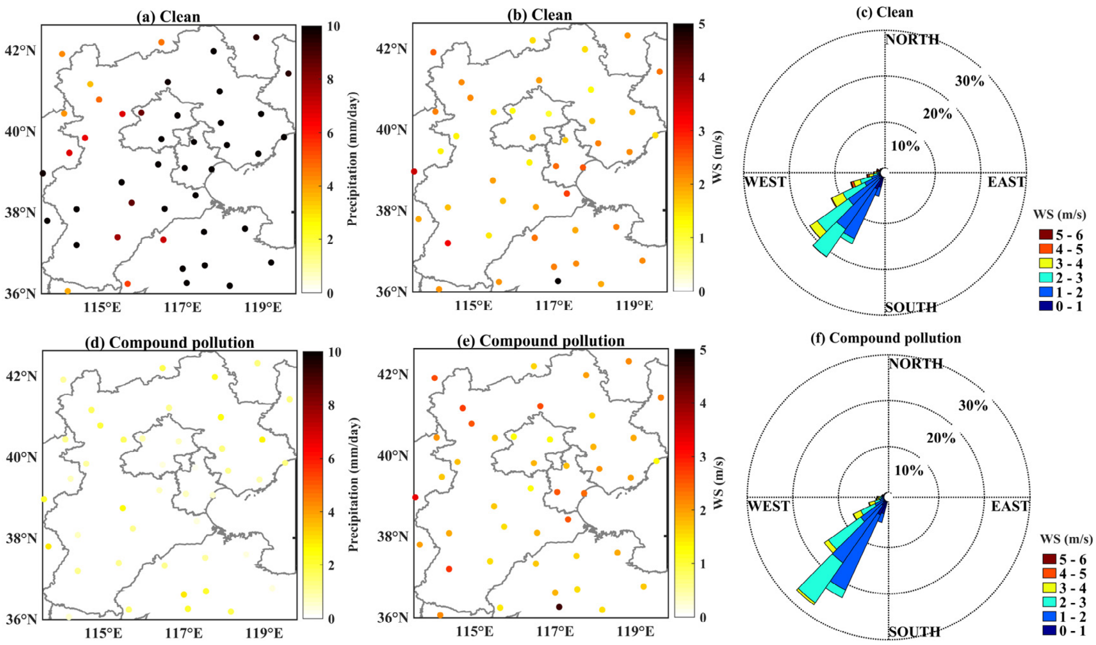

Fig. S11. Same as Fig. S8 but for Type 2.

5. In the Results and Discussion sections, the “rain belt”, “Meiyu”, “rain band”, “heavy precipitation” were simply analyzed with very few observational evidence. Since this study focuses on the movement/evolution of WPSH in summer (rainy season), more in-deep analysis on the links between precipitation and pollutions should be given with observational evidence and typical episodes.

RESPONSE: Thanks for your suggestion. It is indeed our limitation as the position of the rainband could only be sketchily plotted based on the frequency and volume of precipitation under each SWP (Fig. 8i-l). Therefore, this study aimed to characterize the trend and location of rain belt in relation to the movement of WPSH in summer, based on separate discussions with each SWP. More information can be referred as follow: “Type 1 is characterized by humid condition in the southern area and dry condition in the northern region owing to an extensive southwestern flow of the WPSH, resulting in a rain belt found in southeastern coastal area such as PRD and YRD regions. Type 2 is associated with meridional flow and dry and wet anomalies in northern China, resulting in a rain band locating at the central areas of between BTH and YRD regions due to the northern advance of the WPSH compared with Type 1. Furthermore, there is a greater RH for most of the study sites under Type 3 and Type 4, possibly a result of the shifted rain belt in the BTH and NEM regions under Type 3 once the northern boundary of the WPSH reaching at 37.5°N, and an occurrence of heavy precipitation across the western PRD region as well as central areas of between BTH and YRD regions under Type 4 (Fig. S6).”.

Additionally, we have now shown the linkages between precipitation and compound pollution in Figs. S10 and S11 as well as the response of the last question, with evidences showing that precipitation amount during clean period is greater than that of the polluted period over the BTH region.

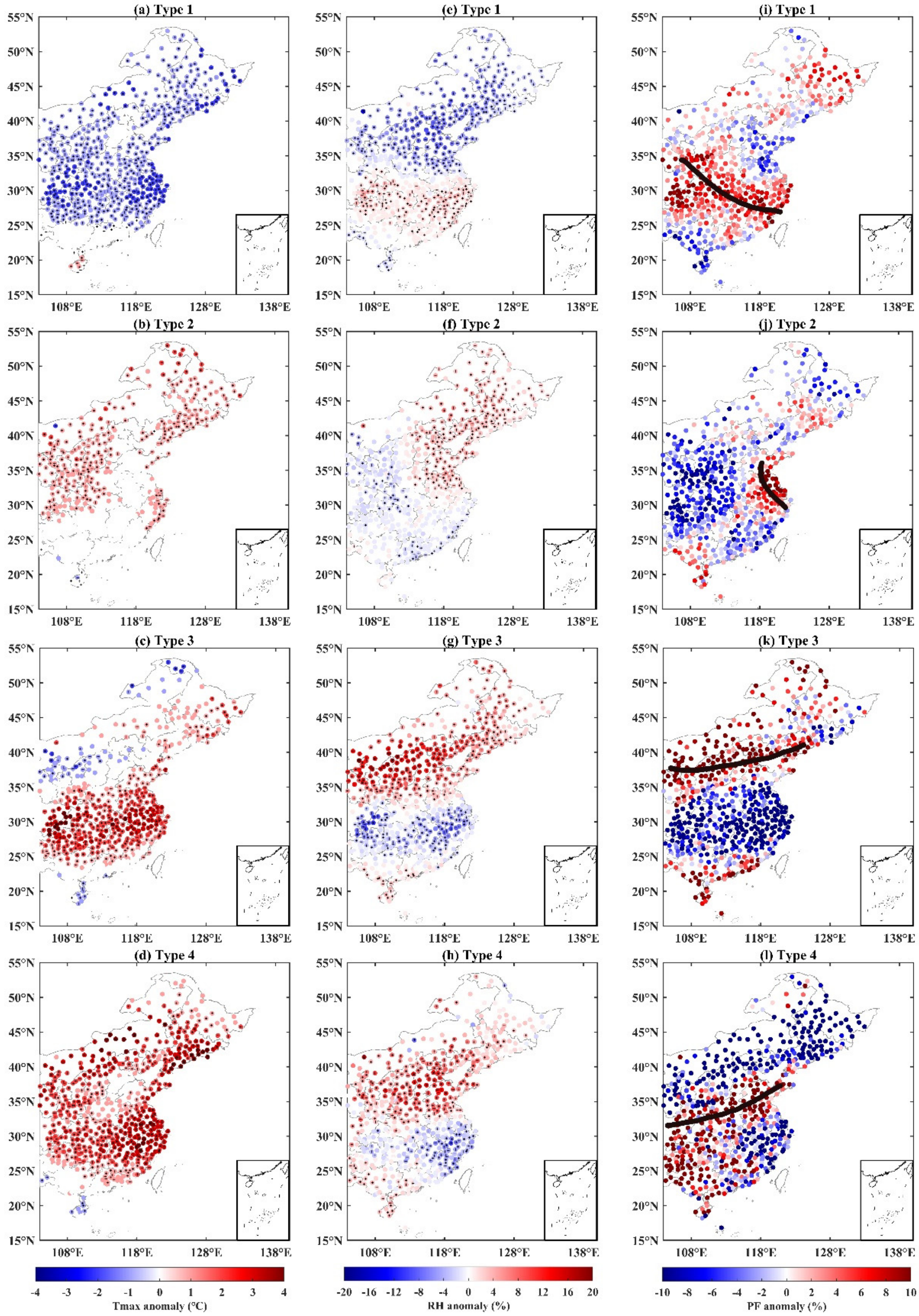

Fig. 8. Same as Fig. 6 but for Tmax (a–d), RH (e–h), and PF (i–l). The black solid line presents the rain belt of each SWP.

6.Section 4.2 "Effects of NO2 on O3". The best proxy of photochemical reactivity is the ozone potential efficiency (OPE) but not the ratio of O3 to NO2. High photochemical reactivity probably appeared with high O3 and NO2 concentration but reasonably with a low O3/NO2 ratio. It is not accurate to take the O3/NO2 ratio as the judging criteria.

RESPONSE: Many thanks for your kind suggestion. Indeed, ozone potential efficiency (OPE)

is the best proxy of photochemical reactivity, however, the related data for calculation was unavailable. As an alternative, previous studies have demonstrated that the photochemical reaction of NO, NO2, and O_3 in the troposphere form could a closed system(Yu et al., 2020), and this photochemical cycle of NOx and O_3 could be the basis of photochemical processes in the troposphere. Therefore, oxidant (Ox, Ox=O_3+NO_2), a conservative quantity over a short temporal scale, could be an alternative parameter to evaluate photochemical processes because NO can quickly react with the equivalent amount of O_3 to generate NO_2(Kley et al., 1994). Particularly, some studies have demonstrated that Ox could be used to represent OPE (Chang et al., 2020; Ge et al., 2013). Therefore, we used Ox to be an alternative of OPE, not the ratio of O_3 to NO_2 in the last manuscript.

Based on these assumptions, we further revised our content. For example, revised, "Figure 10 can present the daily variation of NO_2 and Ox. These include daily variations of NO_2 showing two peaks during a day, including a first peak at the morning and an second peak associated with traffic emissions in the evening (Xie et al., 2016; Yu et al., 2020). As we found the lowest point of NO_2 at 15:00 (BJT), and NO_2 can be photolyzed to produce O_3 during the day, this study assumed that this particular time was the peak formation ozone across the study areas. As NO_2 was consumed through a photochemical reaction with the involvement of other precursors to produce a large amount of O_3, Ox could form a peak during the afternoon. In particular, abundant sunlight in summer is beneficial to the photochemical reaction process, but since most parts of eastern China are in a subtropical climate with the same period of rain and heat, the existence of the rainy season will inevitably inhibit the summer photochemical process. Under different SWP, the photochemical reaction over each area has an obvious relationship with the rain belt. For example, the rainy season in BTH and NEM areas mainly occurs in Type 3, and the Ox of Type 3 in this area is significantly lower than other SWPs.". Therefore, we have changed the section title from "Effects of NO_2 on O_3" to "Potential implications of NO_2".

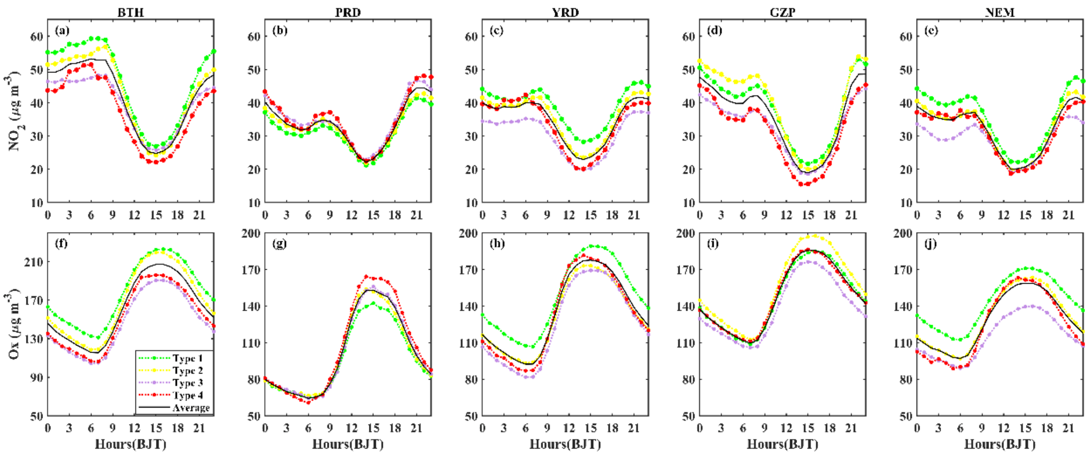

Fig. 10. Daily variation of NO_2 and Ox under four SWPs in key urban clusters.

Reference

Chang, L. S., Choi, J. Y., Son, J., Lee, S., Lee, D., Jo, Y. J. and Kim, C. H.: Interpretation of decadal-scale ozone production efficiency in the Seoul Metropolitan Area: Implication for ozone abatement, Atmos. Environ., 243(April), 117846, doi:10.1016/j.atmosenv.2020.117846, 2020.
Ge, B., Sun, Y., Liu, Y., Dong, H., Ji, D., Jiang, Q., Li, J. and Wang, Z.: Nitrogen dioxide

measurement by cavity attenuated phase shift spectroscopy (CAPS) and implications in ozone production efficiency and nitrate formation in Beijing, China, J. Geophys. Res. Atmos., 118(16), 9499–9509, doi:10.1002/jgrd.50757, 2013.
Kley, D., Geiss, H. and Mohnen, V. A.: Tropospheric ozone at elevated sites and precursor emissions in the United States and Europe, Atmos. Environ., 28(1), 149–158, doi:10.1016/1352-2310(94)90030-2, 1994.
Xie, M., Zhu, K., Wang, T., Chen, P., Han, Y., Li, S., Zhuang, B. and Shu, L.: Temporal characterization and regional contribution to O 3 and NO x at an urban and a suburban site in Nanjing, China, Sci. Total Environ., 551–552(x), 533–545, doi:10.1016/j.scitotenv.2016.02.047, 2016.
Yu, S., Yin, S., Zhang, R., Wang, L., Su, F., Zhang, Y. and Yang, J.: Spatiotemporal characterization and regional contributions of O3 and NO2: An investigation of two years of monitoring data in Henan, China, J. Environ. Sci. (China), 90(November), 29–40, doi:10.1016/j.jes.2019.10.012, 2020.

Specific comments:

1. Fig. 5, two “2017”?

RESPONSE: Thank you for the comment. We have now revised the words on Figure 5 as suggested.

2. “BTH, YRD, PRD, Guanzhong Plain (GZP), Northeast Megalopolis (NEM) regions”, the locations of these studied regions should be clearly described in manuscript and presented in the Figure.

RESPONSE: We have now added more descriptions regard to the location of study regions (Lines 165-171 of page 7). Please also find more information as follow: “Summer hourly data (2015-2018) for 1174 stations were retrieved from an observational network in eastern China (104°–135°E, 17°–53°N), which include the more prominent pollution areas in the eastern urban agglomeration, such as the BTH (113.5°–119.8°E, 36°–42.6°N), YRD (115.3°–122.6°E, 27.2°–34.5°N), PRD (112.5°–113.7°E, 21.3°–23.1°N), Guanzhong Plain [GZP (104.6°–112.2°E, 33.3°–36.8°N)], Northeast Megalopolis [NEM (121.2°–131.0°E, 39.8°–47.3°N)] regions (the specific locations of stations and urban agglomerations are shown in Fig. 1a).”, and the specific locations of stations and urban agglomerations are shown in Fig. 1a.

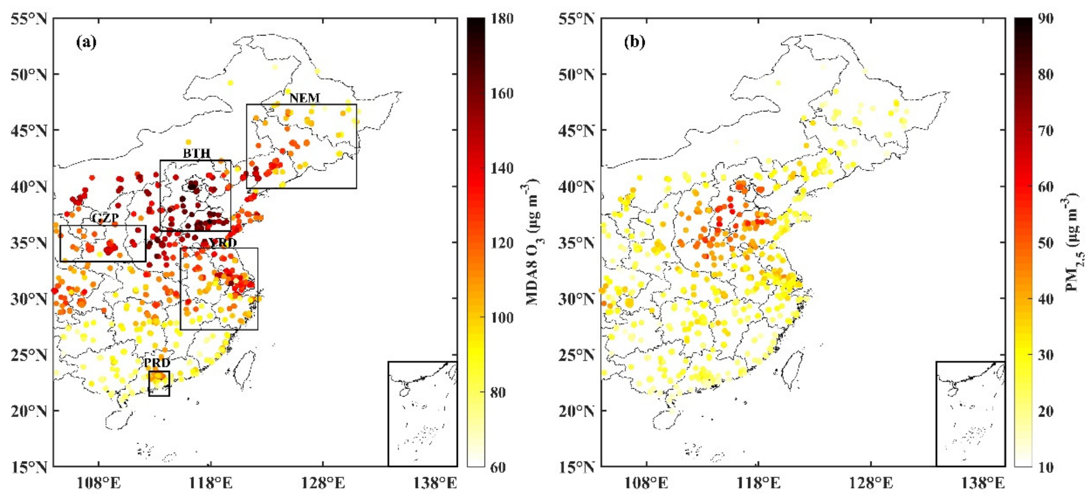

Fig. 1. Average concentration of MDA8 O_3 (a) and $PM_{2.5}$ (b) in eastern China during summers of 2015–2018. Stations and key urban clusters (black boxes) are shown in (a).

3. Line 165-166, "More detailed information about the T-PCA method can be found in Miao et al. (2017)." The detailed information of the method should be directly given.

RESPONSE: More detailed information regarding the T-PCA method is now added to lines 191-197 on pages 7-8:

"The cost733class is a FORTRAN software package consists of several modules for classification, evaluation and comparison of weather and circulation pattern. First, T-PCA classification of the cost733class performs spatial standardization on weather data. Then split data to 10 subsets and estimates principal components (PCs) of weather information based on singular value decomposition, the PC score for each subset can be calculated after oblique rotation, and compares 10 subsets based on contingency tables to select the subset with highest sum and return its types (Miao et al. 2017)."

4. Some literatures were not properly cited. Please carefully check the citations of the whole manuscript. Some are given below. "In general, PM2.5 pollution is featured with obvious diurnal and seasonal changes. Due to the influence of atmospheric diffusion conditions such as precipitation and wind speed (WS), it tends to be enhanced in the morning and evening, lower at noon, and higher in winter and lower in summer." Dose the author mean that the diurnal variations of precipitation and wind speed modulate the pollution level? It is odd. How about the emission and PBL?

RESPONSE: Thanks for your comments. We have revised our content as follow: "In general, a significant diurnal variation of $PM_{2.5}$ pollution was observed, possibly due to obvious the local emissions caused by industrial production and human activities for daily living (Amil et al., 2016; Liu et al., 2019). Particularly, the pollution level was higher during the morning and evening of a normal weekday, with a weakening effect found in the afternoon which may be caused by the co-effects of boundary layer structure as well as anthropogenic emissions. There was also a seasonal variation of $PM_{2.5}$ pollution across China, indicating a higher level of pollution in winter than summer (Ye et al., 2018; Zhang and Cao, 2015)". (lines 66-72 of page 3).

5. "Summer O3 pollution has gradually been prominent, replacing PM2.5 as the primary pollutant in the air…" Is it true? At present, PM2.5 still is the dominant pollutant in China.

RESPONSE: We have revised the sentence as follow: "While $PM_{2.5}$ is still one of the dominant air pollutants across China, surface O_3 pollution in summer has gradually been prominent. Several studies even indicated that O_3 might have replace the role of $PM_{2.5}$ as the primary air pollutant during summer (Li et al., 2019).".

6. "Miao et al. (2015) suggested that strong northwesterly synoptic winds, low BLH (boundary layer height), high RH and stable atmosphere are more prone to aerosol pollution in the BTH region during wintertime …" The strong northwesterly winds would favor the dispersion of pollutants in winter.

RESPONSE: Thank you for the information. We have revised the content as follow: "Miao et al. (2015) suggested that low boundary layer height (BLH) and stable atmosphere would be an unfavorable condition for the dispersion of winter aerosol pollution over the BTH region.".

7. "Shi et al. (2020) studied the spatial distribution of O3-8h (O3 8-hour moving average) and PM2.5, and their sensitivity of meteorological parameters; pronounced positive (negative)

correlation between temperature (BLH and absolute humidity) and O3-8h was found, but the relation between WS and O3-8h was spatially different; for PM2.5, it was negatively (positively) correlated with temperature, WS and BLH (absolute humidity).” It is another inappropriate citation. Please carefully read the previous study (Shi et al., 2020) and properly introduce it.

RESPONSE: Thank you for the information. We have revised the content as follow:

“ Shi et al. (2020) studied the sensitivity of O_3-8h (O_3 8-hour moving average) and $PM_{2.5}$ associated with meteorological parameters. This study focused on the air pollution and meteorological conditions between January and July, 2013, with a result showing that temperature could have the greatest impact on the daily maximum O_3-8h, while the $PM_{2.5}$ sensitivities are negatively (positively) correlated with temperature, WS, and BLH (absolute humidity) in most regions of China.”.

8. “Recently, Han et al. (2020) revealed that meteorological factors can explain ~46% of the daily variability in summertime surface O3, while synoptic factors contribute to ~37% of the overall meteorological effects on the daily variability of surface O3 in eastern China.” More detailed information on Han et al. (2020) should be presented since it is quite similar to this study, such as its studied period, method, and classification results?

RESPONSE: Thanks for your comments. More details regard to the results of Han et al. (2020) have now been presented in the revised manuscript (lines 110-116 of page 5):

“Recently, Han et al. (2020) assessed the impacts of local and synoptic meteorological factors on the daily variability of surface O_3 over eastern China. This study revealed that the meteorological factors could explain ~46% of the daily variations of summer surface O_3. Particularly, synoptic factors contributed to ~37% of the overall effects associated with the meteorological factors. Furthermore, six predominant SWPs were identified by the self-organized map, and the results indicated a weak cyclone system and a southward prevailing wind inducing a positive O_3 anomalies over the eastern China.”.

9. Line 95-97, “The abovementioned indicates that the variation of meteorological factors, which are mainly driven by the evolution of different weather circulation situations, play a non-negligible role in air pollution. Therefore, classification of air pollution according to the meteorological circulation has become particularly important …” The abovementioned literatures cannot support this statement.

RESPONSE: Thank you for the comment. This statement has now been deleted in the revised manuscript.

10. Line 101-102, “In recent years, it has become possible to objectively classify atmospheric circulation conditions using weather data such as GH, sea level pressure…” It is not true. The objective classification method has been used since the 1990s.

RESPONSE: Thank you for pointing out the biased description. We have now revised it based on your suggestion (Lines 121-123 of page 5).

11. Line 104-105, “the objective approach has been widely used in air pollution research (Beck & Philipp, 2010)…” Beck and Philipp (2010) didn’t study the pollution issues.

RESPONSE: We apologize to the inappropriate citation. This citation is now removed from our manuscript.

12. Line 115-118, "Many studies have suggested that PM2.5 and O3 pollution are mainly related to the East Asian summer monsoon (EASM) and western Pacific subtropical high (WPSH) (Li et al., 2018a; Xie et al., 2017; Yin et al., 2019; Zhao et al., 2010)." More detailed information about these previous studies can be given, their studied periods, temporal scale and spatial scale. Seasonal variation? Inter-annual variation? The paper of Xie et al. (2017) has been withdrawn, please check (https://acp.copernicus.org/preprints/acp-2017-500/).

RESPONSE: Thank you for your kind suggestion. We have revised the content as follow:

"Many studies have suggested a moderating effect of East Asian summer monsoon (EASM) and western Pacific subtropical high (WPSH) on air quality over China (Li et al., 2018; Yin et al., 2019; Zhao et al., 2010). In particular, Li et al. (2018) applied RegCM4-CHEM simulation to analyze the differences of ozone level among three strong and weak monsoon years, and found that the concentrations of O_3 over the central and eastern China were higher in strong EASM years than that in weak EASM years.".

13. Line 129-131, "the compound O3-PM2.5 pollution-related meteorological conditions, should be complex and likely to be associated with certain weather types". This statement is not well supported.

RESPONSE: Thank you for your suggestion. We have revised the content as follow: "Due to a variability of local meteorological conditions under the impacts of various synoptic weather types and modulation of large-scale WPSH movement, the causes and consequences of meteorological factors for the formation of compound O_3-$PM_{2.5}$ pollution could be complex.".

Anonymous Referee #2:

This paper investigated the co-occurring of ozone and PM2.5 pollution of eastern China in summer. Four synoptic weather patterns (SWPs) were detected and the air pollution feature under each SWP was analyzed. The paper is not well organized and difficult to follow. The authors should revise the manuscript carefully to meet the standard of ACP. The detailed comments are listed below.

RESPONSE: Thank you so much for your valuable comments. We have carefully addressed your concerns. We have also reorganized our manuscript thoughtfully as suggested.

Major comments:

This paper investigated the co-occurring of ozone and PM2.5 pollution in summer. However, the probability of PM2.5, ozone and compound pollution in each site could not be found in the manuscript. Please show their distribution at beginning of the manuscript. Their distribution under each SWP should be also shown to see the impacts of different weather patterns.

RESPONSE: Thanks for your suggestion. We have now included a figure S11 (supplementary material) to represent the calculation for the probability of compound pollution. Particularly, we found significant O_3-$PM_{2.5}$ compound pollution events over five urban clusters during the study period, especially in the BTH region. Furthermore, BTH-NYRD under Type 1 and BTH region under Type 2 could be concluded as a result of O_3-$PM_{2.5}$ co-occurring pollution due to a greater occurrence of compound pollution. More information regarding spatial distributions of O_3, $PM_{2.5}$ and compound pollution under each SWP were given in Fig. 12.

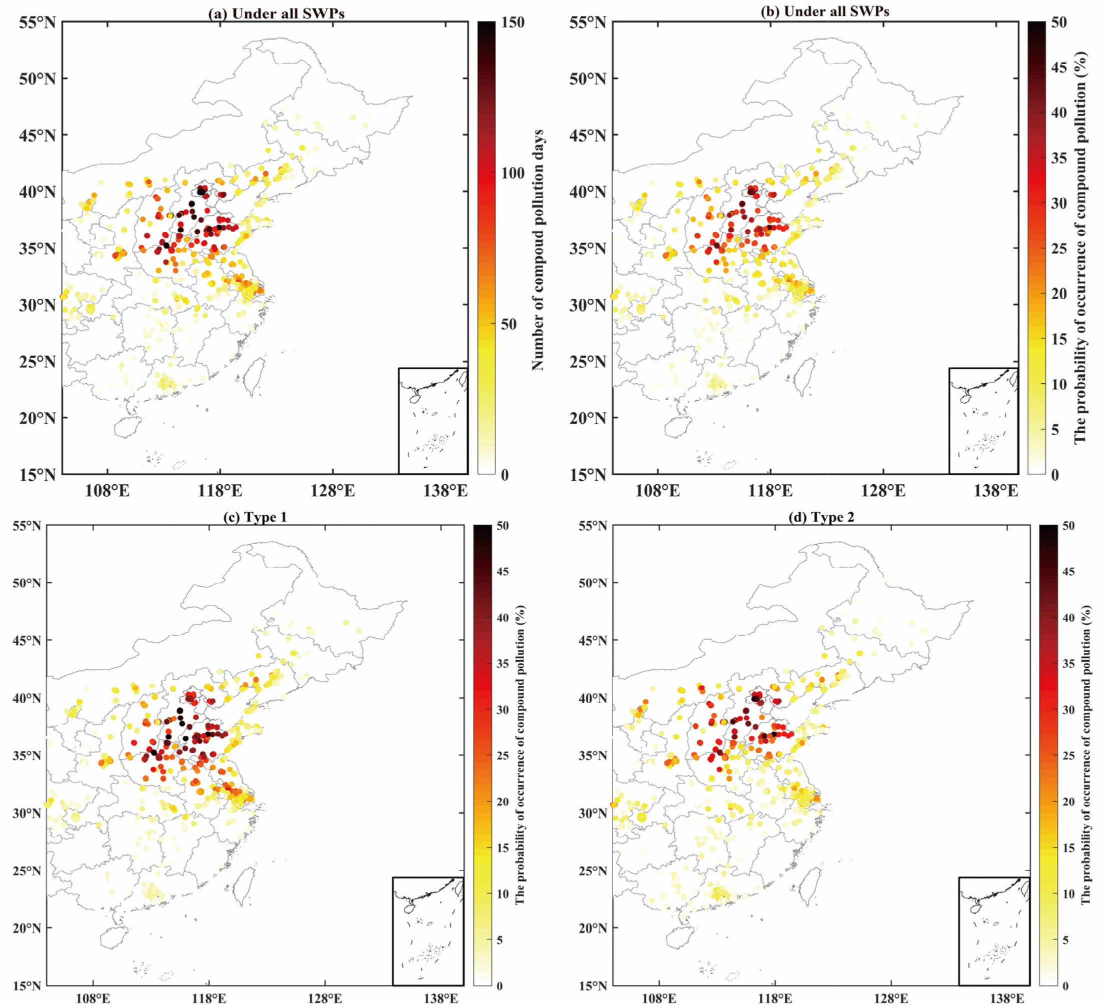

Fig. S12. The number (a) and probability (b) of occurrence of compound pollution days under all SWPs in each site, (c) and (d) is the same as (b), but for Type 1 and Type 2.

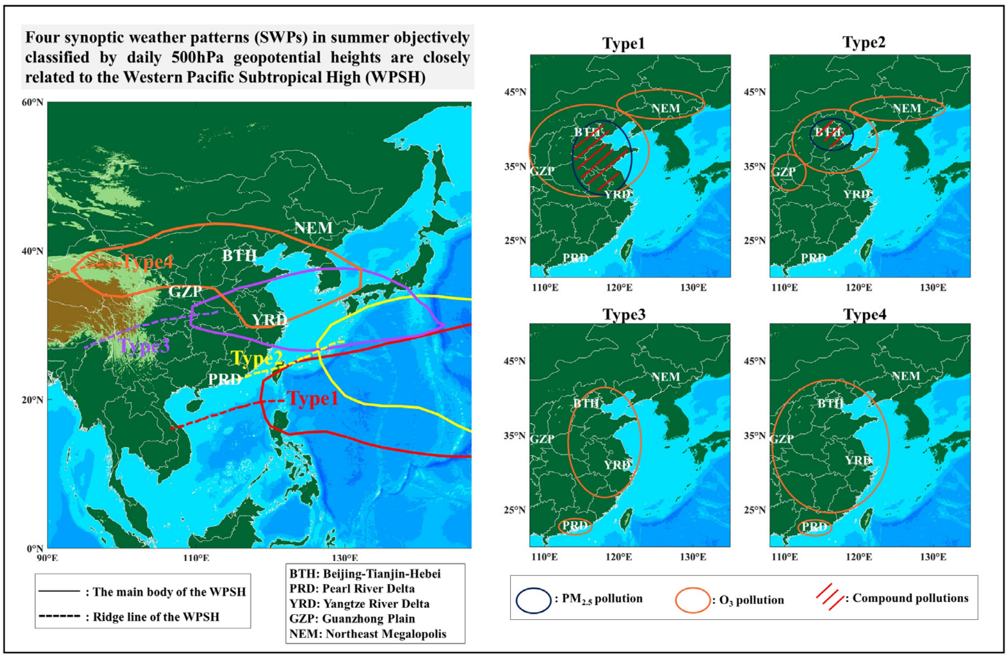

Fig. 12. Schematic diagrams describing the relationships between the WPSH, four SWPs and summertime O_3 and $PM_{2.5}$ pollution in various regions.

In this work, four synoptic weather patterns were detected and their difference were compared. The physical understanding the SWPs could be improved. In my opinion, Type 1 and type 2 represents normal WPSH pattern during early and late summer, respectively. Type 3 and type4 reflects two splitting states (southern mode and northern mode) of the WPSH, which mainly occurs in late summer. The climate background of early and late summer is quite different from each other. Thus, the SWPs of early and late summer should be compared separately.

RESPONSE: Thank you for your comments. For most of the days, Type 1 and Type 2 can represent both regular WPSH pattern during early and late summer. Type 3 and type 4 may demonstrate the two splitting states (southern mode and northern mode) of the WPSH, which mainly occurs in the late summer. Particularly, characteristics of circulation of these synoptic patterns have been described and compared in section 3.2:

"The location of Type 1 related western ridge point and northern boundary of the WPSH at 500 hPa is around 120°E and 30°N, respectively, (Fig. 4a and Table S2). The southwestern flow of this WPSH could chemically transport water vapor to the YRD region, resulting in a southwestward prevailing wind across the YRD region and westward flow from the north of the WPSH forming a convergence area at 850 hPa. These conditions were also associated with high temperature and humidity during the summer with Meiyu season, which Meiyu season is a climate phenomenon with continuous cloudy and rainy days generally occurring during June and July every year in the middle and lower reaches nearby Yangtze river, Taiwan of China, central/southern Japan, and southern Korea. For Type 2, the westerly trough could deepen as the WPSH shifts northward slightly from Type1 or retreats southeast from Type 3 (Fig. 4b). The southerly wind from the ocean could interact with the northern periphery of the WPSH. As a result, the sea-land interaction could affect the southeastern region across China,

while northern China could be mainly controlled by the westerly trough. In compared with Type 2, the impacts of Type 3 could shift the boundary of WPSH to a higher latitude, with a westward extension (Fig. 4c), which disintegrating the closed high-pressure monomer along the eastern coast of China and remaining the main body of the WPSH over the ocean (Figs. 4c and S4). This has led to a condition completely controlled by the monomer of the WPSH over the YRD region, resulting a hot and dry weather at the end the rainy season at the beginning of mid-summer. Figure. 4d indicated that the location of the WPSH monomer was more northern and western with respect to other SWPs, controlling northern China for a long time, the western ridge point was around 95°E and the northern boundary is around 40°N.
Figure 5 presents the daily and annual variations of the SWPs in the summers of 2015–2018. The advance of the WPSH in eastern China occurs in June and July, while a gradual withdrawal of the WPSH mainly occurs in August. Particularly, Type 1 and Type 2 represent normal WPSH characteristics during early and late summer. Type 3 and Type 4 could reflect a split of the WPSH, which mainly occurs in late summer. Consequently, there were 167, 117, 52 and 32 days for the Type 1, Type 2, Type 3 and Type 4 over the study period, respectively. Since WPSH movement is generally affected by the weather phenomenon of its surrounding climate systems (such as typhoons, the Tibetan high, etc.) (Ge et al., 2019; Liu and You, 2020; Shu et al., 2016; Wang et al., 2019), it could result in a short-term southward retreat during the advancement of WPSH (e.g., around 10 August 2018) and a short-term northward advance during its process of retreat (e.g., 21 and 29 August 2016). In general, the WPSH could represent the evidences of intra-seasonal and interannual changes over China, which will inevitably modify the changes of weather, climatic and environmental conditions in eastern China.".
More information for local meteorological factors under the influences of the above climatic background, including related environmental impacts, have now been noted in section 3.4.

The abstract is not well written and following information should be included: 1) The distinct feature of each synoptic weather pattern; 2) the pollution features under each SWP; 3) which SWP mostly favors the co-occurring of ozone and PM2.5 pollution; 4) where the co-occurring of ozone and PM2.5 pollution happens.
RESPONSE: Thanks for your suggestion. We have revised the abstract to be more focusing on the co-occurrence of O_3 and $PM_{2.5}$ pollution under Type 1 and Type 2 synoptic weather patterns, including more details in the results. The revised abstract is as follow: "Surface ozone (O_3) pollution during summer (June-August) over eastern China has become more severe, resulting in a co-occurrence of surface O_3 and $PM_{2.5}$ (particulate matter with aerodynamic diameter ≤ 2.5 μm in the air) pollution recently. However, the mechanisms regarding how synoptic circulation pattern could influence this compound pollution remains unclear. This study here applied a T-mode principal component analysis (T-PCA) method to objectively classify the occurrence of four synoptic weather patterns (SWPs) over eastern China, based on geopotential heights at 500 hPa during summer (2015-2018). Four SWPs of eastern China are closely related to the western Pacific subtropical high (WPSH), exhibiting, significant intraseasonal and interannual variations. Based on ground-level air quality information and meteorological observations, remarkable spatial and temporal disparities of surface O_3 and $PM_{2.5}$ pollution were also found under the impacts of the four SWPs.

Particularly, there were two SWPs sensitive to compound pollution (Type 1 and Type 2). Type 1 is characterized by a stable WPSH ridge with axis at about 22°N and the rain belt located in the south of Yangtze River Delta (YRD). High temperature, moderate humidity and low precipitation occurred in the region from BTH to northern YRD (BTH – NYRD), resulting in a co-occurrence of O_3 and $PM_{2.5}$ pollution. Additionally, air pollutants can be transported by the prevailing southerly winds from southern plains and accumulated in the southern BTH, resulting in a worsen pollution. Type 2 exhibits a WPSH dominance (the ridge axis ~25°N) and rain belt (over the YRD) in a higher latitude compared with Type 1. High temperature, medium-high humidity and low precipitation over the BTH were the conducive factors related to the occurrence of the compound pollution events under Type 2. Furthermore, low boundary layer height (BLH) and high frequency of light-wind days (FLWD) could create favorable conditions for pollution maintenance. Overall, synoptic weather patterns have played an important role as driving factors of surface O_3-$PM_{2.5}$ compound pollution in a regional context. In addition to the impacts of local emissions, our results may provide further insights regarding how regional environmental changes due to co-occurrence of high $PM_{2.5}$ and high O_3 level may be driven by the effects of meteorological factors. Overall, our findings demonstrate the important role played by synoptic weather patterns in driving regional surface O_3-$PM_{2.5}$ compound pollution, in addition to the large quantities of emissions, and may also provide insights into the regional co-occurring high $PM_{2.5}$ and high O_3 level via the effects of certain meteorological factors.”.

Other comments:

1. Line 26: Please describe details of SWPs here.

RESPONSE: The details of SWPs are given as follows: “Type 1 is characterized by a stable WPSH ridge with axis at about 22°N and the rain belt located in the south of Yangtze River Delta (YRD).” And “Type 2 exhibits a WPSH dominance (the ridge axis ~25°N) and rain belt (over the YRD) in a higher latitude compared with Type 1”. See lines 30-37 of page 2 in the revised version.

2. Line 30: How about the ozone pollution over the regions where are not controlled by the WPSH or the prevailing westerlies. Where are these regions?

RESPONSE: Most of the regions we focus on are controlled by the WPSH or the prevailing westerlies under four SWPs except for PRD region under Type 3 and Type 4. In the revision, we have focused on the SWPs which are more prone to the compound pollution.

3. Line 34: Please explain the meaning of “some local areas”.

RESPONSE: “Some local areas” refers to “the BTH region under impacts of Type 1 and Type 2”. Thanks and revised.

4. Line 35: Please clarify where the co-occurring surface O3 and PM2.5 pollution happens.

RESPONSE: The co-occurring surface O_3 and $PM_{2.5}$ pollution happened in the BTH – NYRD regions under Type 1 and BTH region under Type 2.

5. Line 35-36: How the WPSH affects the boundary layer height and frequency of lightwind days?

RESPONSE: The area controlled by the WPSH usually have shallow BLH and high FLWD. In the revised manuscript, we have added the structural characteristics of the boundary layer to better explain the causes of compound pollution.

6. Line 36: What does the “different roles” mean? Please provide some explanations.

RESPONSE: It should be “an important role”. Sorry for incorrect description and thanks.

7. Line 118-120: In abstract, it is mentioned that high temperature, moderate humidity and slight precipitation favors the ozone formation. It is not consistent with the statements here.

RESPONSE: Thanks for your comment. Indeed, hot and dry air can enhance the photochemical reactions of O_3. Eastern China has a monsoon climate with dry winters and humid summers, so moderate humidity actually presents negative anomaly for summers, and it could be considered as a dry summer. In addition, we also analyzed the RH condition under different pollution scenarios (Fig. S14), and found RH is low-medium when O_3-only pollution occurs, and moderate RH would favor the co-occurrence of O_3 and $PM_{2.5}$. Therefore, the results were not inconsistent. In order to address the comments, we have now revised this description as follow: "High temperature, moderate humidity and low precipitation occurred in the region from BTH to northern YRD (BTH – NYRD), resulting in co-occurring O_3 and $PM_{2.5}$ pollution".

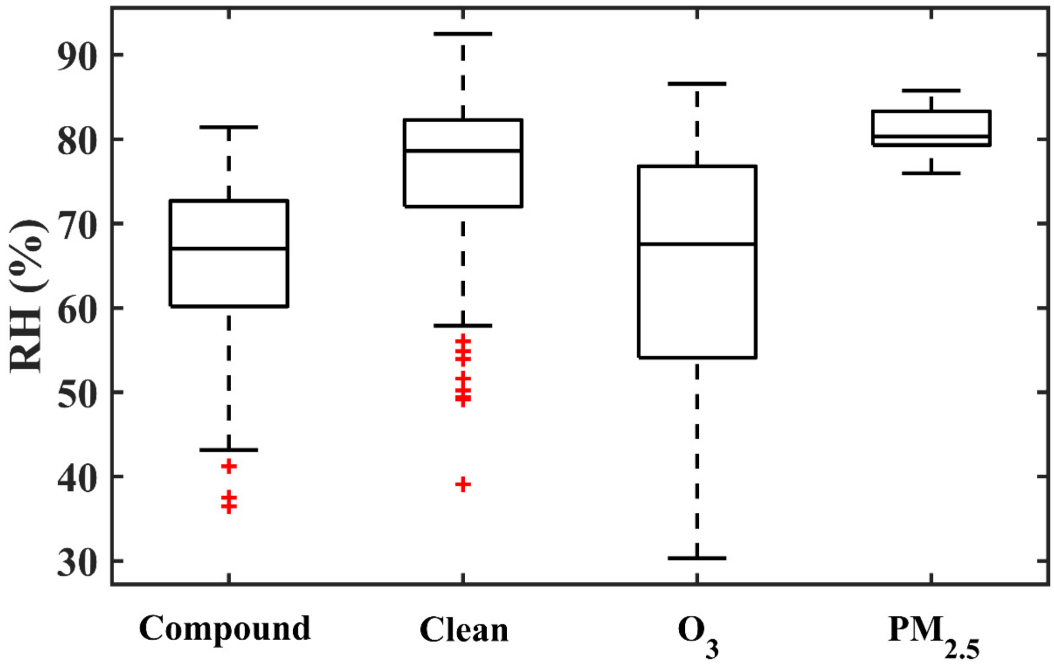

Fig. S14. Box-Whiskers for the RH under compound pollution, clean, O3-only, PM2.5-only period. In the Box-Whiskers plot, the central box represents the values from the lower to upper quartile (25th to 75th percentile). The vertical line extends from the maximum to the minimum value. The middle solid line represents the median, and the red plus represents the outlier.

8. Line 124: It is not consistent with the conclusions in abstract. In abstract, it is found that the warm moist flow brought by the WPSH result in co-occurring surface O3 and PM2.5 pollution.

RESPONSE:

Sorry for the unclear description. We have revised our conclusion as follow: "On one hand, the appropriate warm moist flow brought by the WPSH can promote hygroscopic growth of the fine particulate matter in some local areas (i.e., BTH-NYRD under Type 1 and BTH under Type 2), resulting in the increase of $PM_{2.5}$ concentrations. On the other hand, transboundary O_3 was transported to these local areas at the same time, which may contribute to the co-occurring surface O_3 and $PM_{2.5}$ pollution"

9. Line 148: I cannot find the position of the urban agglomeration in Figure 1a. Please check.

RESPONSE: We have changed the Figure 1a, and the black boxes shown in Figure 1a indicate the locations of key urban clusters.

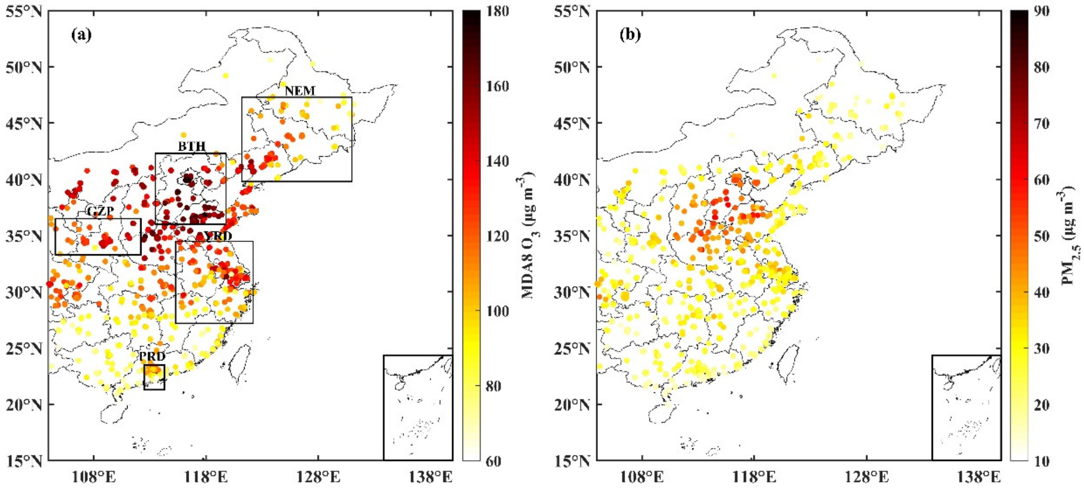

Fig. 1. Average concentration of MDA8 O_3 (a) and $PM_{2.5}$ (b) in eastern China during summers of 2015–2018. Stations and key urban clusters (black boxes) are shown in (a).

10. Line 207: Please show the temporal variations of co-occurring events.

RESPONSE: We have added the temporal variations of co-occurring events in Fig. 3. The asterisks indicate the co-occurred events under Chinese standard (WHO interim target 1, IT-1), and the circles indicate the co-occurred events under WHO IT-2 in Fig. 3. The specific description is "China has implemented strict policies for emission control, and the effects of these policies were remarkable. However, despite a decrease in $PM_{2.5}$ in the last five years, there was also an increase in ozone pollution over China (Fan et al., 2020; Sun et al., 2016), although "double-high" pollution reported on the weather scale has been decreased. As the limit of $PM_{2.5}$ concentration for pollution control is relatively loose in China, previous studies usually referred the interim target 1 (IT-1) of the World Health Organization (WHO) as the standard threshold. Our study pushed forward to the next stage, in which we used IT-2 of WHO (24-h average concentration of $PM_{2.5}$ is 35 μg m^{-3}) as our target limit to count the number of compound pollution days across each region. Based on this target, the pollution days for 4 SWPs were 194, 52, 16, 47, and 20, respectively (Fig. 3). These results indicated a severe situation of compound pollution that is still deserved a public attention."

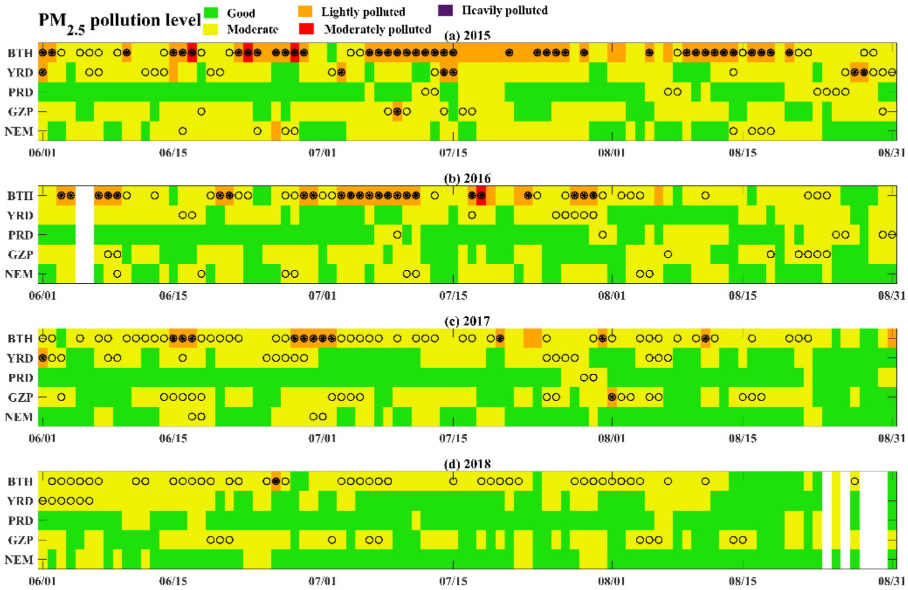

Fig.3. Time series of $PM_{2.5}$ pollution levels in key urban clusters, the black dots indicate the co-occurred events. The asterisks indicate the co-occurred events under Chinese standard (WHO interim target 1, IT-1), and the circles indicate the co-occurred events under WHO IT-2.

11. Line 229: Please focus on the position and strength of WPSH.

RESPONSE: The location of WPSH is shown on Table S2. Description regarding WPHS is now added to lines 266-285 of pages 10-11: "The location of western ridge point and northern boundary of the WPSH at 500 hPa in Type 1 is around 120°E and 30°N, respectively (Fig. 4a and Table S2). …… For Type 2, the westerly trough could deepen as the WPSH shifts northward slightly from Type 1 or retreats southeast from Type 3 (Fig. 4b). …… In compared with Type 2, Type 3 presents the boundary of WPSH in a higher latitude with a westward extension (Fig. 4c), disintegrating a closed high-pressure monomer along the eastern coast of China and the main body of the WPSH over the ocean (Figs. 4c and S4). …… Figure. 4d indicated that the location of WPSH monomer was more western and northern with respect with other SWPs, controlling the northern China for a long time; the western ridge point was around 95°E and the northern boundary was around 40°N.".

Table S2. The location index of the WPSH under four SWPs.

WPSH	Type 1	Type 2	Type 3	Type 4
The western ridge point	120°E	127.5°E	110°E	95°E
The northern boundary	30°N	32.5°N	37.5°N	40°N
The ridge axis	22°N	25°N	32.5°N	37.5°N

12. Line 229: It should be the north advance of WPSH.

RESPONSE: Yes, WPSH is slight shifting northward. We have now revised the content (lines 274-275 page 10).

13. Line 234: Type 1 and type 2 represents normal WPSH pattern during early and late summer,

respectively. Type 3 and type4 reflects splitting of the WPSH, which mainly occurs in late summer.

RESPONSE: Thanks for your advice. Based on your suggestions, we have now added the following information to the revised manuscript: (lines 286-290): "The advance of the WPSH in eastern China occurs in June and July, while gradual withdrawal of the WPSH occurs mainly in August, Type 1 and Type 2 represent normal WPSH characteristics during early and late summer. Type 3 and Type 4 could reflect a split of the WPSH, which mainly occurs in late summer.".

14. Line 260: Type1 mainly occurs in June and it explains why the O3 concentration is higher.

RESPONSE: Yes.

15. Line 295: Please show the spatial distribution of the co-occurring surface O3 and PM2.5 pollution under each SWP.

RESPONSE: The spatial distributions of the co-occurring surface O_3 and $PM_{2.5}$ pollution under impacts of each SWP are shown in Fig.12.

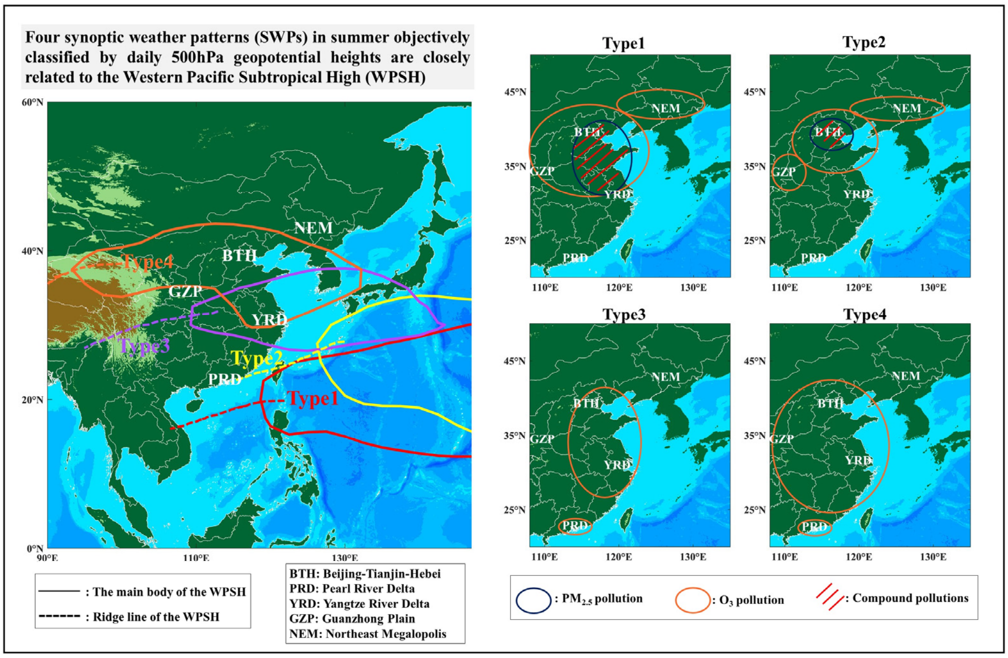

Fig. 12. Schematic diagrams describing the relationships between the WPSH, four SWPs and summertime O_3 and $PM_{2.5}$ pollution in various regions.

16. Line 300: Potential meteorological factors should be included in the results of this paper.

RESPONSE: Thanks for your suggestion. We have now moved the corresponding information to the "Result" section. Please refer to lines 347-376 on pages 13-14.

17. Line 305-310: This part should be mentioned in introduction.

RESPONSE: Thanks for the comment. We have moved this part to the introduction. Please refer to lines 93-110 on pages 4-5.

18. Line 315-316: It is because the type 1 mainly occurs in early summer.

RESPONSE: We have added more information to describe the occurrence of type 1 in early summer (lines 363-364, page 13).

19. Line 365: Figure S6 shows probability of occurrence of compound pollution days under all four types. Please show the situation under type1.

RESPONSE: The situation under Type 1 and Type 2 are shown in Figure S10.

Figures and tables:

1. Figure 2 and 3: Please Mark the heavy polluted cases with dark color.

RESPONSE: Replotted.

2. Figure 4: Please draw the ridgeline of the subtropical high.

RESPONSE: Replotted.

3. Figure 8 and Figure 11: Please compare the difference of daily mean values. An introduction of daily variations makes things difficult to follow.

RESPONSE: Thanks for your kind suggestion. We have changed Fig. 8 to daily anomalies variation of O_3 and $PM_{2.5}$ under impacts of four SWPs over key urban clusters (Fig. 7). Additionally, original Fig. 8 has now been updated to Fig. S5 instead. Original Fig. 11 has now been the revised Fig. 10, with add average value adding to the revised figure.

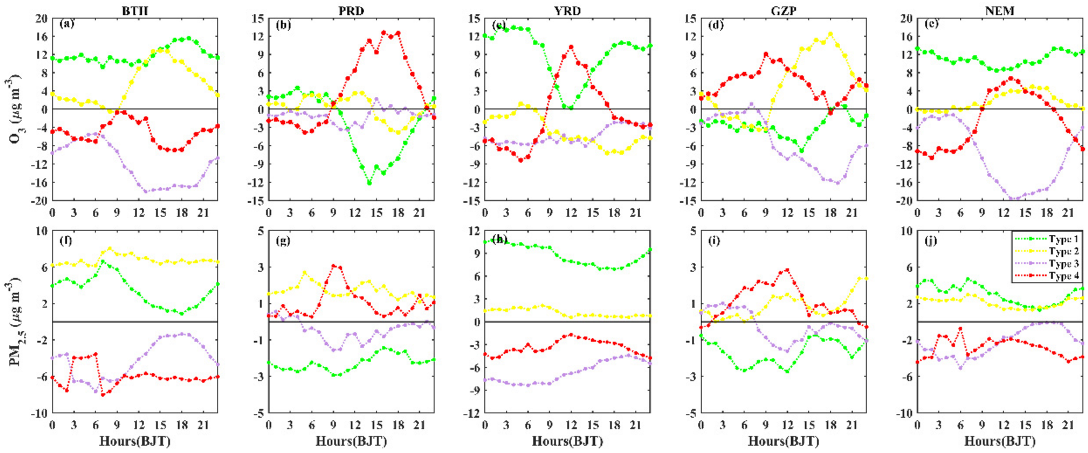

Fig. 7. Daily anomalies variation of O_3 and $PM_{2.5}$ under four SWPs in key urban clusters. The black solid line presents the averaged value of each urban cluster.

Anonymous Referee #3:

The authors use the T-mode PCA to objectively classify the summertime synoptic weather pattern across East-Asia and the western Pacific Basin aiming to identify the mode(s) most favorable for compound pollution events across sub-regions in China, specifically for PM2.5 and O3. Many factors governing these events operating across an array of scales are explored. The PCA identified 4 synoptic regimes characterizing the seasonal set up of the 500 hPa WPSH from 2015-2018. An additional large-scale circulation is also at work here, the East-Asian monsoon, which is discussed in context to the WPSH. Additionally, the authors discuss the effects of precipitation frequency and boundary layer characteristics on regulating compound pollution events. Occurrences of pollution are based on Chinese governmental standards.

While this work has great upward potential to be a significant contribution to the community, many revisions are required before publication.

RESPONSE: We highly appreciate your positive and constructive comments.

Secs. 1-2 are written quite well and motivate the questions at hand. Beyond that however, I believe that more concrete connections can be and must be made between processes unfolding at different scales (synoptic down to the mesoscale) of motion that lead to Types 1 and 2 dominating the regulation of compound pollution events. For instance, connecting the modulations in the WPSH to changes in favorable PBL conditions and thermal stratification need to be made, in addition to changing precipitation amounts between the types. All of these processes dictate the amount of pollution in the atmosphere at any given time. The final sentence of Sec. 1 states that this manuscript will examine the SWPs responsible for co-occurring pollution events, but the synoptic scale processes have bearing on finer scale processes such as PBL characteristics that are critical for air quality (e.g. inversions associated with tropospheric sinking motion). The authors analyze changes in PBL height between the types and provide loose discussion of their implications for air quality, but further analysis is needed.

RESPONSE: Thank you for valuable comments. Yes, our motivation is to demonstrate the causes of meteorological processes of the compound O_3-$PM_{2.5}$ pollution, as it is believed that the processes should be likely associated with local meteorological conditions (e.g., temperature, wind, humidity, rainfall, and PBL) under the influences of various weather types and modulation of large-scale WPSH movement. In addition, the impacts of PBL characteristics on air quality have been further discussed (lines 414-424 on page 15).

Please refer to the following information for more details:

"Particularly, Type1 has a significantly warmer temperature over the boundary layer during the compound pollution period of BTH region than that of the clean period. The daytime BLH under compound pollution condition was also higher than that of the clean condition. In addition, there were different directions of prevailing during the two periods, which prevailing winds during the compound pollution period were usually southward and could be driven by air pollutants transported from the southern plains (Fig. 11; see also Miao et al., 2019b, 2020). Co-influencing by the topographical effect of the northern mountainous areas, air pollutants could be trapped in the BTH region. In comparison, although there was southward wind prevailing in the BTH region (Figs. 11 and S11), the rain belt also located in the southern area of BTH might lead to the potential removal of $PM_{2.5}$ (Fig. 9j). Therefore, compound pollution across the BTH region might mainly be due to local emissions of air pollutants."

Major comments:

1. The abstract needs to be shorted and be more specific.

RESPONSE: We have reorganized the abstract. Our abstract has been revised as follows: "Surface ozone (O_3) pollution during summer (June-August) over eastern China has become more severe, resulting in a co-occurrence of surface O_3 and $PM_{2.5}$ (particulate matter with aerodynamic diameter ≤ 2.5 μm in the air) pollution recently. However, the mechanisms regarding how synoptic circulation pattern could influence this compound pollution remains unclear. This study here applied the T-mode principal component analysis (T-PCA) method is used to objectively classify the occurrence of four synoptic weather patterns (SWPs) over eastern China, based on the geopotential heights at 500 hPa during summer (2015-2018). Four SWPs of eastern China are closely related to the western Pacific subtropical high (WPSH), exhibiting, significant intraseasonal and interannual variations. Based on the ground-level air quality and meteorological observations, remarkable spatial and temporal disparities of surface O_3 and $PM_{2.5}$ pollution were also found under the impacts of the four SWPs. Particularly, there were two SWPs sensitive to compound pollution (Type 1 and Type 2). Type 1 is characterized by a stable WPSH ridge with axis at about 22°N and the rain belt located in the south of Yangtze River Delta (YRD). High temperature, moderate humidity and low precipitation occurred in the region from BTH to northern YRD (BTH – NYRD), resulting in a co-occurrence of O_3 and $PM_{2.5}$ pollution. Additionally, air pollutants can be transported by the prevailing southerly winds from southern plains and accumulated in the southern BTH, resulting in a worsen pollution. Type 2 exhibits a WPSH dominance (the ridge axis ~25°N) and rain belt (over the YRD) in a higher latitude compared with Type 1. High temperature, medium-high humidity and low precipitation over the BTH were the conducive factors related to the occurrence of the compound pollution events under Type 2. Furthermore, low boundary layer height (BLH) and high frequency of light-wind days (FLWD) could create favorable conditions for pollution maintenance. Overall, synoptic weather patterns have played an important role as driving factors of surface O_3-$PM_{2.5}$ compound pollution in a regional context. In addition to the impacts of local emissions, our results may provide further insights regarding how regional environmental changes due to co-occurrence of high $PM_{2.5}$ and high O_3 level may be driven by the effects of meteorological factors. Overall, our findings demonstrate the important role played by synoptic weather patterns in driving regional surface O_3-$PM_{2.5}$ compound pollution, in addition to the large quantities of emissions, and may also provide insights into the regional co-occurring high $PM_{2.5}$ and high O_3 level via the effects of certain meteorological factors.".

2. How do the percentages of the PCs sum to 100%? Shouldn't there be other relevant synoptic patterns than just those 4, meaning that the leading 4 patterns account for most of the synoptic-scale pattern but not all?

RESPONSE: Thanks for your question. By using T-PCA, users can customize the number of synoptic patterns and determine the domain pattern(s), based on the following information: 1) a distinct direction of the air flow and its related short-term changes, 2) a regime of the pressure field (and vertical movements resulting from the field), 3) particular pattern(s) of front passages, and 4) an inflow of air masses of a particular origin and their related changes.

Based on the above method, the similarity of circulation pattern of each day to a particular type expressed by the corresponding loading(s), the greater similarity is expected between the day's type and the pattern(Huth, 1996). Therefore, no matter how many synoptic patterns are predefined, the sum of PCs could be 100%. The final number of patterns is determined by ΔECV, which larger ΔECV means an improved classification performance with stability (Ning et al., 2019). In our study, the highest ΔECV was used to classify to the four patterns. More information has been noted in the supplementary materials.

Reference:

Huth, R.: An intercomparison of computer-assisted circulation classification methods, Int. J. Climatol., 16(8), 893–922, doi:10.1002/(SICI)1097-0088(199608)16:8<893::AID-JOC51>3.0.CO;2-Q, 1996.

3. The language used to describe the synoptic scale features needs to be presented in a manner consistent with meteorological standards (see Bluestein 1992). In its present form, it is very difficult to follow the discussion. Here is an example. On lines 226-227, the authors state "The westward extension and southward motion of the WPSH in Type 1, as shown in Fig. 4a, transports water vapor into the YRD region, and the prevailing southwesterly in the YRD region and westward flow from the north form a cyclonic convergence area, with high temperature and high humidity during the Meiyu season." The 850 hPa flow associated with each PC correlates highly with the gradient in 500 hPa GH as rather expected, but what is meant by "southward motion of the WPSH?" Are the authors referring to the anticyclonic flow about the WPSH (i.e. northerlies to the west of the GH maximum)? Also, the sign of the relative vorticity should differ with height in the troposphere. For instance, should vorticity be negative in the lower troposphere (i.e. anticyclonic), it should be positive (i.e. cyclonic) in the upper troposphere (assuming a thermally direct circulation on a rotating sphere). Are the authors referring to the cyclonic shear vorticity anomaly apparent in the 850 hPa arrows around 120E/30N? The authors should use GH anomalies as reference points to describe the flow patterns, and they should make sure that it is clear which level in the atmosphere is being referenced in the text. More examples are given below.

RESPONSE: Thank you for your valuable suggestions. We apologize for the unclear descriptions regarding the location of the WPSH. More information regard to the location of the WPSH has now been reported in Table S2 of the revised manuscript. Following your suggestion, we have deleted the following word "cyclonic". We have also reworded the description of synoptic scale's features carefully (lines 266-274: "The location of western ridge point and northern boundary of the WPSH at 500 hPa in Type 1 is around 120°E and 30°N, respectively (Fig. 4a and Table S2). The southwestern flow of this WPSH could transport water vapor to the YRD region, resulting in a southwestward prevailing wind across the YRD region and westward flow from the north of the WPSH forming a convergence area at 850 hPa. These conditions were also associated with high temperature and humidity during the summer with Meiyu season, which Meiyu season is a climate phenomenon with continuous cloudy and rainy days generally occurring during June and July every year in the middle and lower reaches of Yangtze river, Taiwan of China, central/southern Japan, and southern Korea.".

4. Sec. 3.2: I feel as though the discussion of the PCs could be tied more explicitly to the vertical motion field. Obviously, the WPSH is characterized by mid-tropospheric downward vertical motion and doesn't need much justification. However, the strength of the sinking motion and its co-occurrence with low wind events is driven by the synoptic pattern and could be shown. I would suggest at least a supplemental figure showcasing how the vertical motion varies with PC, perhaps overlaid with the 10-m windspeed. This would set up the next section nicely, which returns to examining the spatial characteristics of PM2.5 and O3.

RESPONSE: We appreciate these valuable suggestions. We have now added supplementary information for the vertical motion under impact of four SWPs, and latitude-height cross-sections of mean and anomalous vertical velocity averaged by longitudes over each region under four SWPs. in (Fig. S9). The strong updrafts and positive anomalies, which occurred in some regions (south YRD under Type 1, BTH and GZP under Type 3), is favorable for the formation of precipitation to decrease air pollution. In particular, the downward vertical motion and negative anomalies over BTH under Type 1 and Type 2 are associated with the co-occurrence of O_3-$PM_{2.5}$ pollution.

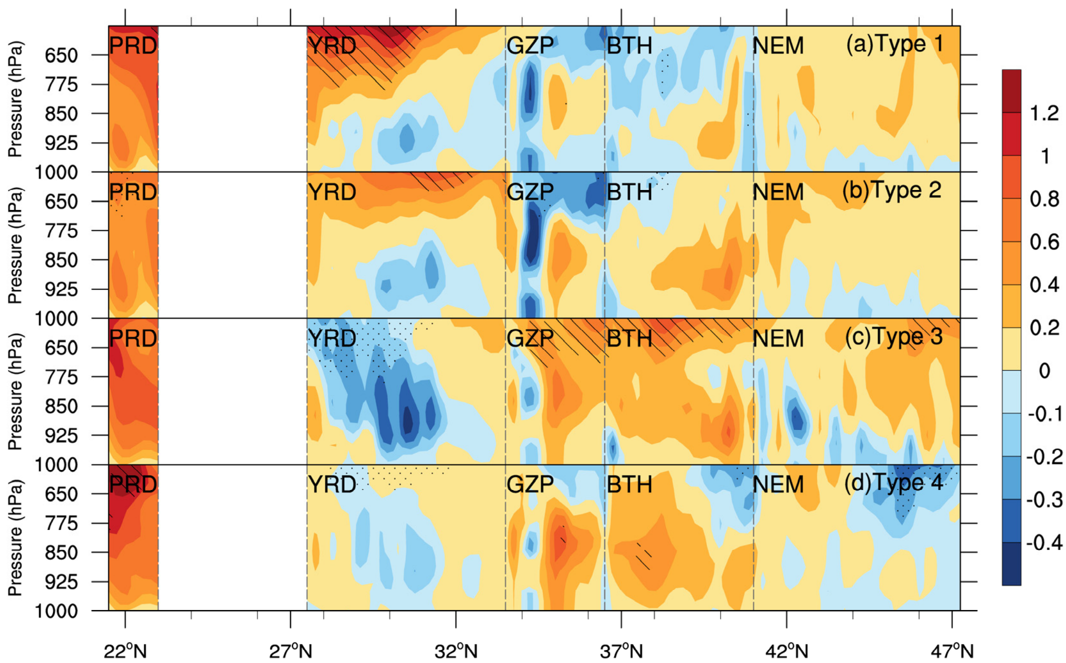

Fig. S9. Vertical cross-sections of the means (shading) and anomalies (filled patterns) of vertical velocity (unit: 10^{-2} m s^{-1}, derived from ERA5 reanalysis data) averaged by longitudes over each region of (a) Type 1, (b) Type 2, (c) Type 3, and (d) Type 4. The dotted and hatched areas represent the negative anomalies less than -3×10^{-2} m s^{-1} and positive anomalies greater than 3×10^{-2} m s^{-1}, respectively. The gray dashed lines indicate the boundaries of PRD, YRD, GZP, BTH and NEM, and the blank area (23°-27.2°N) is not our study region.

5. Diffusion of pollutants between the PBL and the free atmosphere is fundamentally related to the turbulent mixing and thermal stratification of the overlying atmosphere. While referenced here, I believe that this is an integral component of this work and must be explicitly addressed across the various subregions. How do the vertical profiles of temperature, moisture, and wind compare across the multiple PCs and subregions? How are these anomalies physically related to the different

synoptic weather pattern differences between the PCs?

RESPONSE: Thank you for your comments. The vertical profiles of temperature, moisture, and wind, as well as their anomalies under sub-regions of each SWP are provided in Fig. S8. Lower WS and its negative anomalies at low level over BTH under Type 1 and Type 2, is not conductive to the diffusion of pollutants. Meanwhile, the moderate RH and its negative anomalies also favor the formation of compound pollution. For GZP, Type 1 and Type 2 correspond to negative anomalies of WS and RH, favoring the occurrence of compound pollution. Note that the probability of compound pollution is relatively small, and it might be related to the local emissions. In other sub-regions, WS mainly affects the diffusion of air pollutants, and precipitation affects the occurrence of ozone and $PM_{2.5}$ pollution to a certain extent.

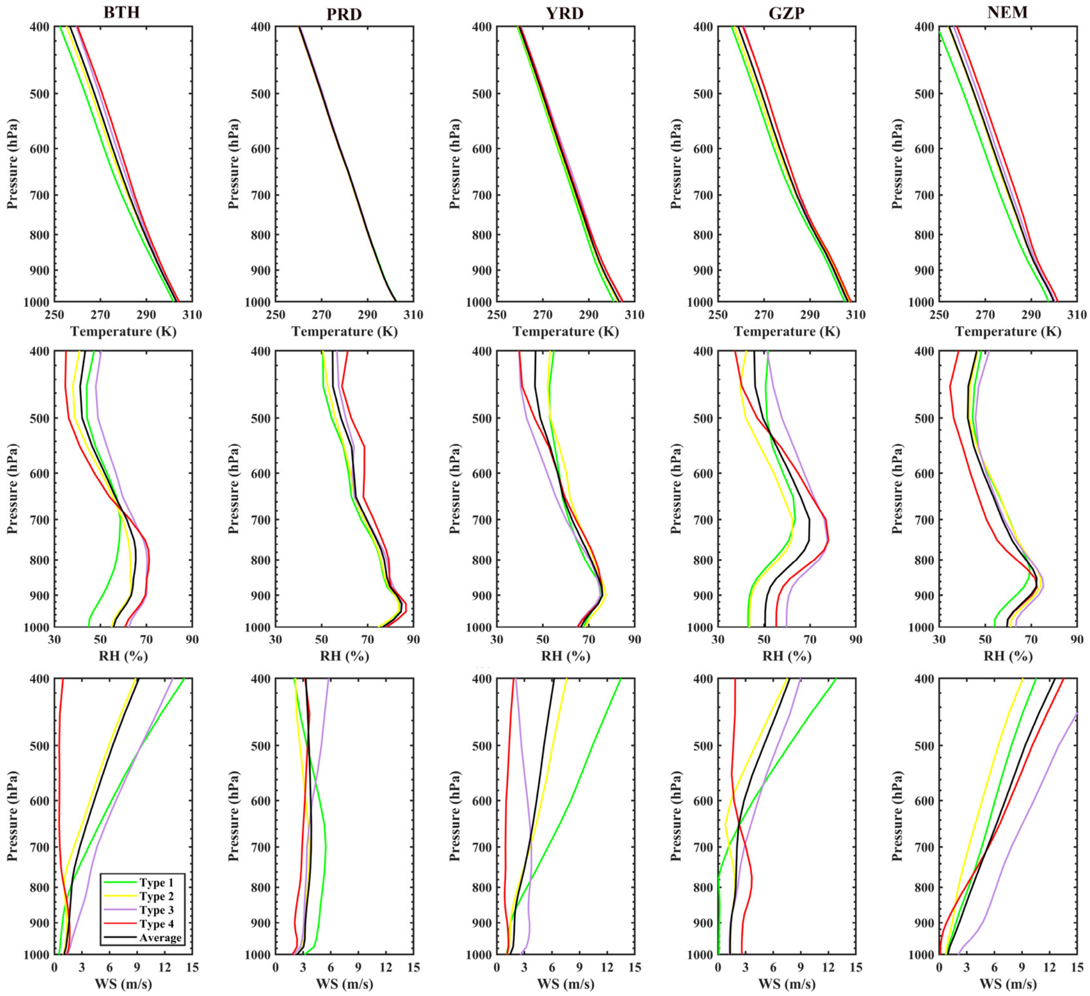

Fig. R5. The vertical profile of temperature, RH, WS (derived from ERA5 reanalysis data) over subregions under each SWP.

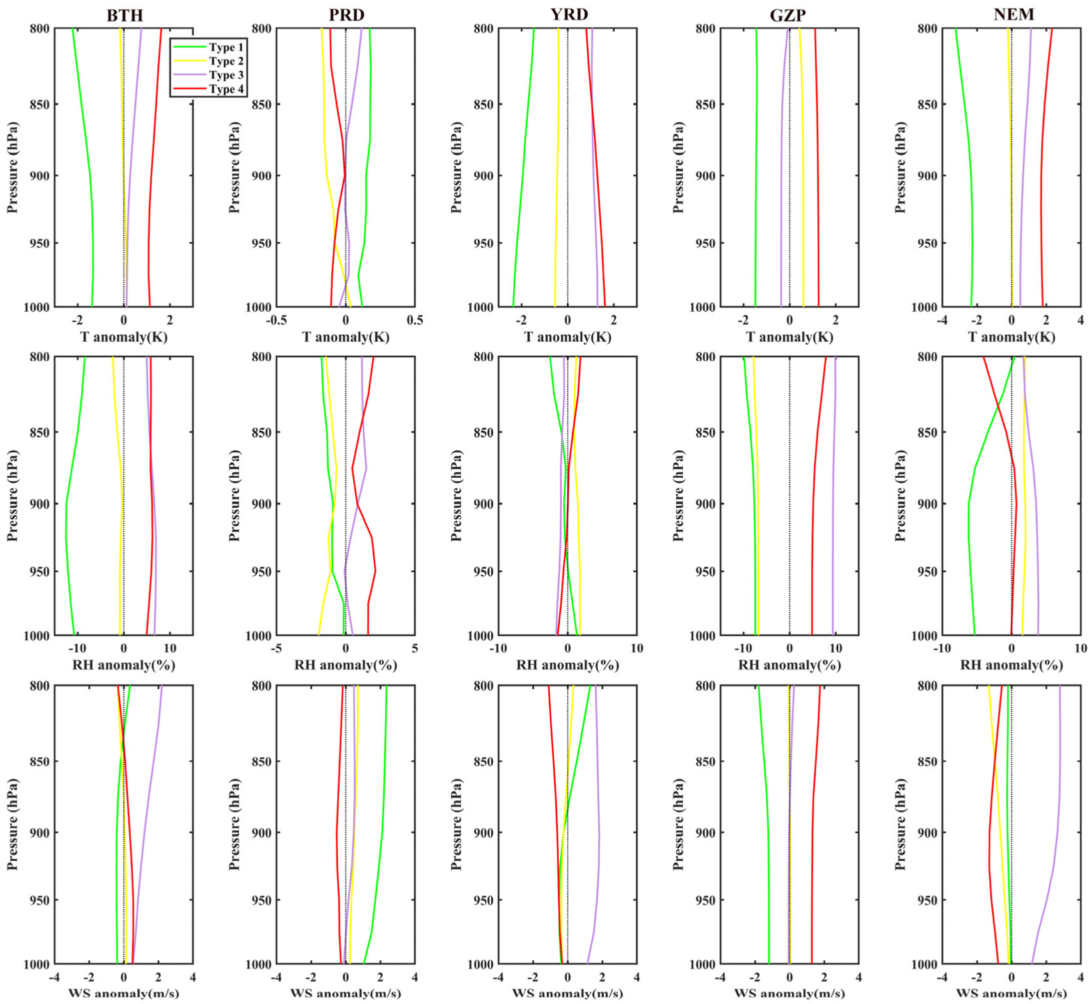

Fig. S8. The vertical profile of temperature, RH, WS anomalies over subregions under each SWP.

Other comments:

1. Line 32: “Slight” should be “low”

RESPONSE: Changed and thanks.

2. Line 57: insert a “the” before “economy”

RESPONSE: Inserted and thanks.

3. Line 72: Change “attached” to “caught”

RESPONSE: Changed and thanks.

4. Line 85: “US” should be “United States”

RESPONSE: Changed and thanks.

5. Line 105: The Miao et al. findings should be reproducible here but for a multitude of areas. Cross-sections similar to their Figs. 6-7 would work, but regionally averaged vertical profiles would work as well. Vertical profiles of state variables (temperature, stability, vertical velocity, etc.) should be included in this manuscript as these quantities’ vertical variation help to significantly modulate PBL and free atmosphere exchange of heat, moisture, pollution, etc. I would also suspect that summertime surface winds would be lower due to more infrequent midlatitude cyclone occurrences, so pollution “pooling” would be more frequent.

RESPONSE: Thank you for your suggestion. Similar analysis as the Figs. 6-7 of Miao et al has been added to the revised manuscript (lines 402-425 on page 15 and Fig. 11). Vertical profiles of state variables are presented in Fig. S8.

Please also find the information as follow:

"In the last section, we have discussed how the SWPs and local meteorological factors modify summer O_3 and $PM_{2.5}$ pollution. However, how does the boundary layer structure interact with the co-occurrence of O_3-$PM_{2.5}$ pollution? In order to address this question, we conducted a further analysis. As mentioned, co-occurrence of O_3 and $PM_{2.5}$ pollution were mainly found in the BTH – NYRD under Type 1 and over BTH region under Type 2. Lower WS and its negative anomalies at lower boundary layer over BTH– NYRD under Type 1 and over BTH under Type 2 may not enhance the diffusion of air pollutants (Fig. S8). In contrast, moderate RH and its negative anomalies might favor the formation of compound pollution. Downward vertical motion and negative anomalies could also stabilize the atmospheric characteristics of boundary layer (Fig. S9). Furthermore, we summarized boundary layer structure, precipitation, and ground-level wind flow across the BTH region. Based on the characteristics, we separately defined Type 1 and Type 2 into clean (both concentrations of the O_3 and $PM_{2.5}$ are less than polluted level) and compound pollution periods (Figs. 11 and S10-S11). Particularly, Type1 has a significantly warmer temperature over the boundary layer during the compound pollution period of BTH region than that of the clean period. The daytime BLH under compound pollution condition was also higher than that of the clean condition. In addition, there were different directions of prevailing during the two periods, which prevailing winds during the compound pollution period were usually southward and could be driven by air pollutants transported from the southern plains (Fig. 11; see also Miao et al., 2019b, 2020). Co-influencing by the topographical effect of the northern mountainous areas, air pollutants could be trapped in the BTH region. In comparison, although there was southward wind prevailing in the BTH region (Figs. 11 and S11), the rain belt also located in the southern area of BTH might lead to the potential removal of $PM_{2.5}$ (Fig. 9j). Therefore, compound pollution across the BTH region might mainly be due to local emissions of air pollutants."

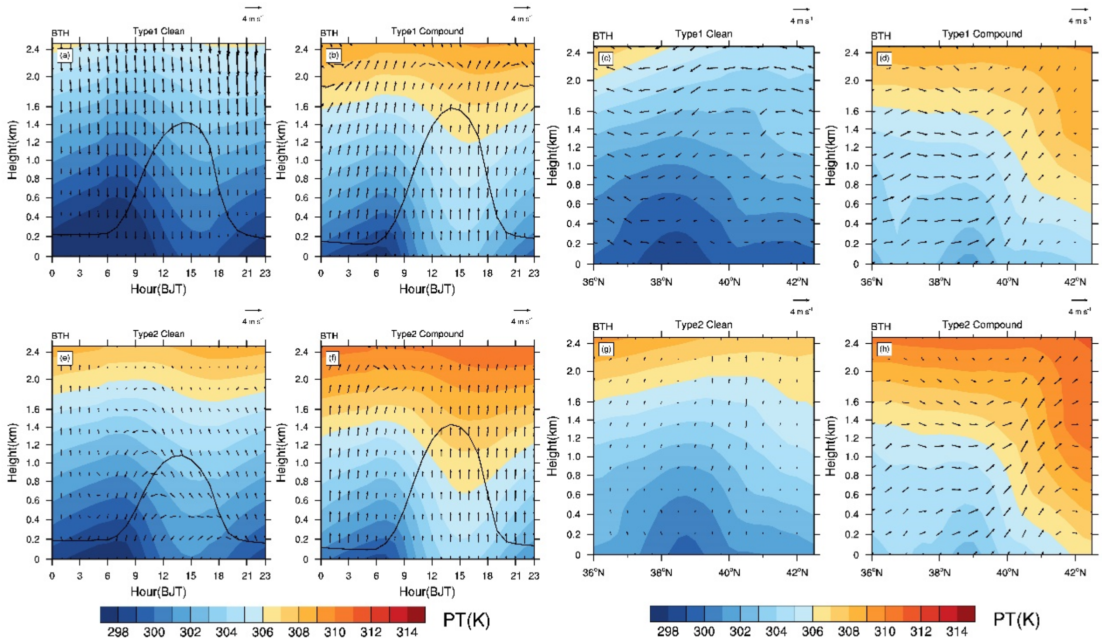

Fig. 11. The daily variation of horizontal wind, potential temperature (PT) and BLH of boundary layer in the BTH under clean and compound pollution period of Type 1 and Type 2 (a, b, e, f). The vertical cross-section of u-wind, w-wind and PT for the same situation of BTH (c, d, g, h). The w-wind is multiplied by 100 when used. The data has been derived from ERA5 reanalysis data.

6. Lines 146-147: Subregions should be labeled in a figure to orient the reader. This can be done in panel (a) of Fig. 1.

RESPONSE: Revised.

7. Fig 1.: There is no "red box"? If there is, it is not clear

RESPONSE: We have changed to the "black box".

8. Figs. 2 and 3: Please change the color of "heavily polluted" regions to something other than turquoise. It can easily be misinterpreted as a "good" category

RESPONSE: Changed.

9. Line 200: How is "pollution day defined" for O3? By the thresholds laid out earlier (160 ug/m3 threshold)? Also, what constitutes "moderate" pollution? Same question applies for PM2.5.

RESPONSE: The pollution levels of O_3 and $PM_{2.5}$ over each key area were verified according to the limit of air pollutant concentration, based on the Technical Regulation on Ambient Air Quality Index (on trial) (HJ633-2012) issued by the Ministry of Ecology and Environment of the People's Republic of China Specific standard limits are now shown in Table S1 of the supplementary materials.

Table S1. Thresholds for each pollution level of $PM_{2.5}$ and O_3-8h.

AQI	Pollution level	$PM_{2.5}$($\mu g\ m^{-3}$)	O_3-8h ($\mu g\ m^{-3}$)
0~50	Good	0~35	0~100
51~100	Moderate	36~75	101~160
101~150	Lightly polluted	76~115	161~215
151~200	Moderately polluted	116~150	216~265
201~300	Heavily polluted	151~250	266~800

10. Line 219-220: This low-level transport feature and its variation with PC is not shown in any figure but is referenced. I believe that at least one figure should show this feature since it is being discussed in forthcoming results

RESPONSE: The low-level transport feature is shown in Fig. 11.

11. Line 226: How can you infer that water vapor is being transported into the YRD regions? The 850-hPa flow vectors are at best directed parallel to the YRD coastline. Otherwise they are directed offshore. Additionally, inferences about moisture transport should be made by wind/water vapor overlays or by integrated vapor transport/moisture convergence analysis (see Rahimi et al. 2018), which this figure does not have.

RESPONSE: Thank you for your valuable suggestion. We added the water vapor flux (WVF) in Fig. 4. WVF denotes the direction and magnitude of atmospheric moisture transport, which is simplified as : WVF = $V*q/g$, where q is specific humidity, g is the gravitational acceleration (= 9.8 g/m^2), and V is the horizontal wind. It can be seen that the southwesterly flow transports sufficient water vapor to the YRD region.

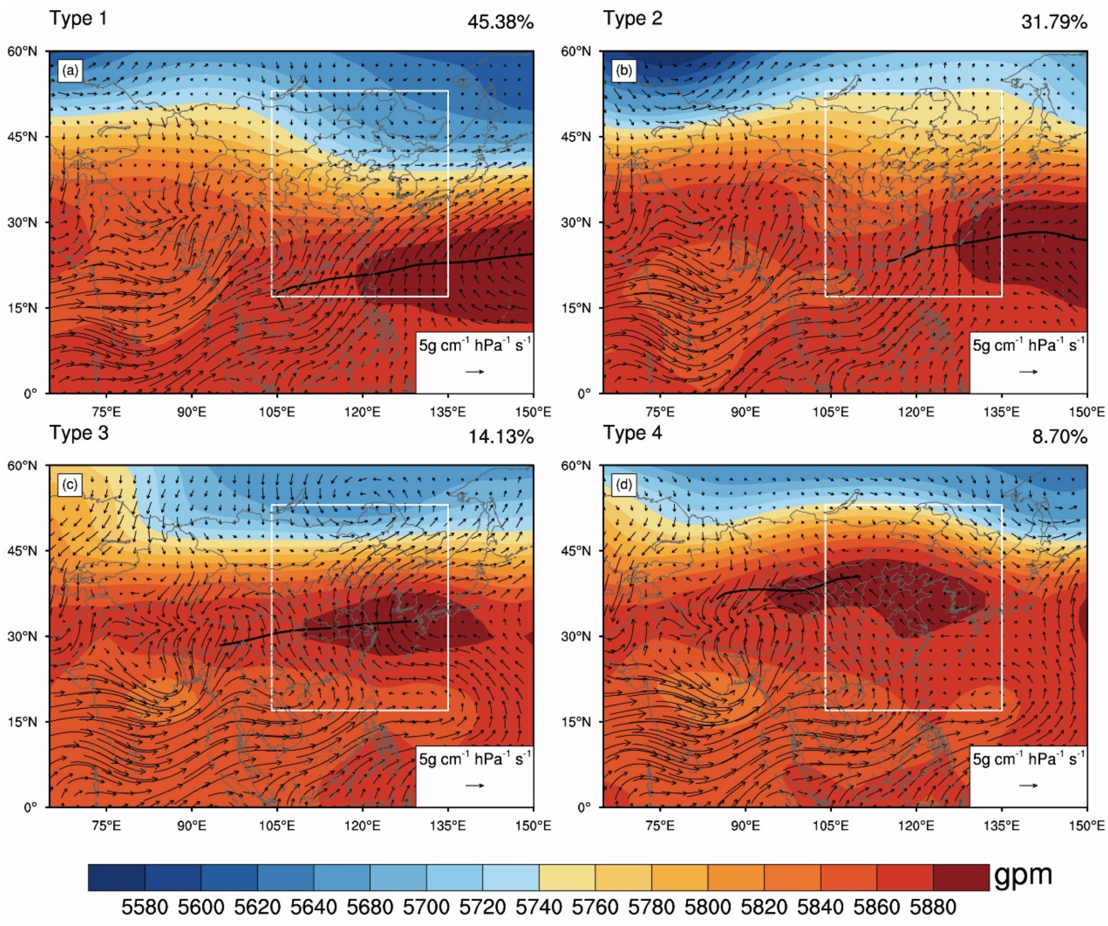

Fig. 4. 850-hPa water vapor flux (WVF =V*q/g, q is specific humidity, g is gravitational acceleration, V is horizontal wind; vectors; see scale arrow at the bottom right in units of 5 g $cm^{-1}hPa^{-1}s^{-1}$) and 500-hPa GH (contours; see scale bar at bottom in units of gpm) patterns based on objective classification (see text for details). White box area is for the area of eastern China, the number at the upper right corner of each panel indicates the frequency of the occurrence of each pattern type, the black line of each panel presents the ridge axis of the WPSH.

12. Line 227: Flow shifting from southwesterly to westerly with northward extent is anticyclonic, which we see in the figure. At the same time, we see a cyclonic sped shear maximum, so it is impossible without quantifying the vorticity explicitly to say if this is anticyclonic or cyclonic. Please remove “cyclonic.”

RESPONSE: Thanks for your comment. Removed.

13. Line 229: Is it the WPSH retreating or advancing? Its axis appears to shift north slightly. . .

RESPONSE: The WPSH shifts northward slightly from Type 1 to Type 2; and it retreat southeastward from Type 3 to Type 2. Thanks for the suggestion and we have now revised the content (Lines 274-275 on page 10).

14. Line 230: Consider deleting, “and the GH over northern China at 500 hPa is higher compared with Type 1 (Fig. 4b).” The change in the magnitudes of GH are not terribly important; it is the change in their gradients that regulates the winds in each PC. Line 231: The only Type 2 onshore flow (at 850 hPa) I see is around 120E by 30N, which lies directly west of the Type 2 GH maximum. This is an example of how you can use certain language relating flow properties to GH anomalies

for specific PCs. Currently the authors state, ". . .southerly wind blowing from the ocean to the continent lies in front of the bottom of the high pressure,. . .", which is very unclear. More generally, I recommend the authors refrain from using "top" and "bottom" unless they are referring to the vertical axis (i.e. up and down).

RESPONSE: Thank you for your comment. The related sentence in Line 230 has been deleted. We also changed ". . .southerly wind blowing from the ocean to the continent lies in front of the bottom of the high pressure,. . ." to "The southerly wind from the ocean could interact with northern periphery of the WPSH".

15. Line 233: "and the rain belt moves northwards to the east of the YRD region." Are the authors referring to the belt as it compares to other PCs? If so, the different PCs may be compared to one another, but it is not guaranteed that any type will necessarily evolve from another type. Please clarify and reword throughout the text.

RESPONSE: Thank you for your suggestion. We have reworded the descriptions for the rain belt and plotted the rain belt in Fig. 8 (i-l). The discussion about rain belt is moved to Sec.3.4 as follows:

"Type 1 is characterized by humid condition in the southern area and dry condition in the northern region owing to an extensive southwestern flow of the WPSH, resulting in a rain belt found in southeastern coastal area such as PRD and YRD regions. Type 2 is associated with meridional flow and dry and wet anomalies in northern China, resulting in a rain band locating at the central areas of between BTH and YRD regions due to the northern advance of the WPSH compared with Type 1. Furthermore, there is a greater RH for most of the study sites under Type 3 and Type 4, possibly a result of the shifted rain belt in the BTH and NEM regions under Type 3 once the northern boundary of the WPSH reaching at 37.5°N, and an occurrence of heavy precipitation across the western PRD region as well as central areas of between BTH and YRD regions under Type 4 (Fig. S6)".

16. Lines 237-238: ". . .which implies that the rainy season in the YRD region ends in midsummer and the weather becomes hot and dry." How is this implied? 850-hPa flow is onshore beneath the western edge of the 500 hPa monomer of the WPSH. This linkage is not implicit and should be explained. Moreover, references made to shifts in precipitation need to be explicitly shown if they are going to be frequently referred in the text.

RESPONSE: We appreciate your advice. We have revised this sentence as follow: "This has led to a condition completely controlled by the monomer of the WPSH over the YRD region, resulting a hot and dry weather at the end the rainy season at the beginning of mid-summer.". As for rainy season, we have determined the location of the rain belt based on the amount of precipitation and PF under each SWP, which can be seen at Fig.8(i-l).

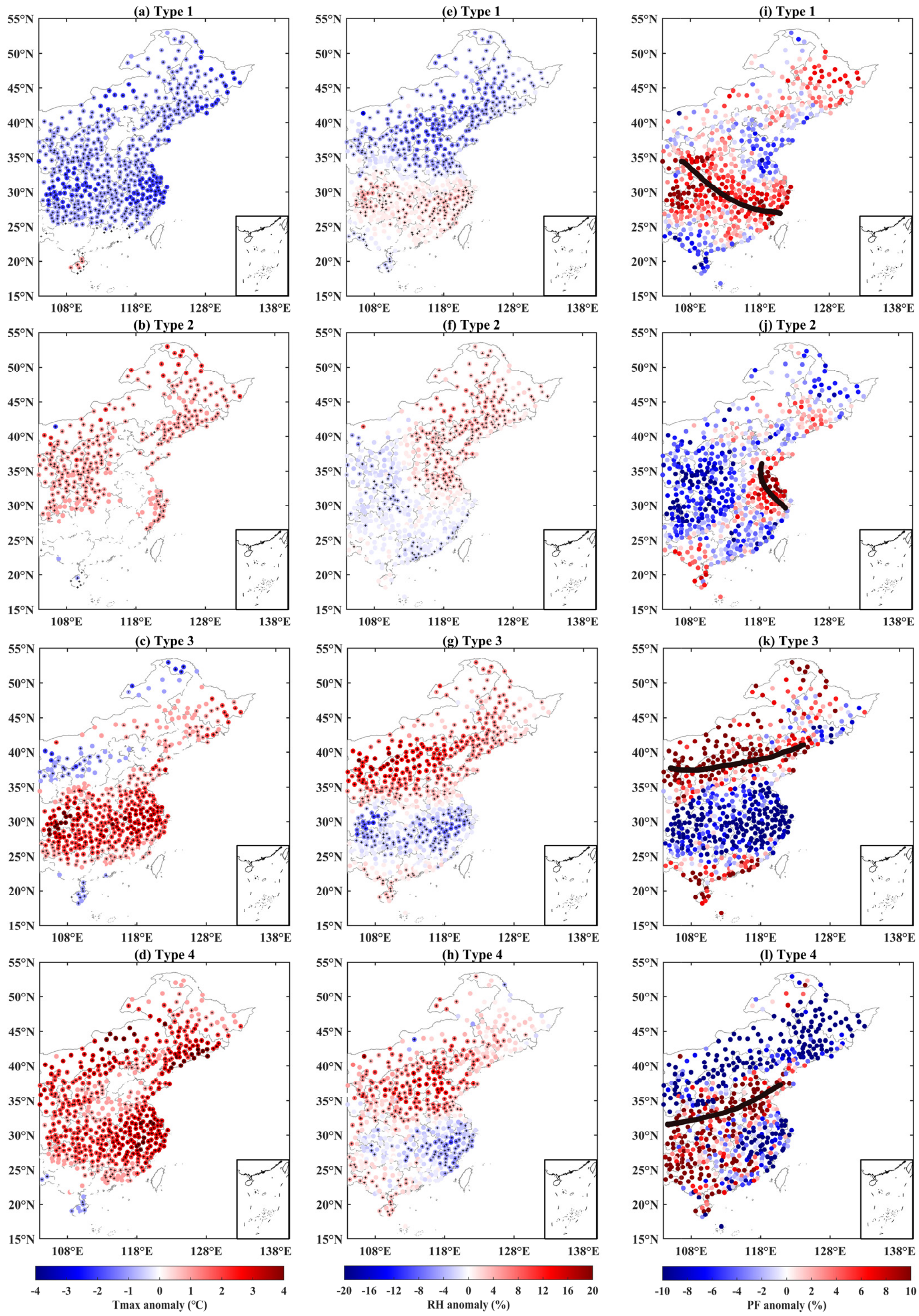

Fig. 8. Same as Fig. 6 but for Tmax (a–d), RH (e–h), and PF (i–l). The black solid line presents the rain belt of each SWP.

17. Lines 239-240: "continues to extend westwards and shift northwards," shifts westward and northward compared to PC3. Again, please indicate it's the synoptic pattern's position more explicitly. Something like, "In Fig. 4d, the monomer is located north and west of the feature in Fig. 4c". The word accordingly relates this sentence to the previous one, but it isn't clear what that

linkage actually is. Also, please explain the linkage or remove the word "accordingly."

RESPONSE: This sentence has been changed as follow: "Figure. 4d indicated that the location of WPSH monomer was more western and northern with respect to other SWPs, controlling the northern China for a long time; the western ridge point was around 95°E and the northern boundary was around 40°N.".

18. Line 241: Heat wave? How is PC4 related to a heat wave? Where is this shown in the figures or analyses?

RESPONSE: Sorry for the confusion. The words related to "heat wave" have now been removed from this sentence.

19. Figs 3-4: How are levels of air quality defined? Are they arbitrary? If so, then a brief justification is required. If they are a community standard, then a source is needed.

RESPONSE: The pollution levels of O_3 and $PM_{2.5}$ over each key area were verified according to the limit of air pollutant concentration, based on the Technical Regulation on Ambient Air Quality Index (on trial) (HJ633-2012) issued by the Ministry of Ecology and Environment of the People's Republic of China Specific standard limits are now shown in Table S1 of the supplementary materials.

20. Fig. 4 shows the PCs of the synoptic weather pattern and associated percentages of occurrence for the study period.

RESPONSE: Yes.

21. Fig. 5: 2017 is labeled twice. Should the second instance be 2018?

RESPONSE: Revised and thanks.

22. Line 263: Any hypothesis for why the lowest MDA8O3 occurs for PC3? Could it be related to the synoptic pattern of Fig. 4 and associated precipitation (not shown)?

RESPONSE: The analysis of light O_3 pollution under Type 3 is revised as follow (lines 448-455 on pages 16-17):

"High temperature, low humidity and few precipitations over the YRD region tend to generate a large amount of O_3, while the positive BLH and negative FLWD anomalies are unfavorable to O_3 accumulation. On the other hand, summer typhoon activities might weaken the WPSH intensity over the YRD region, leading to the eastward retreat and northward shift of the WPSH. As a result, high WS across coastal areas could ease the ground-level O_3 pollution (Shu et al., 2016). For the BTH and PRD regions, high PF tends to suppress O_3 production. Only 6.8% of the compound pollution occurrence days at all sites occurred under Type 3, in accordant with the light O_3-only pollution over the areas of the BTH, YRD and PRD (Fig. 12)."

23. Line 279: Delete "in the eastern region"

RESPONSE: Deleted.

24. Fig. 8, Lin3 285: What constitutes "serious?" Perhaps it would be good to plot the pollution threshold values here for O3 and PM2.5. Plotting these curves (they would be straight lines) would help the reader to identify how bad (or good) the air quality actually is in terms of PM2.5 and O3. The authors discuss "over-standard" rates, so a threshold must have been used (plot it). I believe these values are 160 and 75 ug/m3 for O3 and PM2.5, respectively. . .

RESPONSE: We appreciate your comment. The threshold values of O_3 and $PM_{2.5}$ for "over-standard" refer to the 24-h concentrations, and we explained the threshold values for O_3 and $PM_{2.5}$ in the Data and methods as "Based on the Ambient Air Quality Standards (GB3095-2012) issued by the Ministry of Ecology and Environment of the People's Republic of China,

O_3 ($PM_{2.5}$) pollution occurs when the MDA8 O_3 ($PM_{2.5}$ 24-h) concentration exceeds 160 (75) μg m^{-3}." In order to more clearly compare the concentration differences under different SWPs in various regions, we have changed the Fig. 8 to daily anomalies variation.

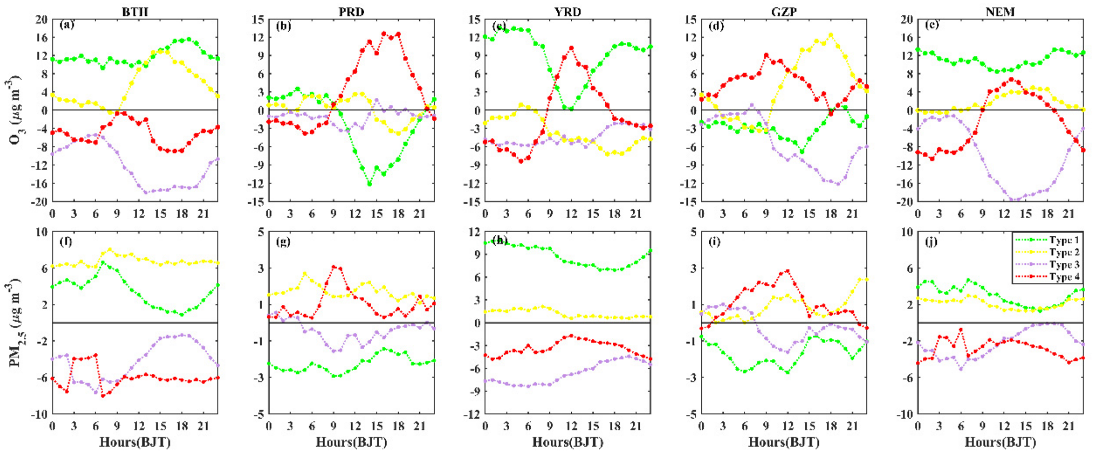

Fig. 7. Daily anomalies variation of O_3 and $PM_{2.5}$ under four SWPs in key urban clusters. The black solid line presents the averaged value of each urban cluster.

25. Line 286: For (2), over-standard rates are not plotted – concentrations are. Please clarify. If the authors are suggesting that O3 an PM2.5 concentrations are similar between PCs, then please reword.

RESPONSE: The over-standard rates are shown in Table 1. Reworded it to "in the PRD region, the over-standard rates and concentrations of O_3 and $PM_{2.5}$ is similar under four SWPs".

26. Line 287: For (3), it looks like Type 4 is leading, not Type 1, for O3 concentrations from 0900-1500. Since this is when concentrations are largest, the "Type 1 > Type 4 > . . ." may mischaracterize your argument.

RESPONSE: The O_3 pollution over-limit ratio is calculated via stations* days, it presents as Type 1 > Type 4 > Type 2 > Type 3" in the YRD. But it is true that Type 4 is leading, not Type 1, for O3 concentrations from 0900-1500, this is because the daily variation is counted by regional average concentrations.

27. Line 302: "Activities"? Do the authors mean "modulations"? This is unclear..

RESPONSE: Thank you for the suggestion. We have now used "modulations" (line 87, page4) as suggested.

28. Line 308: "Makes summer always hot and moist" grammar needs revisions

RESPONSE: Revised. We changed it to "induces a hot and humid condition over the summer".

29. Line 316: "presents negative" should be followed by "(Fig. 9a)" to guide the reader. Also, why are Tmax anomalies negative under this PC?

RESPONSE: We have added the tags to guide the reader. The reason of negative Tmax anomalies under Type 1 is that Type 1 is always occurring early summer.

30. Lines 312-321: Precipitation is integral to the lifecycle of PM2.5 and O3. The linkages between the precipitation anomalies and Fig. 4 should be explicitly discussed. I believe the authors attempt to do this in Sec. 3.2, but that discussion is more appropriate here.

RESPONSE: Thanks for your advice. We have moved the discussion of precipitation to subsection 3.4. Please refer to lines 352-361 on page 13: "Type 1 is characterized by humid

condition in the southern area and dry condition in the northern region owing to an extensive southwestern flow of the WPSH, resulting in a rain belt found in southeastern coastal area such as PRD and YRD regions. Type 2 is associated with meridional flow and dry and wet anomalies in northern China, resulting in a rain band locating at the central areas of between BTH and YRD regions due to the northern advance of the WPSH compared with Type 1. Furthermore, there is a greater RH for most of the study sites under Type 3 and Type 4, possibly a result of the shifted rain belt in the BTH and NEM regions under Type 3 once the northern boundary of the WPSH reaching at 37.5°N, and an occurrence of heavy precipitation across the western PRD region as well as central areas of between BTH and YRD regions under Type 4 (Fig. S6).".

31. Lines 328-331: This sentence is unclear and should be revised. Also, there is an instance here where the authors use an acronym in one part of the sentence but not the other. Please be consistent. Also, how do negative FLWD anomalies result in a deeper PBL?

RESPONSE: Thank you for your comment. It has been revised to "As can be seen from Fig. 9, when the BLH has a positive anomaly, on the contrary FLWD has a negative anomaly (e.g., BTH in Type 1), which indicates the higher BLH, the lower FLWD, the more conducive to the diffusion of pollutants, otherwise, lower BLH and higher FLWD (BTH in Type 2) do not support the diffusion.". The averaged WS would be higher when negative FLWD anomalies, usually the BLH is higher in this case.

32. Sec. 4.1, P3: I believe that stability should be discussed here in addition to a more detailed discussion of precipitation "anomalies" associated with each PC. Thermal stratification of the PBL will dictate the mixing depth of the PBL and thus regulate the pooling of these aerosol/pollution plumes. Looking at the correlation between Tmax, PF, FLWD, etc. is not enough.

RESPONSE: Thank you for your suggestion. The stability discussion is linked to thermal stratification of the PBL in Sec. 4. Please refer to the response to major comments 3 of referee #1 and major comments 4-5 of yours.

33. Lines 346-349: Here is a wonderful chance to discuss what is special about PC4 on a synoptic level. Why is PC4 leading to the largest O3 events synoptically? Do these same conditions favor the co-occurrence of O3 and PM2.5?

RESPONSE: We appreciate your suggestions. We have discussed these questions in the Discussion as follows:

"High temperatures, medium-high humidity and few precipitations in the GZP and PRD regions can cause O_3-$PM_{2.5}$ compound pollution, but $PM_{2.5}$ pollution in the both regions is are not heavy, which is possibly in relation to local lower pollutant emissions. The probability of compound pollution occurrence under Type 4 is about 5.1%. Under the control of the WPSH, there are strong photochemical reactions at high temperatures and little rainfall in some eastern region (such as North BTH, YRD), which is also conducive to O_3 generation (Fig. 12). Meanwhile, relative to Type 1, O_3 pollution is lighter in the BTH, due to the differences of RH, BLH and FLWD."

34. What is the difference between the Yangtze River and the YRD? These should be labeled on a map for readers. . .

RESPONSE: It should be "YRD" there.

35. It seems as though there is a window of moisture availability that is large enough to allow

hygroscopic growth of PM2.5 but is sufficiently small to allow for the important photochemical processes that regulate O3. It would seem to me that identifying this moisture window, as well as its sensitivity to PCs, would be a very significant contribution and I recommend that it be studied further to more precisely identify the PCs responsible for co-occurring O3/PM2.5 events. Identification of this moisture window can be based on an optimal relative humidity for compound pollution events too. This window can change by region and PC type.

RESPONSE: Thank you for your valuable comment. We selected the BTH region, an area with high frequency of compound pollution, to analyze the RH condition under four period (compound pollution, clean, O_3-only, $PM_{2.5}$-only). Indeed, there is a moisture window here, higher RH would restrain the production of O_3, and lower RH would not favor hygroscopic growth of $PM_{2.5}$. The moderate RH is more conducive to the formation of compound pollution.

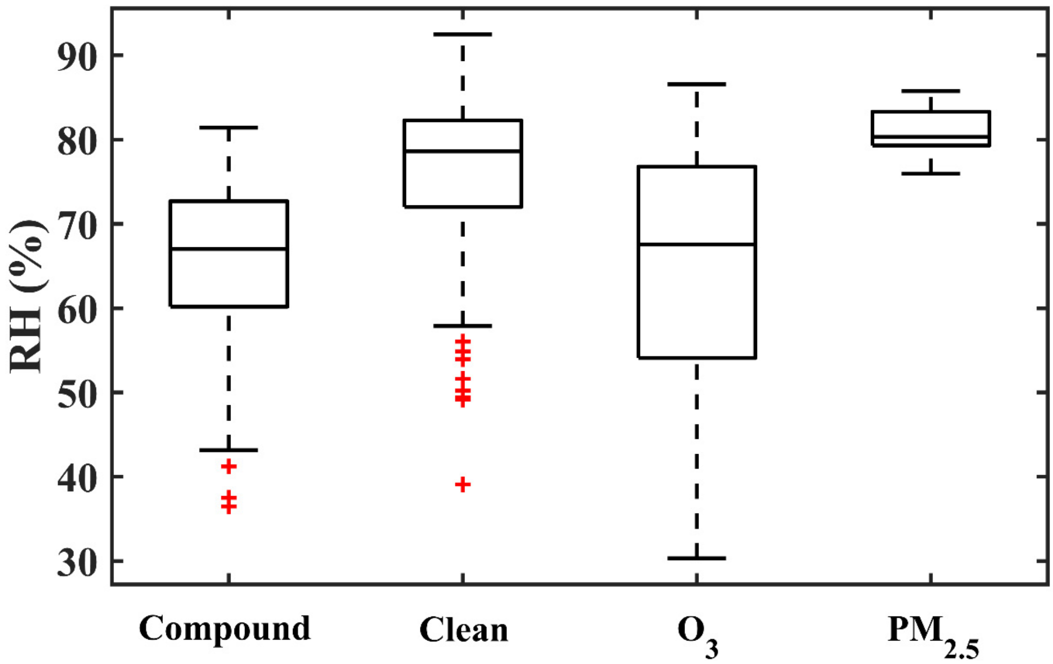

Fig. S14. Box-Whiskers for the RH under compound pollution, clean, O_3-only, $PM_{2.5}$-only period. In the Box-Whiskers plot, the central box represents the values from the lower to upper quartile (25th to 75th percentile). The vertical line extends from the maximum to the minimum value. The middle solid line represents the median, and the red plus represents the outlier.

36. Line 368: Strengthens compared to Type 1? Type 2's trough does not necessarily strengthen from the Type 1 pattern. Please reword.

RESPONSE: Thank you for your suggestion. We have reworded it to "As the northern advance of WPSH from Type 1 or the retreat from Type 3 or Type 4, and the northern region is still controlled by the westerly zone".

37. Lines 357-387: The authors give the percentage of days with compound pollution for types 1 and 2. However, this does not elucidate which type is more efficient at producing compound pollution. The authors should include the percentages of compound pollution days for types 3 and 4. From the results here, I'd suspect that types 1 and 2 are the most efficient compound pollution setups, but this can be confirmed by including the percentages as for types 1 and 2.

RESPONSE: Thanks for your suggestion. The probability of compound pollution occurrence

under Type 3 and Type 4 are 6.8% and 5.1%, which are added in lines 453 and 459.

38. Lines 396-397: These percentages need to be presented for Types 3 and 4 as higher percentages may indicate that PCs 3 and 4 are more efficient setups for co-occurring pollution events, even if the PCs occur less frequently.

RESPONSE: Thanks and added.

39. Line 398: "line" should be "axis"

RESPONSE: Revised and thanks.

40. Line 400: Again, what is "Meiyu" season for non-local readers?

RESPONSE: The explanation about "Meiyu" is added to lines 270-274 on page 10: "These conditions were also associated with high temperature and humidity during the summer with Meiyu season, which Meiyu season is a climate phenomenon with continuous cloudy and rainy days generally occurring during June and July every year in the middle and lower reaches of Yangtze river, Taiwan of China, central/southern Japan, and southern Korea".

41. Lines 400-401: How do higher temperatures suppress O3 production? I would suspect that the higher relative humidifies are primarily responsible. . ..

RESPONSE: Yes, you are right. We have revised it.

42. Line 403: Is the low pressure trough at the surface or at 500 hPa?

RESPONSE: It is referring to the condition at 500 hPa. We have added related information to Lines 478, page 17.

43. Lines 402-404: Again, this "small amount of water vapor transport" suggests that there is a nominal vapor pressure deficit conducive to compound pollution events. In an environment of appropriate stability and PBL characteristics, compound pollution may be especially severe.

RESPONSE: Thank you for your valuable suggestion. We have revised it as "The hygroscopic growth of $PM_{2.5}$ occurs in the corresponding area in front of the trough with a small amount of water vapor transported by the WPSH. Particularly, the prevailing southerly winds in the boundary layer can transport the pollutants emitted from southern cities to the BTH region, and the atmospheric stratification is stable when the air mass is sinking. Thus, the compound pollution can be severe. In general, the synoptic circulation might be responsible for the concentration of pollutants under this SWP".

44. Lines 407-408: It appears that the WPSH only shifts north in your objective PC analysis, not southwards and eastwards. . .can the authors clarify?

RESPONSE: From Type 1 or Type 2 to Type 3 or Type 4 presents the shift north of WPSH in early summer, in the contrary, from Type 3 or Type 4 to Type 2 or Type 1 presents southwards and eastwards retreat. We have added the location of the WPSH (Table S1) and re-described the motion of the WPSH. Please refer to lines 266-285 on pages 10-11, lines 474-475 and 486-489 on pages 17-18.

45. Line 411: Why does water vapor lead to a sink of O3? Water vapor by itself cannot remove O3 from the atmosphere or prevent its formation. Are the authors referring to the supersaturation, dew point depression, etc.?

RESPONSE: Sorry for the confusion. We did not refer to the supersaturation or dew point depression. Instead, we are referring to water vapor flux at 850 hPa (Fig. 4). This is based on the following context: as water vapor can absorb part of the short-wave solar radiation, and this can weaken the photochemical reaction and reduce ozone production. The details have now been revised in the manuscript (Lines 489-490 of Pages 18).

Marked-up manuscript with track changes

Large-scale ~~S~~synoptic drivers of co-occurring summertime ozone and $PM_{2.5}$ pollution in eastern China

Lian Zong[1], Yuanjian Yang[1,*], Meng Gao[2], Hong Wang[1], Peng Wang[3], Hongliang Zhang[4], Linlin Wang[5], Guicai Ning[6], Chao Liu[1], Yubin Li[1], Zhiqiu Gao[1,5]

1. School of Atmospheric Physics, Nanjing University of Information Science & Technology, Nanjing, China
2. Department of Geography, Hong Kong Baptist University, Hong Kong SAR, China
3. Policy Research Center for Environment and Economy, Ministry of Ecology and Environment of the People's Republic of China, Beijing, China
4. Department of environmental science and engineering, Fudan University, China
5. State Key Laboratory of Atmospheric Boundary Layer Physics and Atmospheric Chemistry (LAPC), Institute of Atmospheric Physics, Chinese Academy of Sciences, Beijing, China
6. Institute of Environment, Energy and Sustainability, The Chinese University of Hong Kong, Shatin, N.T., Hong Kong, China

* Correspondence to: Dr./Prof. Y. Yang (yyj1985@nuist.edu.cn)

Abstract

~~In recent years, s~~Surface ozone (O_3) pollution during summer~~time~~ (June-August) over eastern China has become more ~~serious~~severe, resulting in a co-occurrence of ~~and it is even the case that~~ surface O_3 and $PM_{2.5}$ (particulate matter with aerodynamic diameter ≤ 2.5 µm in the air) pollution recently~~can co-occur~~. However, the mechanisms regarding how synoptic circulation pattern could influence~~related to~~ this compound pollution remains unclear. ~~In t~~This study~~,~~ here applied the T-mode principal component analysis (T-PCA) method is used to objectively classify the occurrence of four synoptic weather patterns (SWPs) ~~that occur~~ over eastern China, based on the geopotential heights at 500 hPa during summer~~time from~~ (2015~~ to~~ -2018). Four SWPs of eastern China are closely related to the western Pacific subtropical high (WPSH), exhibiting, significant intraseasonal and interannual variations. Based on the ground-level air quality and meteorological observations, ~~Note that~~ remarkable spatial and temporal disparities of surface O_3 and $PM_{2.5}$ pollution ~~are~~ were also found~~given~~ under the impacts of the~~se~~ four ~~different~~ SWPs ~~according to the ground-level air quality and meteorological observations~~. Particularly, there were two SWPs sensitive to compound pollution (Type 1 and Type 2). Type 1 is characterized by a stable WPSH ridge with axis at about 22°N and the rain belt located in the south of Yangtze River Delta (YRD). High temperature, moderate humidity and low precipitation occurred in the region from BTH to northern YRD (BTH – NYRD), resulting in a co-occurrence of O_3 and $PM_{2.5}$ pollution. Additionally, air pollutants can be transported by the prevailing southerly winds from southern plains and accumulated in the southern BTH, resulting in a worsen pollution. Type 2 exhibits a WPSH dominance (the ridge axis ~25°N) and rain belt (over the YRD) in a higher latitude compared with Type 1. High temperature, medium-high humidity and low precipitation over the BTH were the conducive factors related to the occurrence of the compound pollution events under the impacts of Type 2. Furthermore, low boundary layer height (BLH) and high frequency of light-wind days (FLWD) could create favorable conditions for pollution maintenance. Overall, synoptic weather patterns have played an important role as driving factors of surface O_3-$PM_{2.5}$ compound pollution in a regional context. In addition to the impacts of local emissions, our results may provide further insights regarding how regional environmental changes due to co-occurrence of high $PM_{2.5}$ and high O_3 level may be driven by the effects of meteorological factors ~~Two SWPs are identified as sensitive to compound pollution. One~~

pattern (Type 1) is characterized by a stable WPSH ridge axis at about 22°N, with the rain belt located in the south of Yangtze River Delta (YRD). High temperature, moderate humidity and low precipitation occurred in the region from BTH to northern YRD (BTH – NYRD), resulting in co-occurring O_3 and $PM_{2.5}$ pollution, in addition to the pollutants can be transported by the prevailing southerly winds from southern plains and accumulated in the southern BTH, resulting in worse pollution. The other pattern (Type 2) is featured as more northerly WPSH (the ridge axis ~25°N) and rain belt (over the YRD) compared with Type 1, high temperature, medium-high humidity and low precipitation in the BTH are conducive to occurrence of the compound pollution events. In addition, the low boundary layer height (BLH) and high frequency of light-wind days (FLWD) tend to create favorable conditions for pollution maintenance. In areas controlled by the WPSH or the prevailing westerlies, O_3 pollution is mainly caused by photochemical reactions of nitrogen oxides and volatile organic compounds under weather conditions of high temperature, moderate humidity and slight precipitation. In particular, the warm moist flow brought by the WPSH can promote hygroscopic growth of fine particulate matter in some local areas, resulting in the increase of $PM_{2.5}$ concentrations, which may form co-occurring surface O_3 and $PM_{2.5}$ pollution. In addition, the low boundary layer height and frequency of light-wind days are closely related to the transmission and diffusion of pollutants under the different SWPs, modulating the levels of O_3-$PM_{2.5}$ compound pollution. Overall, our findings demonstrate the different important roles played by synoptic weather patterns in driving regional surface O_3-$PM_{2.5}$ compound pollution, in addition to the large quantities of emissions, and may also provide insights into the regional co-occurring high $PM_{2.5}$ and high O_3 level via the effects of certain meteorological factors.

Keywords: Synoptic weather pattern, ozone, $PM_{2.5}$, compound pollution, western Pacific subtropical high (WPSH)

1. Introduction

In recent years, China has been experiencing serious air pollution problems due to the enormous emissions of polluting gases [e.g., sulfur dioxide, nitrogen dioxide (NO_2), etc.] and aerosol particulates [e.g., particulate matter with aerodynamic diameter ≤ 2.5 (10) μm in the air

$PM_{2.5}$ (PM_{10}), etc.] associated with its rapid economic development, industrialization and urbanization, together with certain unfavorable meteorological conditions (Wang & Chen, 2016; Zhang et al., 2014; Y. Zhang et al., 2016). Particularly, atmospheric compound pollution has become serious (Li et al., 2019; Saikawa et al., 2017; ~~C.~~ Zhang et al., 2019), especially for the economically developed and densely populated eastern urban agglomerations of China, such as the Beijing–Tianjin–Hebei (BTH), Yangtze River Delta (YRD) and Pearl River Delta (PRD) regions (Cai et al., 2017; Du et al., 2019; Ji et al., 2018; Li et al., 2020), exerting a severe threat in terms of public health, economy and society (Chen et al., 2019; Cohen et al., 2017; Day et al., 2017; Yim et al., 2019).

In general, a significant diurnal variation of $PM_{2.5}$ pollution was observed,~~is featured with obvious diurnal and seasonal changes~~ possibly due to obvious the local emissions caused ~~because of the local emissions brought~~ by industrial production and human activities for daily living ~~activities~~(Amil et al., 2016; Liu et al., 2019a). ~~Due to the influence of atmospheric diffusion conditions such as precipitation and wind speed (WS), i~~Particularly, the pollution level was higher ~~It tends to be enhanced in~~during the morning and evening of a normal weekday, with a weakening effect found in the ~~lower at~~ afternoon which may be caused by the co-effects of ~~related to~~ the boundary layer structure ~~and~~as well as anthropogenic emissions~~,~~. There was also a seasonal variation of ~~in terms of seasonality, and higher~~ $PM_{2.5}$ pollution across China, indicating a higher level of pollution ~~occurs~~ in winter ~~and lower in~~than summer ~~in China~~(Ye et al., 2018; Zhang and Cao, 2015)~~(Amil et al., 2016; H. Liu et al., 2019; Ye et al., 2018; Zhang & Cao, 2015)~~. The $PM_{2.5}$ level of China showed a steady increase from 2004 to 2007, and has since stabilized (Ma et al., 2016); however, there are still frequent $PM_{2.5}$ pollution events in autumn and winter (Song et al., 2017; Yang et al., 2018; Ye et al., 2018; Zhang et al., 2014). In the past few years, the $PM_{2.5}$ concentration in China has decreased significantly as a result of measures introduced across the country that have reduced multi-pollutant emissions, adjusted energy structure, and increased supply of clean energy (Gui et al., 2019; Yang et al., 2020; Q. Zhang et al., 2019; Zhang et al., 2020). While $PM_{2.5}$ is still one of the dominant air pollutants across China,~~In contrast,~~ ~~summer~~ surface O_3 pollution in summer has gradually been prominent~~,~~. Several studies even indicated that O_3 might have ~~replacing~~ replace the role of $PM_{2.5}$ as the primary air pollutant ~~in the air~~during summer (Li et al., 2019), which has caught the attention of ~~experts and scholars~~researchers in recent years. ~~As a secondary pollutant, ozone in the troposphere is mainly formed by photochemical reactions between NO_x, carbon monoxide (CO) and VOCs in the exposure of sunlight (Sillman, 2002). The prominent problem of O_3 pollution has attracted the attention of experts and scholars in recent years.~~ For instance, Sun et al. (2016) showed that the observed summertime O_3 at Mt. Tai has increased significantly by 1.7 ppbv yr^{-1} for June and 2.1 ppbv yr^{-1} for July–August during the period of 2003 to 2015. An increase of the maximum daily 8-h average concentration of O_3 (MDA8 O_3) at an annual-average rate of 4.6%, was reported by Fan et al. (2020), albeit with a decrease of the frequency of $PM_{2.5}$ pollution.

The modulations of atmospheric circulation system often lead to changes in meteorological elements, and to a large extent, affect the processes of pollutant formation, transmission and diffusion. And many~~Many~~ studies have indicated that $PM_{2.5}$ and O_3 pollution are strongly correlated with local meteorological factors such as temperature, relative humidity (RH) and WS (Huang et al., 2016;~~—~~Miao et al., 2015; Shu et al., 2019; Tai et al., 2010). Miao et al. (2015) suggested that ~~strong northwesterly synoptic winds,~~ low ~~BLH (~~boundary layer height (BLH)~~), high RH~~ and stable atmosphere ~~are more prone to~~would be an unfavorable condition for ~~disfavor~~ the dispersion of winter aerosol pollution ~~in~~ over the BTH region ~~during wintertime~~. Zhang et al. (2017) found that the majority of O_3 extremes occurred with daily maximum temperature (Tmax) between 300 K and 320 K, minimum RH (RHmin) less than 40%, and minimum WS less than 3 m s^{-1}, through the analysis of extreme O_3 and $PM_{2.5}$ events from historical data (30 years for O_3 and 10 years for $PM_{2.5}$) in the ~~US~~United States. Furthermore, the number of annual extreme $PM_{2.5}$ days was highly positively correlated with the extreme RHmin/Tmax days, and the correlation coefficient between $PM_{2.5}$ and RHmin (Tmax) was highest in urban and suburban (rural) regions. Shi et al. (2020) studied the ~~spatial distribution~~sensitivity of O_3-8h (O_3 8-hour moving average) and $PM_{2.5}$~~, and their sensitivity of to~~associated with meteorological parameters. This study focused on the air pollution and meteorological conditions between January and July, 2013~~;~~ ~~–~~, with a result showing that ~~pronounced~~ temperature could hasve the greatest impact on the daily maximum O_3-8h, ~~and~~while the $PM_{2.5}$ sensitivities are negatively (positively) correlated ~~to~~with temperature ,WS, and BLH (absolute humidity)~~and positive to absolute humidity~~ in most regions of China.~~positive (negative) correlation between temperature (BLH and absolute humidity) and O_3-8h was found, but the relation between~~

WS and O_3-8h was spatially different; for $PM_{2.5}$, it was negatively (positively) correlated with temperature, WS and BLH (absolute humidity). Miao et al. (2015) showed that RH is high when aerosol pollution occurs in the BTH region. However, O_3 pollution in China is more frequent in summer, and the warm and humid flow brought by the East Asian summer monsoon (EASM) induces a hot and humid condition over the summermakes summer always be hot and moist. Zhao et al. (2019) investigated the RH of O_3 pollution in Shijiazhuang between 15 June and 14 July 2016, and found that the O_3 concentration was higher at moderate humidity (RH average during daytime from 10:00 to 17:00 LT was 40%–50%).Recently, Han et al. (2020) assessed the impacts of local and synoptic meteorological factors on the daily variability inof surface O_3 inover eastern China,. This study and revealed that the meteorological factors can could explain ~46% of the daily variability variations ofin summertime surface O_3, while Particularly, synoptic factors contributed to ~37% of the overall meteorological effects associated with the meteorological factorson the daily variability of surface O_3 in eastern China. Furthermore, six predominant SWPs were identified by They employed the self-organizinge map to identify six predominant SWPs, and result indicated finding when eastern China is under a weak cyclone system or and under the a southward prevailing southerly wind inducing would bring a positive O_3 anomalies over the eastern China. The abovementioned indicates that the variation of meteorological factors, which are mainly driven by the evolution of different weather circulation situations, play a non-negligible role in air pollution. Therefore, classification of air pollution according to the meteorological circulation has become particularly important, not least because of its worth when applied to air quality monitoring, forecasting and evaluation (Liu et al., 2019; Ning et al., 2019; Yang et al., 2018; Zheng et al., 2015).

In recent years, iIt has become possible to objectively classify atmospheric circulation conditions using weather data such as GH, sea level pressure, WS and temperature since 1900s, so that the weather mechanism of extreme weather can be better understood and analyzed. Compared with subjective weather classification, the objective approach has been widely used in air pollution research (Beck & Philipp, 2010; Miao et al., 2017, 2019; Ning et al., 2018). Miao et al. (2019), based on the daily 900 hPa GH fields during winter in Beijing, identified seven synoptic patterns using an objective approach, and found that the weak northwesterly prevailing winds and strong elevated thermal inversion layer, along with the local emissions of aerosols play a decisive role in the formation of heavy pollution in Beijing; noted also that the southerly prevailing winds can transport the pollutants emitted from southern cities to Beijing. Zheng et al. (2015) studied the relationship between regional pollution and the patterns of large-scale atmospheric circulation over eastern China in October from 2001 to 2010 and identified six pollution types and three clean types. Specifically, weather patterns such as a uniform surface pressure field in eastern China or a steady straight westerly in the middle troposphere, particularly when at the rear of an anticyclone at 850 hPa, were found to be typically responsible for heavy pollution events. Many studies have suggested a moderating effect of East Asian summer monsoon (EASM) and WPSH on ~~that the~~ air quality over China ~~is regulated by~~~~$PM_{2.5}$ and O_3 pollution are mainly related to the East Asian summer monsoon (EASM) and western Pacific subtropical high (WPSH)~~ (Li et al., 2018a; ~~Xie et al., 2017;~~ Yin et al., 2019; Zhao et al., 2010). In particular, ~~(~~Li et al.~~,~~ (2018a) applied RegCM4-CHEM simulation to analyze~~d~~ the differences of ozone between three strong and weak monsoon years ~~by RegCM4-CHEM simulation~~, and found that the concentrations of O_3 over the central and eastern part of China ~~is~~were higher in strong EASM years than that in weak EASM years ~~over the central and eastern part of China.~~ The anomalous high-pressure system at 500 hPa, associated with downward dry, hot air and intense solar radiation can enhance the photochemical reactions to elevate the production of tropospheric O_3 (Gong and Liao, 2019; Yin et al., 2019). Furthermore, Zhao & Wang (2017) and Yin et al. (2019) noted that the positive GH anomalies at high latitudes tend to significantly weaken the cold-air advection from the north and result in local high temperatures near the surface in northern China, while the WPSH can transport sufficient water vapor to the YRD region and lead to a decrease in surface O_3. In addition, different subregions can exhibit various distributions of pollutant, even with identical emission scenarios (Li et al., 2019; Saikawa et al., 2017; ~~C.~~ Zhang et al., 2019). Also, it is still unclear how the distribution of pollution responds locally to large-scale atmospheric circulation patterns. ~~Considering the reduced surface solar radiation due to $PM_{2.5}$ pollution (Haywood & Boucher, 2000; He & Wang, 2020; Huang et al., 2018; Yang et al., 2020) and thus suppressed the photochemical production of O_3 (Li et al., 2017), the compound O_3-$PM_{2.5}$ pollution-related meteorological conditions, should be complex and likely to be associated with certain weather types modulated by large-scale WPSH movement.~~ Due to a variability of local meteorological conditions under the impacts of various synoptic weather types and modulation of large-scale WPSH movement(Li et al., 2018; Wang et al., 2019c; Zhao and Wang, 2017), the causes and consequences of meteorological factors for the formation of compound O_3-$PM_{2.5}$ pollution could be complex. Overall, the mechanism by which the synoptic weather pattern (SWP) modulates the characteristics of O_3-$PM_{2.5}$ compound pollution has yet to be comprehensively described.

In this study, the SWPs corresponding to the co-occurrence O_3-$PM_{2.5}$ pollution during summertime are analyzed, focusing on the eastern China (~~108~~104°–135°E, 17°–53°N). Then, the causes of O_3-$PM_{2.5}$ compound pollution, as well as O_3-only pollution, from the perspective of the objective classification of atmospheric circulation patterns, are revealed. The findings are expected to provide a scientific reference for the monitoring, forecasting and evaluation of summertime air pollution in eastern China.

2. Data and methods

The air quality data, including $PM_{2.5}$, NO_2, O_3, and O_3-8h, are from the national 24-h continuous air quality observation published by the China Environmental Monitoring Station (http://www.cnemc.cn/). ~~The~~ Summer hourly ~~observation~~ data (2015–2018) ~~of a total from~~for ~~949~~ 1174 stations ~~(108°–135°E, 17°–53°N)~~ were retrieved form an observational network in eastern China (104°–135°E, 17°–53°N) ~~during summertime of 2015–2018~~, which include the more prominent pollution areas in the eastern urban agglomeration, such as the BTH (113.5°–119.8°E, 36°–42.6°N), YRD(115.3°–122.6°E, ~~—~~27.2°–34.5°N), PRD(112.5°–113.7°E, 21.3°–23.1°N, Guanzhong Plain [~~(~~GZP~~)~~ (104.6°–112.2°E, 33.3°–36.8°N)], Northeast Megalopolis [~~(~~NEM~~)~~ (121.2°–131.0°E, 39.8°–47.3°N)] regions (the specific locations of stations and urban agglomerations are shown in Fig. 1a). Surface meteorological data, such as Tmax, precipitation, WS and RH from ~~517~~ 611 meteorological observation stations and radiosonde data from 63 stations in eastern China, were obtained from the China National Meteorological Information Center of the China Meteorological Administration (http://data.cma.cn/site/index.html). The BLH was calculated according to the method given by Guo et al. (2016, 2019) (the detailed method can be seen in supplementary materials), and the FLWD [frequency of light wind (< 2 m s^{-1}) days, which can be defined as the ratio between the number of the days with average daily WS lower than 2 m s^{-1} and the total days of each pattern], precipitation frequency (PF, which can be defined as the ratio of the number of the rainy days to the total days under each pattern), and MDA8 O_3 were also counted.

Additionally, for synoptic analysis of particulate matter and O_3 pollution in summer, we use the GH field at 500 hPa~~ and~~, wind and specific humidity field at 850 hPa from the NCEP/NCAR (National Centers for Environmental Prediction/National Center for Atmospheric Research) daily reanalysis dataset on a 2.5° × 2.5° latitude/longitude grid during the study period.

The ~~T-mode principal component analysis (~~T-PCA~~)~~ is an objective mathematical computer-based method that can be used to classify the synoptic circulation patterns of regional gridded data in the troposphere at the lower level. Indeed, it is commonly regarded as the most promising weather pattern classification method at present (Huth et al., 2008). Moreover, this approach has been widely used in the studies of aerosols and O_3 pollution-related atmospheric circulation in China (Miao et al., 2017, 2019; Ning et al., 2018, 2019). The T-PCA analysis module of the COST733 software (http://cost733.met.no/) developed by the European Scientific and Technical Research Cooperation, was used to classify the synoptic circulation pattern based on the 500 hPa GH field. The cost733class is a FORTRAN software package consists of several modules for classification, evaluation and comparison of weather and circulation pattern. First, T-PCA classification of the cost733class performs spatial standardization on weather data. Then split data to 10 subsets and estimates principal components (PCs) of weather information based on singular value decomposition, the PC score for each subset can be calculated after oblique rotation, and compares 10 subsets based on contingency tables to select the subset with highest sum and return its types~~The cost733software includes several modules for classification, evaluation and comparison. The T-PCA classification on cost733 performs spatial standardization on data, splits data into 10 subsets, achieves the principal components (PCs) according to singular value decomposition, then applies oblique rotation to PCs, calculates the PC score of each subset, finally compares 10 subsets and selects the most consistent one with other classification~~ (Miao et al. 2017).~~More detailed information about the T-PCA method can be found in Miao et al. (2017).~~ To assess the performance of synoptic classification and determine the number of classes, the explained cluster variance (ECV) is selected in this study (Hoffmann & SchlüNzen, 2013; Ning et al., 2019; Philipp et al., 2014). The detailed information about the ECV is provided in the supplementary document.

Based on the Ambient Air Quality Standards (GB3095-2012) ~~environmental air quality~~

~~standard~~ issued by the Ministry of Ecology and Environment of the People's Republic of China, O_3 ($PM_{2.5}$) pollution occurs when the MDA8 O_3 ($PM_{2.5}$ 24-h) concentration exceeds 160 (75) μg m^{-3}. For a region, when haze occurs in more than 50% of the observed sites, the day can be defined as a haze day(Chen and Wang, 2015). In this study, we used the average value of higher 50% O_3 and $PM_{2.5}$ concentrations in each region as the regional values. The specific standard limits of each pollution level are according to their concentration limits based on the Technical Regulation on Ambient Air Quality Index (on trial) (HJ633-2012) issued by the Ministry of Ecology and Environment of the People's Republic of China (Table S1). ~~To investigate the temporal variations of air pollution in various regions in summer, the pollution levels of O_3 and $PM_{2.5}$ in each key area were verified according to their concentration limits.~~

Finally, in order to make it clear in the analysis of different weather types of O_3 and $PM_{2.5}$ concentration change, we calculated the average distribution of O_3 and $PM_{2.5}$, as well as the meteorological conditions for each type, and further calculated the anomalous distribution of these variables, i.e., the average of O_3 and $PM_{2.5}$ and the average of the meteorological conditions under the respective patterns minus the average during summertime of 2015–2018, were given as well. The statistical significance was tested with a 0.05 confidence level via analysis of variance, which enabled us to distinguish the significant differences of spatial distribution characteristics between O_3 and $PM_{2.5}$ pollution under four SWPs.

3. Results

3.1 Spatial and temporal distribution of O_3 and $PM_{2.5}$ during summer 2015–2018

Figure 1 shows the summer averaged MDA8 O_3 and $PM_{2.5}$ concentrations at ~~949~~ 1174 stations in the eastern region of China for 2015–2018. Among these stations, the MDA8 O_3 concentration at most stations (~~662~~795/~~949~~1174) exceeds 100 μg m^{-3}, of which 45 sites exceed 160 μg m^{-3}. The highest O_3 pollution is found in Zibo, Shandong, with a value of 181.5 μg m^{-3}. The averaged $PM_{2.5}$ at most sites (~~680~~844/~~949~~1174) is below 35 μg m^{-3}, while reaches 62.6 μg m^{-3} in Handan, Hebei Province. On the whole, the MDA8 O_3 and $PM_{2.5}$ in the BTH region and its surrounding areas is significantly higher than in other regions; and besides, the level of O_3 in some urban clusters, such as the PRD, YRD, GZP and NEM regions, is particularly higher than that of the surroundings, thus, we focus on analyzing these key areas later.

Figures 2 and 3 respectively show the daily variation of pollution levels of O_3 and $PM_{2.5}$. In recent years, The reduced visibility of haze days weakens the solar radiation reaching the ground and inhibits photochemical reactions from generating O_3 (Li et al., 2019; Z. Zhang et al., 2015), as a result, the concentration of O_3 continues to increase with the mitigation of $PM_{2.5}$ pollution. The days of O_3 pollution in BTH, YRD, PRD, GZP, and NEM regions were 254, 133, 84, 165 and 96 days respectively, while the days of $PM_{2.5}$ pollution were only 93, 8, 0, 2 and 1, of which compound pollution occurred 76, 7, 0, 2, ~~,~~and 0 days according to Chinese standards (the asterisks in Fig. 3 indicate the co-occurred events). China has implemented strict emission control policies and the effects ~~has been~~were remarkable. China has implemented strict policies for emission control, and the effects of these policies were remarkable. However, despite a decrease in $PM_{2.5}$ in the last five years, there was also an increase in ozone pollution over China (Fan et al., 2020; Sun et al., 2016), although "double-high" pollution reported on the weather scale has been decreased. As the limit of $PM_{2.5}$ concentration for pollution control is relatively loose in China, previous studies usually referred the interim target 1 (IT-1) of the World Health Organization (WHO) as the standard threshold. Our study pushed forward to the next stage, in which we used IT-2 of WHO (24-h average concentration of $PM_{2.5}$ is 35 μg m^{-3}) as our target limit to count the number of compound pollution days across each region. Based on this target, the pollution days for 4 SWPs were 194, 52, 16, 47, and 20, respectively (Fig. 3). These results indicated a severe situation of compound pollution that is still deserved a public attention. ~~It is true that there has been a decrease in $PM_{2.5}$ in the last five years and an increase in ozone, so that the double-high pollution on the weather scale has decreased. As $PM_{2.5}$ pollution concentration limit is relatively loose in China, it is currently in the interim target 1 (IT-1) of the World Health Organization (WHO). Our target limit for the next stage (IT-2 of WHO, the 24-h average concentration of $PM_{2.5}$ is 35 μg m^{-3}) has counted the number of compound pollution days in each region, which are 194, 52, 16, 47, and 20, respectively. Which shows that~~Thus, the situation of compound pollution is still serious and deserves attention. ~~The temporal variations of O_3 pollution levels in key areas are displayed in Fig. 2, revealing an obvious increase in O_3 pollution levels and duration in the five priority areas for the period 2015–2018. The O_3 pollution in June is more severe than that in July and August, which is consistent with the fact that the peak~~

concentration of MDA8 O_3 in northern China is in June (Gong and Liao, 2019). In spatial terms, O_3 pollution is particularly prominent in the BTH and GZP regions, with the number of pollution days reaching 148 and 109, of which even 23 and 17 are moderate pollution, respectively. Figure 3 illustrates the $PM_{2.5}$ pollution-level variations and, although it is not difficult to see that $PM_{2.5}$ pollution weakens year by year, the number of days of $PM_{2.5}$ pollution in the BTH region reaches 192 (25 days for moderate pollution), which is higher than the number of days of O_3 pollution. The reduced visibility of haze days weakens the solar radiation reaching the ground and inhibits photochemical reactions from generating O_3 (Li et al., 2019; Z. Zhang et al., 2015), as a result, the concentration of O_3 continues to increase with the mitigation of $PM_{2.5}$ pollution. It is worth noting that O_3 and $PM_{2.5}$ co-occurred in both the BTH (120 days) and GZP (60 days) regions. Overall, the O_3 and $PM_{2.5}$ concentration in eastern China exhibits distinct intraseasonal and interannual variations, indicating that, aside from the changes in emission sources (because it is considered that inter-seasonal and short-term changes in emission sources are not significant), it may also be regulated by meteorological conditions, which is further analyzed below.

3.2 Objective classification of large-scale synoptic circulation patterns in summer

To analyze the effect of meteorological conditions on the changes of O_3 and $PM_{2.5}$ concentration, it is necessary to statistically analyze the large-scale weather circulation situation in summer. Existing studies have shown that the WPSH (500 hPa GH field with obvious anticyclonic characteristics, and downward flow around the center) in summer prominently regulates the weather and climate of East Asia (Lu, 2002), owing to its various location, shape and intensity (Ding, 1994). A low-level southerly monsoon formed at the periphery of the WPSH can transport warm and humid air from the ocean to East Asia, which might also be responsible for the asymmetric spatial distribution in response to an enhanced WPSH for ground-level O_3, i.e. a decrease in southern China but an increase over northern China (Zhao & Wang, 2017).

Therefore, we used the T-PCA method to objectively classify the weather circulation of the 500-hPa GH field in the summers of 2015–2018, and finally obtained four SWPs related to the movement and development of the WPSH. The location of western ridge point and northern boundary of thewestward extension and southward motion of the WPSH at 500 hPa in Type 1 is aboutround 120°E and 30°N, respectively,-(Fig. 4a and Table S2).-as shown in Fig. 4a,The southwestern flow of theis WPSH could transports water vapor into the YRD region, and resulting in a southwestwardthe prevailing windsouthwesterly in across the YRD region and westward flow from the north of the WPSH forming a cyclonic convergence area at 850 hPa,. These conditions were also associated with high temperature and high humidity during the summer with Meiyu season, which Meiyu season is a climate phenomenon with continuous cloudy and rainy days generally occurring during June and July every year in the middle and lower reaches of Yangtze river, Taiwan of China, central/southern Japan, and southern Korea). For Type 2, it is noticed that the westerly trough could deepens accompanying as the WPSH shifts northward slightly from Type1 or retreats southeast from Type 3 (or southward) advance (retreat) of WPSH, and the GH over northern China at 500 hPa is higher compared with Type 1 (Fig. 4b). The southerly wind blowing from the ocean to the continent lies in front of thecould interact with northern peripherybottom of the high pressureWPSH,. As a result, the sea-land interaction could interact withaffecting the southeastern region across China, while northern China is could be mainly controlled by the westerly trough, and the rain belt moves northwards to the east of the YRD region. In compared with Type 2, Under Type 3, presents the boundary of WPSH shifts further northin a higher latitude, with a westward extension compared with Type 2 (Fig. 4c), and disintegrates disintegrating a closed high-pressure monomer along the eastern coast of China, while and the main body of the WPSH remains on over the ocean (Figs. 4c and S4). This has led to a condition completely controlled by the monomer of the WPSH over the YRD region, resulting a hot and dry weather at the end the rainy season at the beginning of mid-summer.In this case, the YRD region is completely controlled by the monomer of the WPSH, the region ends the rainy season and enters midsummer, becoming hot and dry., which implies that the rainy season in the YRD region ends in midsummer and the weather becomes hot and dry. At the same time, the rain belt moves gradually northwards to the BTH and NEM regions. According to In Figure. 4d, indicated that the locationmonomer of the WPSH monomer iwas more western and northern with respect to other SWPslocated the north and west of the feature in Fig.4c, under Type 4 continues to extend westwards and shift northwards, controlling the northern China for a long time,; the western ridge point iwas aboutaround 95°E and the northern boundary iwas aboutaround 40°N, which location of the WPSH is more west and north than other SWPsand with

~~persistent high temperatures and a heat wave occurring in most parts of the eastern China~~.

Fig~~.~~ure 5 presents the daily and annual variations of the SWPs in the summers of 2015–2018. The advance of the WPSH in eastern China occurs in June and July, while gradual withdrawal of the WPSH occurs mainly in August, ~~so~~ Type 1 and Type 2 represent normal WPSH ~~pattern~~characteristics during early and late summer. Type 3 and Type 4 could reflect a splitt~~ing~~ of the WPSH, which mainly occurs in late summer~~mainly appears in June, while Type 2, Type 3 and Type 4 occurs mainly in July and August~~. Consequently, there were167, 117, 52 and 32 days for the Type 1, Type 2, Type 3 and Type 4 ~~appear for 167, 117, 52 and 32 days, respectively, during~~over the study period, respectively. Since the ~~movement of the~~ WPSH movement is ~~often~~ generally affected by the ~~activities~~ weather phenomenon of ~~the~~ its surrounding ~~weather~~ climatic system (such as typhoons, the Tibetan high, etc.) (Ge et al., 2019; Liu and You, 2020; Shu et al., 2016; Wang et al., 2019c)~~(Ge et al., 2019; Liu & You, 2020; Shu et al., 2016)~~, ~~there may~~it could ~~be~~ result in a short-term southward retreat during the advancement of the WPSH~~'s advancement~~ (e.g., around 10 August 2018) and a short-term northward advance during its process of retreat (e.g., 21 and 29 August 2016). In general, ~~it can be seen that~~ the WPSH ~~also shows~~could represent the ~~evident~~ evidences of intra-seasonal and interannual changes over China, which will inevitably ~~regulate~~ modulate the weather, ~~climate~~ climatic and environmental changes in eastern China.

3.3 O_3 and $PM_{2.5}$ pollution characteristics under four SWPs

3.3.1 Spatial characteristics

We calculated the averaged (Fig. S2) and anomalous (Fig. 6) spatial distributions of the MDA8 of O_3 and $PM_{2.5}$ under the four SWPs. ~~The averaged MDA8 O_3 under the four SWPs can be seen in Fig. S2.~~ The O_3 concentration is relatively high in the area north of the Yangtze River under Type 1, and the high values of the MDA8 O_3 are mainly concentrated in the North China Plain (NCP) region, with a total of ~~94~~ 100 stations surpassing 160 μg m^{-3}. Type 2 O_3 pollution is slightly weaker than that for Type 1, and the MDA8 O_3 at the 72 sites exceeds 160 μg m^{-3}. The O_3 high-value areas lie mainly in the NCP, GZP and YRD regions under Type 4, and there are 37 stations larger than 160 μg m^{-3}. Of the four SWPs, the lowest overall MDA8 O_3 occurs under Type 3, with only one site exceeding 160 μg m^{-3} (Figs. S2a-d). It is also found that the regions experiencing significant positive deviations of the MDA8 O_3 from the summer mean are as follows: the BTH, YRD and NEM regions under Type 1, the BTH and GZP regions under Type 2, the middle of the YRD and PRD regions under Type 3, and the YRD, GZP and PRD regions under Type 4 (Figs. 6a-d).

Analogously, Figs. ~~7~~ 6e-h shows the anomaly and significance of difference of $PM_{2.5}$ under the four weather types, presented as positive anomalies in the south of the BTH and YRD regions under Type 1, in the BTH, GZP and PRD regions under Type 2, and in the GZP and PRD regions under Type 4. Due to the obvious seasonal variations of $PM_{2.5}$ concentration (higher in winter and lower in summer) (H. Liu et al., 2019; Miao et al., 2015), no site exceeds 75 μg m^{-3} for the averaged $PM_{2.5}$ concentration. Even so, the level of $PM_{2.5}$ in the BTH region is still significantly higher under the four types than that for the other urban agglomerations (Figs. ~~S3~~S2e-h).

3.3.2 Pollution pattern differences in key areas

Air pollution~~ in eastern China~~ is principally found in dense urban areas such as the BTH and YRD regions (Gui et al., 2019; Han et al., 2019), so we took the BTH, PRD, YRD, GZP and NEM regions in the eastern region as key areas, counted the ~~average~~ daily anomalies and average variation~~changes~~ of O_3 and $PM_{2.5}$ in each key region under different weather patterns (Figs. ~~8~~7 and S5), and calculated the over-limit ratio in key regions via the stations × days statistics (see Table 1). The diurnal variation of O_3 is more obvious, peaking at about 15:00 (Beijing time), while contrasting diurnal variations of $PM_{2.5}$ are given for different regions. According to Figure ~~8~~ 7 and Table 1, the following characteristics can be identified for different urban clusters: (1) in the BTH region, the O_3 ~~pollution~~ concentration of Type 1 and Type 2 is relatively ~~serious~~high, their over-standard rates reach 47.1% and 54.2%, and the $PM_{2.5}$ pollution rates of Type 2 and Type 1 reach 18.8% and 16.3%, respectively; (2) in the PRD region, the over-standard rates and concentrations~~variation~~ of O_3 and $PM_{2.5}$ is similar under four SWPs~~equable~~; (3) in the YRD region, the O_3 pollution over-limit ratio presents as Type 1 > Type 4 > Type 2 > Type 3, $PM_{2.5}$ pollution largely appears in Type1, and both O_3 and $PM_{2.5}$ in Type 1 are higher than those in the other types; (4) in the GZP region, the O_3 pollution frequency is higher in Type 2 and Type 4, and $PM_{2.5}$ pollution occurs more frequently in Type 2; and (5) in the NEM region, O_3 pollution is always found in Type 1, Type 2 and Type 4, but the over-standard rate is no more than 15% and $PM_{2.5}$ pollution in Type 1 is more than in Type 2.

In summary, Type 1 is prone to the formation of compound pollution of O_3-$PM_{2.5}$ (that is, when the ground MDA8 O_3 concentration exceeds 160 μg m^{-3}, the $PM_{2.5}$ concentration also exceeds 75 μg m^{-3}) in the area from ~~southern~~ BTH ~~and~~ to northern YRD regions (Fig. S11), which can be denoted as "~~South~~ BTH – N~~orth~~ YRD O_3-$PM_{2.5}$ compound pollution". Similarly, Type 2 can also be denoted as "BTH~~ – GZP~~ O_3-$PM_{2.5}$ compound pollution", Type 3 as "BTH – ~~GZP~~ YRD – PRD O_3-only pollution", and Type 4 as "~~GZP O_3-$PM_{2.5}$ compound pollution with~~ BTH – GZP – YRD – PRD O_3-only pollution" (Fig.12).

3.4 Analysis of potential meteorological factors

Therefore, to explore the meteorological causes of O_3 and $PM_{2.5}$ pollution, we analyzed the distribution of the average and anomalies for Tmax, RH, PF, BLH and FLWD under the four SWPs (Figs. S6, S7, 8 and 9). Under the influence of the EASM, over 80% of the stations experience high temperatures (Tmax > 27℃) in each SWP, although the anomaly of Tmax in Type 1 (early summer) presents negative (Fig.8a). Type 1 is characterized by humid condition in the southern area and dry condition in the northern region owing to an extensive southwestern flow of the WPSH. resulting in a rain belt found in southeastern coastal area such as PRD and YRD regions. Type 2 is associated with meridional flow and dry and wet anomalies in northern China, resulting in a rain band locating at the central areas of between BTH and YRD regions due to the northern advance of the WPSH compared with Type 1. Furthermore, there is a greater RH for most of the study sites under the influences of Type 3 and Type 4, possibly a result of the shifted rain belt in the BTH and NEM regions under Type 3 once the northern boundary of the WPSH reaching at 37.5°N, and an occurrence of heavy precipitation across the western PRD region as well as central areas of between BTH and YRD regions under the impacts of Type 4 (Fig. S6).

In terms of their anomalous spatial distribution, the positive anomalies of Tmax are located in the southern region of Type 3 and most of the eastern region of Type 4; and since Type 1 always appears in early summer, most areas are negative (Figs. 8a–d). For RH, Types 2, 3 and 4 are negative for the south and positive for the north, while Type 1 is opposite (Figs. 8e–h). PF is characterized by positive anomalies in the area south of the Yangtze River under Type 1, in the YRD region under Type 2, in the BTH and NEM regions under Type 3, and in the area between the BTH and YRD regions under Type 4 (Figs. 8i–l). As can be seen from Fig. 9, when the BLH at 14:00 (BJT) has a positive anomaly, on the contrary FLWD has a negative anomaly (e.g., BTH in Type 1), which indicates the higher BLH, the lower FLWD, the more conducive to the diffusion of pollutants, otherwise, lower BLH and higher FLWD (such as BTH in Type 2) do not support the diffusion. After further inspection of Fig. S7, we found the YRD region in Type 1, the YRD in Type 2, the BTH and PRD regions in Type 3 and 4 have shallow BLHs and high FLWDs, which is detrimental to the transportation of pollution in these areas, thus corresponding to high levels of pollution under these weather patterns. But in some higher BLH areas, there were also more serious pollution, such as BTH under Type 1, which we will discuss next.

3.5 ~~Effects of NO_2 on O_3~~Potential implications of NO_2

Photochemical production of O_3 mainly involve emissions of VOCs and NO_x from anthropogenic, biogenic and biomass burning sources (Deng et al., 2019; Gvozdić et al., 2011; Sillman, 2002). The photochemical reaction of NO, NO2, and O_3 in the troposphere form a closed system(Yu et al., 2020), and this photochemical cycle of NOx and O_3 is the basis of photochemical processes in the troposphere. Oxidant (Ox, Ox=O_3+NO_2), a conservative quantity over short time scales, is defined as a parameter to evaluate the photochemical processes due to the unstable nature of NO, it can quickly react with the equivalent amount of O_3 to generate NO_2 (Kley et al., 1994). In order to compare the photochemical reaction efficiency of five urban clusters under different SWPs, Figure 10 can present the daily variation of NO_2 and Ox. These include daily variations of NO_2 showing two peaks during a day, including a first peak at the morning and an second peak associated with traffic emissions in the evening (Xie et al., 2016; Yu et al., 2020). As we found the lowest point of NO_2 at 15:00 (BJT), and NO_2 can be photolyzed to produce O_3 during the day, this study assumed that this particular time was the peak formation ozone across the study areas. As NO_2 was consumed through a photochemical reaction with the involvement of other precursors to produce a large amount of O_3, Ox could form a peak during the afternoon. In particular, abundant sunlight in summer is beneficial to the photochemical reaction process, but since most parts of eastern China are in a subtropical climate with the same period of rain and heat, the existence of the rainy season will inevitably inhibit the summer photochemical process. Under different SWP, the photochemical reaction ofover each area has an obvious relationship with the rain belt. For example, the rainy season in BTH and NEM areas mainly occurs in Type 3, and the Ox of Type 3 in this area is significantly lower than other SWPs.

Photochemical production of O_3 mainly involve emissions of VOCs and NO_x from anthropogenic, biogenic and biomass burning sources (Deng et al., 2019; Gvozdić et al., 2011; Sillman, 2002). Due to the implementation of a number of pollution abatement measures, the abundance of NO_2 has decreased significantly in eastern China in the past few years, leading to the sensitive precursor of O_3 formation changing from VOCs to a mixture of VOCs and NO_x indicating the overall increasing sensitivity to NO_x especially in the afternoon (Wang et al., 2019b). As a result, both NO_x and VOCs need being cooperatively controlled to mitigate O_3 pollution. Figure 11 shows the diurnal variations of NO_2 and the ratio of O_3 to NO_2 (O_3/NO_2) in five urban clusters, where the larger the O_3/NO_2 ratio, the more O_3 is generated by the photochemical reaction of NO_2 when NO_2 is lower. The NO_2 concentration reaches its lowest and O_3/NO_2 reaches a peak at around 15:00 (Beijing time) in the day, owing to the rapid consumption of NO_2 by the photochemical reaction under high temperature and strong solar radiation in the afternoon. As far as O_3/NO_2 (NO_2) is concerned, it can be seen that the daytime O_3/NO_2 (NO_2) values under Type 4 in the five regions is greater than (less than) under the other types, indicating that O_3 photochemical reactions are stronger under this type than the others. But it seems that due to the influence of heavy precipitation and low RH, few sites will have compound pollution. In contrast, the photochemical reaction of the BTH and NEM regions under Type 3 and the YRD region under Type 1 is weaker owing to the warm and humid air brought by the WPSH, and the rainy weather is also unconducive to the occurrence of photochemical reactions to generate O_3. For the PRD region, the photochemical processes of the four SWPs are not significantly different, the O_3 concentration under each type is very low. It can be seen that different weather patterns also have an important regulatory effect on the photochemical production of O_3.

4. Discussion

4.1 Analysis of potential meteorological factors

The activities of atmospheric circulation system often lead to changes in meteorological elements, and to a large extent, affect the processes of pollutant formation, transmission and diffusion. Zhang et al. (2017) revealed that the extreme O_3 and $PM_{2.5}$ pollution events in the United States always occur under the conditions of high temperature, low humidity and low WS, while Miao et al. (2015) showed that RH is high when aerosol pollution occurs in the BTH region. However, O_3 pollution in China is more frequent in summer, and the warm and humid flow brought by the EASM makes summer always hot and moist. Zhao et al. (2019) investigated the RH of O_3 pollution in Shijiazhuang between 15 June and 14 July 2016, and found that the O_3 concentration was higher at moderate humidity (RH average during daytime from 10:00 to 17:00 LT was 40%–50%).

Therefore, to explore the meteorological causes of O_3 and $PM_{2.5}$ pollution, we analyzed the distribution of the average and anomalies for Tmax, RH, PF, BLH and FLWD under the four SWPs (Figs. S4, S5, 9 and 10). Under the influence of the EASM, over 80% of the stations experience high temperatures (Tmax > 27°C) in each SWP, although the anomaly of Tmax in Type 1 presents negative. Type 1 is characterized by humid condition in the south and dry condition in the north, with the rain belt mainly in the PRD and YRD regions; Type 2 has dry and wet anomalies meridionally in northern China, and the rain band is located in the middle of the BTH and YRD regions; the RH is large for most sites under Type 3 and Type 4, corresponding to the shifted rain belt to the BTH and NEM regions under Type 3, and the heavy precipitation appeared in the western PRD region and the middle of the BTH and YRD regions under Type 4 (Fig. S4).

In terms of their anomalous spatial distribution, the positive anomalies of Tmax are located in the southern region of Type 3 and most of the eastern region of Type 4; and since Type 1 always appears in June, most areas are negative (Figs. 9a–d). For RH, Types 2, 3 and 4 are negative for the south and positive for the north, while Type 1 is opposite (Figs. 9e–h). PF is characterized by positive anomalies in the area south of the Yangtze River under Type 1, in the YRD region under Type 2, in the BTH and NEM regions under Type 3, and in the area between the BTH and YRD regions under Type 4 (Figs. 9i–l). As can be seen from Fig. 10, when the BLH has a positive anomaly, on the contrary FLWD has a negative anomaly, which indicates the higher the height of the boundary layer, the lower the frequency of light wind days, the more conducive to the diffusion of pollutants, and vice versa. After further inspection of Fig. S4, we found the YRD region in Type 1, the area north of the Yangtze River in Type 2, the BTH and PRD regions in Type 3, and most regions of Type 4 have shallow BLHs and high FLWDs, which is detrimental to the transportation of pollution in these areas, thus corresponding to high levels of pollution under these weather patterns.

4.21.1 Effects of NO_2 on O_3

Photochemical production of O_3 mainly involve emissions of VOCs and NO_x from anthropogenic, biogenic and biomass burning sources (Deng et al., 2019; Gvozdić et al., 2011; Sillman, 2002). Due to the implementation of a number of pollution abatement measures, the abundance of NO_2 has decreased significantly in eastern China in the past few years, leading to the sensitive precursor of O_3 formation changing from VOCs to a mixture of VOCs and NO_x (Wang et al., 2019b). As a result, both NO_x and VOCs need being cooperatively controlled to mitigate O_3 pollution. Figure 11 shows the diurnal variations of NO_2 and the ratio of O_3 to NO_2 (O_3/NO_2) in five urban clusters, where the larger the O_3/NO_2 ratio, the more O_3 is generated by the photochemical reaction of NO_2. The NO_2 concentration reaches its lowest and O_3/NO_2 reaches a peak at around 15:00 (Beijing time) in the day, owing to the rapid consumption of NO_2 by the photochemical reaction under high temperature and strong solar radiation in the afternoon. As far as O_3/NO_2 (NO_2) is concerned, it can be seen that the daytime O_3/NO_2 (NO_2) values under Type 4 in the five regions is greater than (less than) under the other types, indicating that O_3 photochemical reactions are stronger under this type than the others. In contrast, the photochemical reaction of the BTH and NEM regions under Type 3 and the YRD region under Type 1 is weaker owing to the warm and humid air brought by the WPSH, and the rainy weather is also unconducive to the occurrence of photochemical reactions to generate O_3. For the PRD region, the photochemical processes of the four SWPs are not significantly different. It can be seen that different weather patterns also have an important regulatory effect on the photochemical production of O_3.

In the last section, we have discussed how the SWPs and local meteorological factors regulate modify summer O_3 and $PM_{2.5}$ pollution during summertime. ButHowever, how does the boundary layer structure interact with respond tothe co-occurringence O_3-$PM_{2.5}$ pollution? In order to address this question, Wwe conducted a further research in this sectionanalysis. We have alreadyAs mentioned that, co-occurringence of O_3 and $PM_{2.5}$ pollution mainly occurs in the BTH – NYRD under the impacts of Type 1 and BTH under the influence of Type 2. Lower WS and its negative anomalies ~~of~~at lower boundary layer over BTH– NYRD under Type 1 and over BTH under Type 2 ~~which is~~may not ~~conductive to~~enhance the diffusion of air pollutants (Fig. S8). In contrast, moderate RH and its negative anomalies might favor the formation of compound pollution.~~, and d~~Downward vertical motion and negative anomalies could also stabilize~~makes~~ the atmospheric characteristic of boundary layer~~ more stable~~ (Fig. S9). Furthermore, we summarized boundary layer structure, precipitation, and ground-level wind flow across the BTH region. Based on the characteristics, we separately defined ~~divided~~ Type 1 and Type 2 into clean (both concentrations of the O_3 and $PM_{2.5}$ are less than polluted level) and compound pollution periods (Figs. 11 and S10-S11). Particularly, Type1 has a significantly warmer temperature over the boundary layer during the compound pollution period of BTH region than that of the clean period. The daytime BLH under compound pollution condition was also higher than that of the clean condition. In addition, there were different directions of prevailing during the two periods, which prevailing winds during the compound pollution period were usually southward and could be driven by air pollutants transported from the southern plains (Fig. 11; see also~~)~~ ~~(~~Miao et al., 2019b, 2020). Co-influencing by the topographical effect of the northern mountainous areas, air pollutants could be trapped in the BTH region. In comparison, although there was southward wind prevailing in the BTH region (Figs. 11 and S11), the rain belt also located in the southern area of BTH might lead to the potential removal of $PM_{2.5}$ (Fig. 9j). Therefore, compound pollution across the BTH region might mainly be due to local emissions of air pollutants.

In summary, the different SWPs can modulate the regional variability of summertime O_3 and $PM_{2.5}$ and their causes in summer as follows:

(1) Type 1: The area to the north of the ~~Yangtze River~~YRD under Type 1 is controlled by the westerly zone in the north of the WPSH at 500 hPa. Under the conditions of high temperature (Tmax > 27°C), moderate humidity (RH ~60%), and low PF, photochemical reactions are largely promoted to cause severe O_3 pollution. Meanwhile, BTH– NYRD~~the area from south of the BTH region to north of the YRD region~~ is located in front of the westerly trough, under the influence of the warm and humid air of the WPSH, and so the hygroscopic growth of fine particulates will cause a certain amount of $PM_{2.5}$ pollution, becoming O_3-$PM_{2.5}$ compound pollution (Fig. 12). Particularly, the prevailing southerly winds in the boundary layer can transport the pollutants emitted from southern

cities to BTH, atmospheric stratification is stable when the air mass is sinking, compound pollution may be especially severe. Although relative higher BLH occurred in the BTH, the prevailing southerly winds in the boundary layer has increased pollution more. In Figure ~~S6~~S12, we counted the number and probability of occurrence of compound pollution days in each site in summer during 2015-2018, indicating that high occurrence probability (maximum values can approach 46.7%) of compound pollution appeared in the Northern China plain (to the north of 32°N). About 55.6% of compound pollution occurrence days at all sites occurred under Type 1.

(2) Type 2: As the northern advance of WPSH from Type 1 or the retreat from Type 3 or Type 4~~The westerly trough strengthens meridionally~~, and the northern region is still controlled by the westerly zone. Ozone pollution is severe under the meteorological conditions of high temperature, moderate humidity, and few precipitations. The $PM_{2.5}$ in the BTH region, which is located in front of the westerly trough, is high since the shallow boundary layer and low wind frequency are unfavorable for pollutant diffusion. Therefore, O_3-$PM_{2.5}$ compound pollution can also be rather frequent (Fig. 12). About 33.~~0~~8% of compound pollution occurrence days at all sites occurred under Type 2 in summer during 2015-2018.

(3) Type 3: High temperature, low humidity and few precipitations ~~in~~ over the YRD region tend to generate~~s~~ a large amount of O_3, while the positive BLH and negative FLWD anomalies are unfavorable to O_3 accumulation. On the other hand, summer typhoon activities ~~will~~ might weaken the WPSH intensity over the YRD region, leading to the eastward retreat and northward shift of the WPSH~~,~~. As a result, high WS ~~in~~ across coastal areas ~~that~~ ~~will~~ could ease the ground-level O_3 pollution ~~on the ground~~ (Shu et al., 2016)~~,~~. ~~and~~ For~~high PF in~~ the BTH and PRD regions, ~~which~~ high PF tends to suppress the O_3 production. Only 6.8% of the compound pollution occurrence days at all sites occurred under Type 3~~,~~. ~~Accordingly, Type 3 is characterized as~~ in accordant with light O_3-only pollution ~~in~~ over the areas of the BTH, YRD and PRD (Fig. 12).

(4) Type 4: High temperatures, medium-high humidity and few precipitations in the GZP and PRD regions can cause O_3-$PM_{2.5}$ compound pollution, but $PM_{2.5}$ pollution in ~~the PRD~~both regions ~~is~~ are not heavy, which is possibly in relation to local lower pollutant emissions. The probability of compound pollution occurrence under Type 4 is about 5.1%. Under the control of the WPSH, there are strong photochemical reactions at high temperatures and little rainfall in ~~the~~ some eastern~~BTH~~

region (such as the northern BTH, YRD), which is also conducive to O_3 generation (Fig. 12). Meanwhile, relative to Type 1, O_3 pollution is lighter in the BTH, due to the differences of RH, BLH and FLWD.

5 Conclusions

In this study, T-PCA, an objective classification method, was applied to classify the 500-hPa weather circulation pattern as four SWPs in the summers of 2015–2018. It was found that these four SWPs are closely related to the development of the WPSH. The spatial and temporal distribution characteristics of O_3 and $PM_{2.5}$ pollution in eastern China under the four SWPs were analyzed to regulate and differentiate O_3 and $PM_{2.5}$ pollution in key areas. We find two synoptic patterns are prone to lead to co-occurrence of O_3 and $PM_{2.5}$ pollution: in ~~the southern BTH and northern YRD~~ BTH– NYRD~~ regions~~ under Type 1 and ~~the areas in the ~~BTH ~~and GZP ~~under Type 2 are associated with the double high level of O_3 and $PM_{2.5}$. The probabilities of compound pollution at all sites under Type 1, 2, 3, and 4 are 54.3%, 33.8%, 6.8%, and 5.1% respectively.~~About 55.6% of compound pollution occurrence days at all sites occurred under Type 1 while 33.0% under Type 2.~~

Type 1 weather pattern appears frequently in ~~June~~early summer, with a stable WPSH ridge ~~line~~ axis at about 22°N, and the warm and humid air brought by the WPSH reaches the area south of the Yangtze River, where a high temperature and high humidity Meiyu season is formed, the high humidity would~~ which~~ suppress~~es~~ the photochemical reaction of O_3 generation. Meanwhile, the north of China is controlled by a low-pressure trough at 500 hPa with high temperatures and little rain. The hygroscopic growth of $PM_{2.5}$ occurs in the corresponding area in front of the trough with a small amount of water vapor transported by the WPSH, causing compound pollution of O_3 and $PM_{2.5}$ in the BTH– NYRD.~~the south of the BTH region and north of the YRD region;~~. ~~particularly~~In addition, the prevailing southerly winds in the boundary layer can transport the pollutants emitted from southern cities to the BTH region, and the atmospheric stratification is stable when the air mass is sinking~~,~~. Thus, the compound pollution ~~may~~can be~~ especially~~ severe. In general, ~~T~~the synoptic circulation in the boundary layer might be responsible for the concentration of pollutants under this SWPs. ~~unfavorable pollution diffusion conditions of a shallow BLH and low WS further exacerbate~~

~~the severity of this compound pollution.~~

Under Type 2, the WPSH shifts northwards from Type 1 or retreats southwards from Type 3 or Type 4 to 32.5°N,~~northwards and retreats eastwards (sometimes retreats southwards and eastwards),~~ with the meridional deepening of the East Asian major trough at 500 hPa, and thus warm and humid airstreams are brought to the Northern China (e.g., the BTH region), gradually elevating temperatures and humidity. Although positive RH anomaly promotes hygroscopic growth of the $PM_{2.5}$, water vapor absorbs solar radiation leading to ~~leads a sink of~~reduced ~~ozone~~ O_3 formation by contrast. As a result, the probability of double high level of O_3 and $PM_{2.5}$ under Type 2 is less than Type 1, the extent of compound pollution in Type 2 is also narrowed, which mainly located in the BTH. On the other hand, weak precipitation, shallow boundary layer and low wind speed in the BTH tend to create favorable conditions for pollution maintenance. In spite of the southerly winds over the BTH, the precipitation in southern cities has reduced pollutants and reduced horizontal transport. The meteorological factors might be responsible for the accumulation of compound pollution.

In general, the location of the WPSH is tightly associated with O_3 pollution in eastern China, and the changes of meteorological conditions in different regions affected by the WPSH can induce significant regional differences in O_3 and $PM_{2.5}$ pollution. On one hand, the appropriate warm moist flow brought by the WPSH can promote hygroscopic growth of the fine particulate matter in some local areas (i.e. BTH-NYRD under Type 1 and BTH under Type 2), resulting in the increase of PM2.5 concentrations; On the other hand, transboundary O_3 was transported to these local areas at the same time, which may contribute to form the co-occurring surface O_3 and $PM_{2.5}$ pollution More importantly, the effects of various large-scale weather circulation patterns on the O_3-$PM_{2.5}$ compound pollution and their corresponding physical and chemical processes, have been clarified, which has important scientific reference value in summer air-quality forecasts, as well as assessment and policy-making services.

Besides, although this study emphasized the important impacts of large-scale synoptic drivers of co-occurring summertime O_3 and $PM_{2.5}$ pollution in eastern China, the presences of $PM_{2.5}$ may play a role in radiation forcing to reduce O_3, the interaction between O_3 and $PM_{2.5}$ which deserves further exploration to better comprehend the mechanism of O_3-$PM_{2.5}$ compound pollution in the future work.

Data availability

Hourly $PM_{2.5}$, NO_2, O_3, and O_3-8h data is published by the China Environmental Monitoring Station (http://www.cnemc.cn/). Surface meteorological data, such as Tmax, precipitation, WS and RH, radiosonde data can be obtained from the China National Meteorological Information Center of the China Meteorological Administration (http://data.cma.cn/site/index.html). The NCEP/NCAR daily reanalysis dataset can be download from https://psl.noaa.gov/data/gridded/data.ncep.reanalysis.html.

Author contributions

L. Zong: Methodology, Data Curation, Formal Analysis, Writing- Original draft preparation, Results Discussion, Writing- Reviewing and Editing；Y. Yang: Conceptualization, Methodology, Formal Analysis, Results Discussion, Writing- Reviewing and Editing；M. Gao, H. Wang, P. Wang, L. Wang, H. Zhang, G. Ning, C. Liu, Y. Li, Z. Gao: Results Discussion, Comments, Writing- Reviewing and Editing

Competing interests

The authors declare that they have no conflict of interests

Acknowledgments

This study was jointly funded by supported by the National Key Research and Development Program of China (2018YFC1506502) and the National Natural Science Foundation of China (41871029).

References

Amil, N., Latif, M. T., Khan, M. F. and Mohamad, M.: Seasonal variability of PM2.5composition and sources in the Klang Valley urban-industrial environment, Atmos. Chem. Phys., 16(8), 5357–5381, doi:10.5194/acp-16-5357-2016, 2016.

~~Beck, C. and Philipp, A.: Evaluation and comparison of circulation type classifications for the European domain, Phys. Chem. Earth, 35(9–12), 374–387, doi:10.1016/j.pce.2010.01.001, 2010.~~

Cai, W., Li, K., Liao, H., Wang, H. and Wu, L.: Weather conditions conducive to Beijing severe haze more frequent under climate change, Nat. Clim. Chang., 7(4), 257–262, doi:10.1038/nclimate3249, 2017.

Chen, C., Saikawa, E., Comer, B., Mao, X. and Rutherford, D.: Ship Emission Impacts on Air Quality and Human Health in the Pearl River Delta (PRD) Region, China, in 2015, With Projections to 2030, GeoHealth, 3(9), 284–306, doi:10.1029/2019GH000183, 2019.

Chen, H. and Wang, H.: Haze days in North China and the associated atmospheric circulations based on daily visibility data from 1960 to 2012, J. Geophys. Res., 120(12), 5895–5909, doi:10.1002/2015JD023225, 2015.

Cohen, A. J., Brauer, M., Burnett, R., Anderson, H. R., Frostad, J., Estep, K., Balakrishnan, K., Brunekreef, B., Dandona, L., Dandona, R., Feigin, V., Freedman, G., Hubbell, B., Jobling, A., Kan, H., Knibbs, L., Liu, Y., Martin, R., Morawska, L., Pope, C. A., Shin, H., Straif, K., Shaddick, G., Thomas, M., van Dingenen, R., van Donkelaar, A., Vos, T., Murray, C. J. L. and Forouzanfar, M. H.: Estimates and 25-year trends of the global burden of disease attributable to ambient air pollution: an analysis of data from the Global Burden of Diseases Study 2015, Lancet, 389(10082), 1907–1918, doi:10.1016/S0140-6736(17)30505-6, 2017.

Day, D. B., Xiang, J., Mo, J., Li, F., Chung, M., Gong, J., Weschler, C. J., Ohman-Strickland, P. A., Sundell, J., Weng, W., Zhang, Y. and Zhang, J. J.: Association of ozone exposure with cardiorespiratory pathophysiologic mechanisms in healthy adults, JAMA Intern. Med., 177(9), 1344–1353, doi:10.1001/jamainternmed.2017.2842, 2017.

Deng, Y., Li, J., Li, Y., Wu, R. and Xie, S.: Characteristics of volatile organic compounds, NO2, and effects on ozone formation at a site with high ozone level in Chengdu, J. Environ. Sci. (China), 75(2), 334–345, doi:10.1016/j.jes.2018.05.004, 2019.

Ding, Y.: The Summer Monsoon in East Asia, in Monsoons over China, pp. 1–90., 1994.

Du, Y., Wan, Q., Liu, H., Liu, H., Kapsar, K. and Peng, J.: How does urbanization influence PM 2.5 concentrations? Perspective of spillover effect of multi-dimensional urbanization impact, J. Clean. Prod., 220, 974–983, doi:10.1016/j.jclepro.2019.02.222, 2019.

Fan, H., Zhao, C. and Yang, Y.: A comprehensive analysis of the spatio-temporal variation of urban air pollution in China during 2014–2018, Atmos. Environ., 220(November), 117066, doi:10.1016/j.atmosenv.2019.117066, 2020.

Ge, J., You, Q. and Zhang, Y.: Effect of Tibetan Plateau heating on summer extreme precipitation in eastern China, Atmos. Res., 218, 364–371, doi:10.1016/j.atmosres.2018.12.018, 2019.

Gong, C. and Liao, H.: A typical weather pattern for ozone pollution events in North China, Atmos. Chem. Phys., 19(22), 13725–13740, doi:10.5194/acp-19-13725-2019, 2019.

Gu, Y., Wong, T. W., Law, S., Dong, G., Ho, K. F., Yang, Y. and Yim, S. H. L.: Impacts of sectoral emissions in China and the implications: Air quality, public health, crop production, and economic costs, Environ. Res. Lett., 13, doi:10.1088/1748-9326/aad138, 2018.

Gui, K., Che, H., Wang, Y., Wang, H., Zhang, L., Zhao, H., Zheng, Y., Sun, T. and Zhang, X.: Satellite-derived PM2.5 concentration trends over Eastern China from 1998 to 2016: Relationships to emissions and meteorological parameters, Environ. Pollut., 247, 1125–1133, doi:10.1016/j.envpol.2019.01.056, 2019.

Guo, J., Miao, Y., Zhang, Y., Liu, H., Li, Z., Zhang, W., He, J., Lou, M., Yan, Y., Bian, L. and Zhai, P.: The climatology of planetary boundary layer height in China derived from radiosonde and reanalysis data, Atmos. Chem. Phys., 16(20), 13309–13319, doi:10.5194/acp-16-13309-2016, 2016.

Guo, J., Li, Y., Cohen, J. B., Li, J., Chen, D., Xu, H., Liu, L., Yin, J., Hu, K. and Zhai, P.: Shift in the Temporal Trend of Boundary Layer Height in China Using Long-Term (1979–2016) Radiosonde Data, Geophys. Res. Lett., 46(11), 6080–6089, doi:10.1029/2019GL082666, 2019.

Gvozdić, V., Kovač-Andrić, E. and Brana, J.: Influence of Meteorological Factors NO2, SO2, CO and PM10 on the Concentration of O3 in the Urban Atmosphere of Eastern Croatia, Environ. Model. Assess., 16(5), 491–501, doi:10.1007/s10666-011-9256-4, 2011.

Han, H., Liu, J., Shu, L., Wang, T. and Yuan, H.: Local and synoptic meteorological influences on daily variability of summertime surface ozone in eastern China, Atmos. Chem. Phys. Discuss., (July), 1–51, doi:10.5194/acp-2019-494, 2019.

Han, H., Liu, J., Shu, L., Wang, T. and Yuan, H.: Local and synoptic meteorological influences on daily variability in summertime surface ozone in eastern China, Atmos. Chem. Phys., 20(1), 203–222, doi:10.5194/acp-20-203-2020, 2020.

Hoffmann, P. and Heinke SchlüNzen, K.: Weather pattern classification to represent the urban heat island in present and future climate, J. Appl. Meteorol. Climatol., 52(12), 2699–2714, doi:10.1175/JAMC-D-12-065.1, 2013.

Huang, X., Ding, A., Liu, L., Liu, Q., Ding, K., Nie, W., Xu, Z., Chi, X., Wang, M., Sun, J., Guo, W. and Fu, C.: Effects of aerosol-radiation interaction on precipitation during biomass-burning season in

East China, Atmos. Chem. Phys. Discuss., (April), 1–37, doi:10.5194/acp-2016-272, 2016.

Huth, R., Beck, C., Philipp, A., Demuzere, M., Ustrnul, Z., Cahynová, M., Kyselý, J. and Tveito, O. E.: Classifications of atmospheric circulation patterns: Recent advances and applications, Ann. N. Y. Acad. Sci., 1146, 105–152, doi:10.1196/annals.1446.019, 2008.

Ji, X., Yao, Y. and Long, X.: What causes PM2.5 pollution? Cross-economy empirical analysis from socioeconomic perspective, Energy Policy, 119(April), 458–472, doi:10.1016/j.enpol.2018.04.040, 2018.

Kley, D., Geiss, H. and Mohnen, V. A.: Tropospheric ozone at elevated sites and precursor emissions in the United States and Europe, Atmos. Environ., 28(1), 149–158, doi:10.1016/1352-2310(94)90030-2, 1994.

Li, K., Jacob, D. J., Liao, H., Zhu, J., Shah, V., Shen, L., Bates, K. H., Zhang, Q. and Zhai, S.: A two-pollutant strategy for improving ozone and particulate air quality in China, Nat. Geosci., 12(11), 906–910, doi:10.1038/s41561-019-0464-x, 2019.

Li, M., Wang, T., Xie, M., Zhuang, B., Li, S., Han, Y., Song, Y. and Cheng, N.: Improved meteorology and ozone air quality simulations using MODIS land surface parameters in the Yangtze River Delta urban cluster, China, J. Geophys. Res., 122(5), 3116–3140, doi:10.1002/2016JD026182, 2017.

Li, M., Wang, L., Liu, J., Gao, W., Song, T., Sun, Y., Li, L., Li, X., Wang, Y., Liu, L., Daellenbach, K. R., Paasonen, P. J., Kerminen, V. M., Kulmala, M. and Wang, Y.: Exploring the regional pollution characteristics and meteorological formation mechanism of PM2.5 in North China during 2013–2017, Environ. Int., 134(November 2019), 105283, doi:10.1016/j.envint.2019.105283, 2020.

Li, S., Wang, T., Huang, X., Pu, X., Li, M., Chen, P., Yang, X. Q. and Wang, M.: Impact of East Asian Summer Monsoon on Surface Ozone Pattern in China, J. Geophys. Res. Atmos., 123(2), 1401–1411, doi:10.1002/2017JD027190, 2018.

Liu, H., Tian, H., Zhang, K., Liu, S., Cheng, K., Yin, S., Liu, Y., Liu, X., Wu, Y., Liu, W., Bai, X., Wang, Y., Shao, P., Luo, L., Lin, S., Chen, J. and Liu, X.: Seasonal variation, formation mechanisms and potential sources of PM2.5 in two typical cities in the Central Plains Urban Agglomeration, China, Sci. Total Environ., 657, 657–670, doi:10.1016/j.scitotenv.2018.12.068, 2019a.

Liu, J. and You, Q.: A diagnosis of the interannual variation of the summer hydrometeor based on ERA-interim over Eastern China, Atmos. Res., 231(October 2018), 104654, doi:10.1016/j.atmosres.2019.104654, 2020.

Liu, N., Zhou, S., Liu, C. and Guo, J.: Synoptic circulation pattern and boundary layer structure associated with PM2.5 during wintertime haze pollution episodes in Shanghai, Atmos. Res., 228(46), 186–195, doi:10.1016/j.atmosres.2019.06.001, 2019b.

Ma, Z., Hu, X., Sayer, A. M., Levy, R., Zhang, Q., Xue, Y., Tong, S., Bi, J., Huang, L. and Liu, Y.: Satellite-based spatiotemporal trends in PM2.5 concentrations: China, 2004-2013, Environ. Health Perspect., 124(2), 184–192, doi:10.1289/ehp.1409481, 2016.

Miao, Y., Hu, X.-M., Liu, S., Qian, T., Xue, M., Zheng, Y. and Wang, S.: Seasonal variation of local atmospheric circulations and boundary layer structure in the Beijing-Tianjin-Hebei region and implications for air quality., J. Adv. Model. Earth Syst., 7, 1602–1626, doi:10.1002/2015ms000522, 2015.

Miao, Y., Guo, J., Liu, S., Liu, H., Li, Z., Zhang, W. and Zhai, P.: Classification of summertime synoptic patterns in Beijing and their associations with boundary layer structure affecting aerosol pollution, Atmos. Chem. Phys., 17(4), 3097–3110, doi:10.5194/acp-17-3097-2017, 2017.

Miao, Y., Liu, S. and Huang, S.: Synoptic pattern and planetary boundary layer structure associated with aerosol pollution during winter in Beijing, China, Sci. Total Environ., 682, 464–474, doi:10.1016/j.scitotenv.2019.05.199, 2019a.

Miao, Y., Liu, S. and Huang, S.: Synoptic pattern and planetary boundary layer structure associated with aerosol pollution during winter in Beijing, China, Sci. Total Environ., 682, 464–474, doi:10.1016/j.scitotenv.2019.05.199, 2019b.

Miao, Y., Che, H., Zhang, X. and Liu, S.: Relationship between summertime concurring PM2.5 and O3 pollution and boundary layer height differs between Beijing and Shanghai, China, Environ. Pollut., doi:10.1016/j.envpol.2020.115775, 2020.

Ning, G., Wang, S., Yim, S. H. L., Li, J., Hu, Y., Shang, Z., Wang, J. and Wang, J.: Impact of low-pressure systems on winter heavy air pollution in the northwest Sichuan Basin, China, Atmos. Chem. Phys., 18(18), 13601–13615, doi:10.5194/acp-18-13601-2018, 2018.

Ning, G., Yim, S. H. L., Wang, S., Duan, B., Nie, C., Yang, X., Wang, J. and Shang, K.: Synergistic effects of synoptic weather patterns and topography on air quality: a case of the Sichuan Basin of China, Clim. Dyn., 53(11), 6729–6744, doi:10.1007/s00382-019-04954-3, 2019.

Philipp, A., Beck, C., Esteban, P., Krennert, T., Lochbihler, K., Spyros, P., Pianko-kluczynska, K., Post, P., Alvarez, R., Spekat, A. and Streicher, F.: Cost733 user guide., 2014.

Riyu, L.: Indices of the Summertime Western North Pacific Subtropical High, Adv. Atmos. Sci., 19(6), 1004–1028, doi:10.1007/s00376-002-0061-5, 2002.

Saikawa, E., Kim, H., Zhong, M., Avramov, A., Zhao, Y., Janssens-Maenhout, G., Kurokawa, J. I., Klimont, Z., Wagner, F., Naik, V., Horowitz, L. W. and Zhang, Q.: Comparison of emissions inventories of anthropogenic air pollutants and greenhouse gases in China, Atmos. Chem. Phys., 17(10), 6393–6421, doi:10.5194/acp-17-6393-2017, 2017.

Shi, Z., Huang, L., Li, J., Ying, Q., Zhang, H. and Hu, J.: Sensitivity Analysis of the Surface Ozone and Fine Particulate Matter to Meteorological Parameters in China, Atmos. Chem. Phys. Discuss., 2020, 1–29, doi:10.5194/acp-2020-173, 2020.

Shu, L., Xie, M., Wang, T., Gao, D., Chen, P., Han, Y., Li, S., Zhuang, B. and Li, M.: Integrated studies of a regional ozone pollution synthetically affected by subtropical high and typhoon system in the Yangtze River Delta region, China, Atmos. Chem. Phys., 16(24), 15801–15819, doi:10.5194/acp-16-15801-2016, 2016.

Shu, L., Wang, T., Xie, M., Li, M., Zhao, M., Zhang, M. and Zhao, X.: Episode study of fine particle and ozone during the CAPUM-YRD over Yangtze River Delta of China: Characteristics and source attribution, Atmos. Environ., 203(July 2018), 87–101, doi:10.1016/j.atmosenv.2019.01.044, 2019.

Sillman, S.: Chapter 12 The relation between ozone, NOx and hydrocarbons in urban and polluted rural environments, Dev. Environ. Sci., 1(C), 339–385, doi:10.1016/S1474-8177(02)80015-8, 2002.

Song, C., Wu, L., Xie, Y., He, J., Chen, X., Wang, T., Lin, Y., Jin, T., Wang, A., Liu, Y., Dai, Q., Liu, B., Wang, Y. nan and Mao, H.: Air pollution in China: Status and spatiotemporal variations, Environ. Pollut., 227, 334–347, doi:10.1016/j.envpol.2017.04.075, 2017.

Sun, L., Xue, L., Wang, T., Gao, J., Ding, A., Cooper, O. R., Lin, M., Xu, P., Wang, Z., Wang, X., Wen, L., Zhu, Y., Chen, T., Yang, L., Wang, Y., Chen, J. and Wang, W.: Significant increase of summertime ozone at Mount Tai in Central Eastern China, Atmos. Chem. Phys., 16(16), 10637–10650, doi:10.5194/acp-16-10637-2016, 2016.

Tai, A. P. K., Mickley, L. J. and Jacob, D. J.: Correlations between fine particulate matter (PM2.5) and meteorological variables in the United States: Implications for the sensitivity of PM2.5 to climate change, Atmos. Environ., 44(32), 3976–3984, doi:10.1016/j.atmosenv.2010.06.060, 2010.

Wang, H., Li, J., Gao, Z., Yim, S. H. L., Shen, H., Ho, H. C., Li, Z., Zeng, Z., Liu, C., Li, Y., Ning, G. and Yang, Y.: High-spatial-resolution population exposure to PM2.5 pollution based on multi-satellite retrievals: A case study of seasonal variation in the Yangtze River Delta, China in 2013, Remote Sens., 11(23), doi:10.3390/rs11232724, 2019a.

Wang, H. J. and Chen, H. P.: Understanding the Recent Trend of Haze Pollution in Eastern China: Roles of Climate Change, Atmos. Chem. Phys. Discuss., 2016(January), 1–18, doi:10.5194/acp-2015-1009, 2016.

Wang, N., Lyu, X., Deng, X., Huang, X., Jiang, F. and Ding, A.: Aggravating O 3 pollution due to NO x emission control in eastern China, Sci. Total Environ., 677(x), 732–744, doi:10.1016/j.scitotenv.2019.04.388, 2019b.

Wang, T., Zhong, Z., Sun, Y. and Wang, J.: Impacts of tropical cyclones on the meridional movement of the western Pacific subtropical high, Atmos. Sci. Lett., 20(5), 1–8, doi:10.1002/asl.893, 2019c.

Xie, M., Zhu, K., Wang, T., Chen, P., Han, Y., Li, S., Zhuang, B. and Shu, L.: Temporal characterization and regional contribution to O 3 and NO x at an urban and a suburban site in Nanjing, China, Sci. Total Environ., 551–552(x), 533–545, doi:10.1016/j.scitotenv.2016.02.047, 2016.

~~Xie, M., Shu, L., Wang, T., Gao, D., Li, S., Zhuang, B., Huang, A., Fang, D., Han, Y., Li, M., Chen, P., Liu, Z., Wu, Z. and Lu, H.: Inter-annual variation of aerosol pollution in East Asia and its relation with strong/weak East Asian winter monsoon, Atmos. Chem. Phys. Discuss., (June), 1–38, doi:10.5194/acp-2017-500, 2017.~~

Yang, Y., Zheng, X., Gao, Z., Wang, H., Wang, T., Li, Y., Lau, G. N. C. and Yim, S. H. L.: Long-Term Trends of Persistent Synoptic Circulation Events in Planetary Boundary Layer and Their Relationships With Haze Pollution in Winter Half Year Over Eastern China, J. Geophys. Res. Atmos., 123(19), 10,991-11,007, doi:10.1029/2018JD028982, 2018.

Yang, Y., Zheng, Z., Yim, S. Y. L., Roth, M., Ren, G., Gao, Z., Wang, T., Li, Q., Shi, C., Ning, G. and Li, Y.: PM2.5 Pollution Modulates Wintertime Urban Heat Island Intensity in the Beijing-Tianjin-Hebei Megalopolis, China, Geophys. Res. Lett., 47(1), 0–3, doi:10.1029/2019GL084288, 2020.

Ye, W. F., Ma, Z. Y. and Ha, X. Z.: Spatial-temporal patterns of PM2.5 concentrations for 338 Chinese cities, Sci. Total Environ., 631–632, 524–533, doi:10.1016/j.scitotenv.2018.03.057, 2018.

Yim, S. H. L., Wang, M., Gu, Y., Yang, Y., Dong, G. and Li, Q.: Effect of Urbanization on Ozone and Resultant Health Effects in the Pearl River Delta Region of China, J. Geophys. Res. Atmos., 124(21), 11568–11579, doi:10.1029/2019JD030562, 2019.

Yin, Z., Cao, B. and Wang, H.: Dominant patterns of summer ozone pollution in eastern China and associated atmospheric circulations, Atmos. Chem. Phys., 19(22), 13933–13943, doi:10.5194/acp-19-13933-2019, 2019.

Yu, S., Yin, S., Zhang, R., Wang, L., Su, F., Zhang, Y. and Yang, J.: Spatiotemporal characterization and regional contributions of O3 and NO2: An investigation of two years of monitoring data in Henan, China, J. Environ. Sci. (China), 90(November), 29–40, doi:10.1016/j.jes.2019.10.012, 2020.

Yue, X., Unger, N., Harper, K., Xia, X., Liao, H., Zhu, T., Xiao, J., Feng, Z. and Li, J.: Ozone and haze pollution weakens net primary productivity in China, Atmos. Chem. Phys., 17(9), 6073–6089, doi:10.5194/acp-17-6073-2017, 2017.

Zhang, C., Liu, C., Hu, Q., Cai, Z., Su, W., Xia, C., Zhu, Y., Wang, S. and Liu, J.: Satellite UV-Vis spectroscopy: implications for air quality trends and their driving forces in China during 2005–2017, Light Sci. Appl., 8(1), doi:10.1038/s41377-019-0210-6, 2019a.

Zhang, H., Wang, Y., Park, T. W. and Deng, Y.: Quantifying the relationship between extreme air pollution events and extreme weather events, Atmos. Res., 188, 64–79, doi:10.1016/j.atmosres.2016.11.010, 2017.

Zhang, Q., Zheng, Y., Tong, D., Shao, M., Wang, S., Zhang, Y., Xu, X., Wang, J., He, H., Liu, W., Ding, Y., Lei, Y., Li, J., Wang, Z., Zhang, X., Wang, Y., Cheng, J., Liu, Y., Shi, Q., Yan, L., Geng, G., Hong, C., Li, M., Liu, F., Zheng, B., Cao, J., Ding, A., Gao, J., Fu, Q., Huo, J., Liu, B., Liu, Z., Yang, F., He, K. and Hao, J.: Drivers of improved PM2.5 air quality in China from 2013 to 2017, Proc. Natl. Acad. Sci. U. S. A., 116(49), 24463–24469, doi:10.1073/pnas.1907956116, 2019b.

Zhang, R. H., Li, Q. and Zhang, R. N.: Meteorological conditions for the persistent severe fog and haze event over eastern China in January 2013, Sci. China Earth Sci., 57(1), 26–35, doi:10.1007/s11430-013-4774-3, 2014.

Zhang, W., Wang, H., Zhang, X., Peng, Y., Zhong, J., Wang, Y. and Zhao, Y.: Evaluating the contributions of changed meteorological conditions and emission to substantial reductions of PM2.5 concentration from winter 2016 to 2017 in Central and Eastern China, Sci. Total Environ., 716, 136892, doi:10.1016/j.scitotenv.2020.136892, 2020.

Zhang, Y., Ding, A., Mao, H., Nie, W., Zhou, D., Liu, L., Huang, X. and Fu, C.: Impact of synoptic weather patterns and inter-decadal climate variability on air quality in the North China Plain during 1980-2013, Atmos. Environ., 124, 119–128, doi:10.1016/j.atmosenv.2015.05.063, 2016a.

Zhang, Y. L. and Cao, F.: Fine particulate matter (PM 2.5) in China at a city level, Sci. Rep., 5(2014), 1–12, doi:10.1038/srep14884, 2015.

Zhang, Z., Zhang, X., Gong, D., Quan, W., Zhao, X., Ma, Z. and Kim, S. J.: Evolution of surface O3 and PM2.5 concentrations and their relationships with meteorological conditions over the last decade in Beijing, Atmos. Environ., 108, 67–75, doi:10.1016/j.atmosenv.2015.02.071, 2015.

Zhang, Z., Zhang, X., Gong, D., Kim, S. J., Mao, R. and Zhao, X.: Possible influence of atmospheric circulations on winter haze pollution in the Beijing-Tianjin-Hebei region, northern China, Atmos. Chem. Phys., 16(2), 561–571, doi:10.5194/acp-16-561-2016, 2016b.

Zhao, C., Wang, Y., Yang, Q., Fu, R., Cunnold, D. and Choi, Y.: Impact of East Asian summer monsoon on the air quality over China: View from space, J. Geophys. Res. Atmos., 115(9), 1–12, doi:10.1029/2009JD012745, 2010.

Zhao, W., Tang, G., Yu, H., Yang, Y., Wang, Y., Wang, L., An, J., Gao, W., Hu, B., Cheng, M., An, X., Li, X. and Wang, Y.: Evolution of boundary layer ozone in Shijiazhuang, a suburban site on the North China Plain, J. Environ. Sci. (China), 83, 152–160, doi:10.1016/j.jes.2019.02.016, 2019.

Zhao, Z. and Wang, Y.: Influence of the West Pacific subtropical high on surface ozone daily variability in summertime over eastern China, Atmos. Environ., 170, 197–204, doi:10.1016/j.atmosenv.2017.09.024, 2017.

Zheng, X. Y., Fu, Y. F., Yang, Y. J. and Liu, G. S.: Impact of atmospheric circulations on aerosol distributions in autumn over eastern China: Observational evidence, Atmos. Chem. Phys., 15(21), 12115–12138, doi:10.5194/acp-15-12115-2015, 2015.

Zhong, M., Chen, F. and Saikawa, E.: Sensitivity of projected PM2.5- and O3-related health impacts to model inputs: A case study in mainland China, Environ. Int., 123(May 2018), 256–264, doi:10.1016/j.envint.2018.12.002, 2019.

Zhu, J., Liao, H. and Li, J.: Increases in aerosol concentrations over eastern China due to the decadal-scale weakening of the East Asian summer monsoon, Geophys. Res. Lett., 39(9), 1–6, doi:10.1029/2012GL051428, 2012.

Table 1. Over-limit ratio and concentration of MDA8 O_3 and PM2.5 calculated via stations × days in key urban clusters under four SWPs

Urban cluster	Month	Type1					Type2					Type3					Type4				
		Stas × days	MDA O_3		$PM_{2.5}$		Stas × days	MDA O_3		$PM_{2.5}$		Stas × days	MDA O_3		$PM_{2.5}$		Stas × days	MDAO_3		$PM_{2.5}$	
			OLR	Con	OLR	Con		OLR	Con	OLR	Con		OLR	Con	OLR	Con		OLR	Con	OLR	Con
BTH	6	6416	57.3%	172.5	16.7%	49.2	122	91.8%	209.6	3.3%	46.0	59	62.7%	176.0	32.2%	67.1	0	0	0	0	0
	7	1716	25.6%	134.2	21.2%	51.8	3681	54.2%	165.6	22.5%	56.9	1356	33.8%	141.8	12.9%	46.7	577	43.5%	153.7	8.8%	49.5
	8	1188	18.9%	118.5	6.9%	33.1	2805	35.3%	143.1	14.7%	44.0	1671	18.9%	121.2	10.1%	42.5	1268	31.9%	144.3	6.0%	39.7
	6~8	9320	46.6%	158.6	16.3%	47.6	365	54.2%	169.8	18.8%	51.2	3086	26.3%	131.3	11.7%	44.8	1845	35.5%	147.3	6.9%	42.8
YRD	6	19329	26.2%	127.2	4.4%	36.8	11098	14.3%	107.0	2.2%	44.5	181	12.7%	102.4	0.6%	32.0	0	0	0	0	0
	7	5207	24.5%	119.8	5.3%	38.6	8459	22.0%	120.1	0.6%	28.0	4135	14.5%	112.6	0.1%	24.0	1743	30.9%	139.5	0.3%	30.0
	8	3593	25.5%	127.6	0.3%	28.6	19922	18.3%	113.8	3.0%	33.3	4993	16.9%	116.7	0.0%	23.7	3817	14.7%	114.8	0.1%	25.1
	6~8	28129	25.8%	125.9	4.0%	36.1	13754	17.4%	112.5	1.7%	30.6	9309	15.8%	114.6	0.1%	24.0	5560	19.7%	122.5	0.1%	26.7
PRD	6	5327	5.2%	80.1	0	16.8	101	31.7%	146.9	0	24.9	48	0	77.6	0	13.2	0	0	0	0	0
	7	1431	20.3%	107.2	0.6%	25.3	3076	7.6%	81.8	0.1%	19.1	1079	13.3%	92.4	0	19.3	461	8.0%	82.1	0	17.9
	8	977	25.4%	122.5	1.1%	27.9	2316	20.6%	108.5	0.6%	28.0	1376	15.5%	103.4	0.3%	24.0	993	17.9%	111.4	0.1%	25.1
	6~8	7735	10.5%	90.5	0.2%	19.8	5493	13.5%	94.3	0.3%	23.0	2503	14.3%	98.2	0.2%	21.8	1454	14.8%	102.1	0.1%	22.8
GZP	6	1549	42.9%	147.6	0.4%	33.2	38	52.6%	165.3	0	30.4	19	26.3%	150.8	0	34.7	0	0	0	0	0
	7	1879	40.7%	145.0	1.9%	33.7	1168	47.4%	160.3	0	30.2	432	24.3%	133.3	1.2%	31.7	173	26.6%	144.1	0	26.4
	8	537	28.5%	134.0	1.6%	31.6	850	36.8%	146.3	1.6%	34.2	530	28.9%	143.1	1.9%	37.2	394	38.6%	154.9	1.3%	39.9
	6~8	368	15.2%	112.9	0.9%	32.4	2056	43.1%	154.6	2.1%	35.9	981	26.8%	138.9	1.5%	34.7	567	34.9%	151.6	0.9%	35.8
NEM	6	13126	17.9%	121.0	1.7%	26.4	243	64.2%	175.3	0.4%	31.1	120	13.3%	123.3	0.8%	37.6	0	0	0	0	0
	7	3422	8.9%	106.8	2.3%	25.2	7338	17.0%	120.7	1.3%	28.1	2722	5.7%	93.0	0.7%	20.8	1141	15.1%	122.4	0.2%	24.3
	8	2341	4.4%	92.6	1.0%	20.1	5520	6.3%	91.0	1.3%	21.0	3282	5.6%	98.3	0.9%	23.2	2507	7.8%	97.8	0.2%	19.5
	6~8	18889	14.6%	114.9	1.7%	25.4	13101	13.4%	109.2	1.3%	25.2	6124	5.8%	96.4	0.8%	22.4	3648	10.1%	105.5	0.2%	21.0

Notes: stas × days, stations × days; OLR, Over-limit ratio; Con, Concentration (μg m^{-3}).

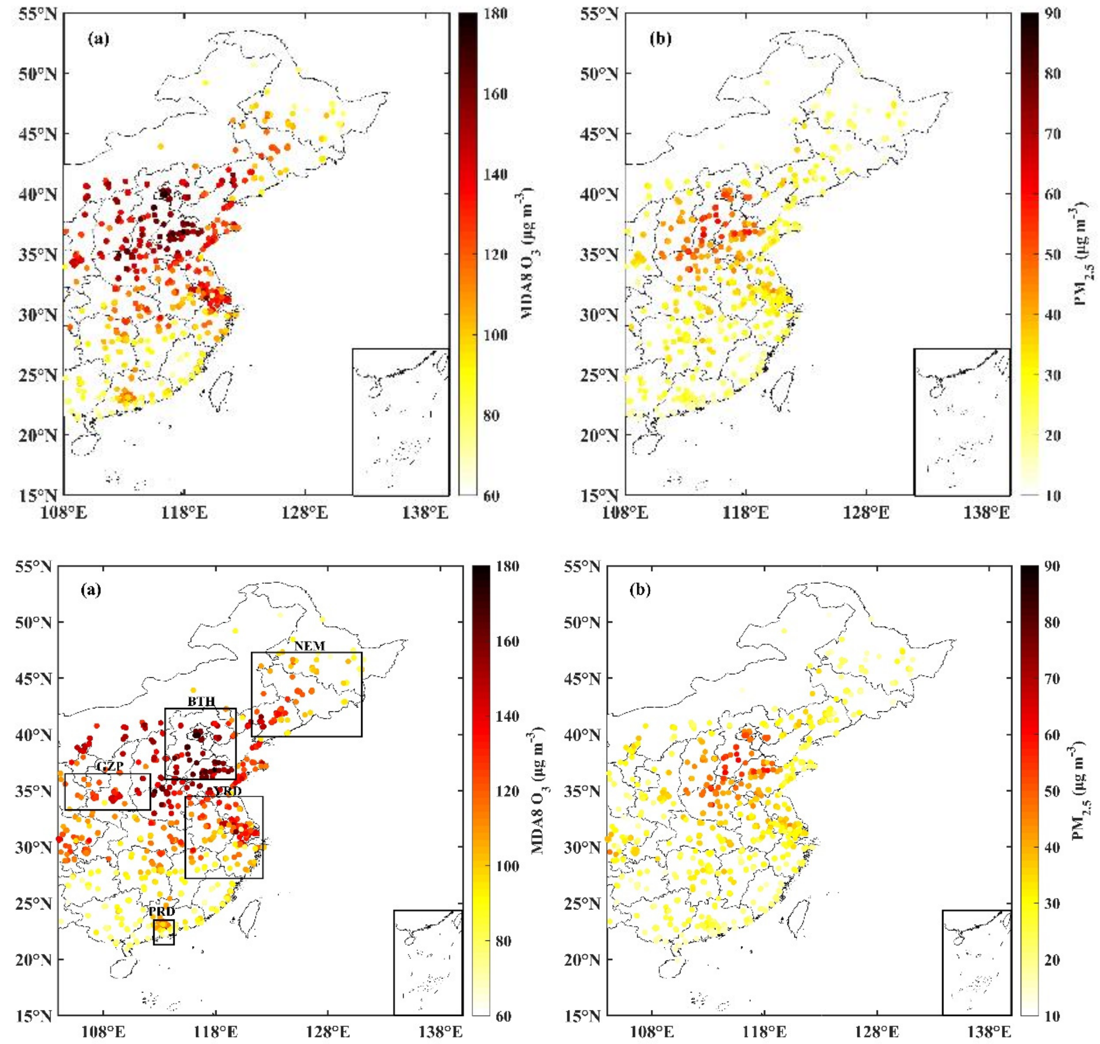

Fig. 1. Average concentration of MDA8 O_3 (a) and $PM_{2.5}$ (b) in eastern China during summers of 2015–2018. Stations and key urban clusters (~~red~~ black box) are shown in (a).

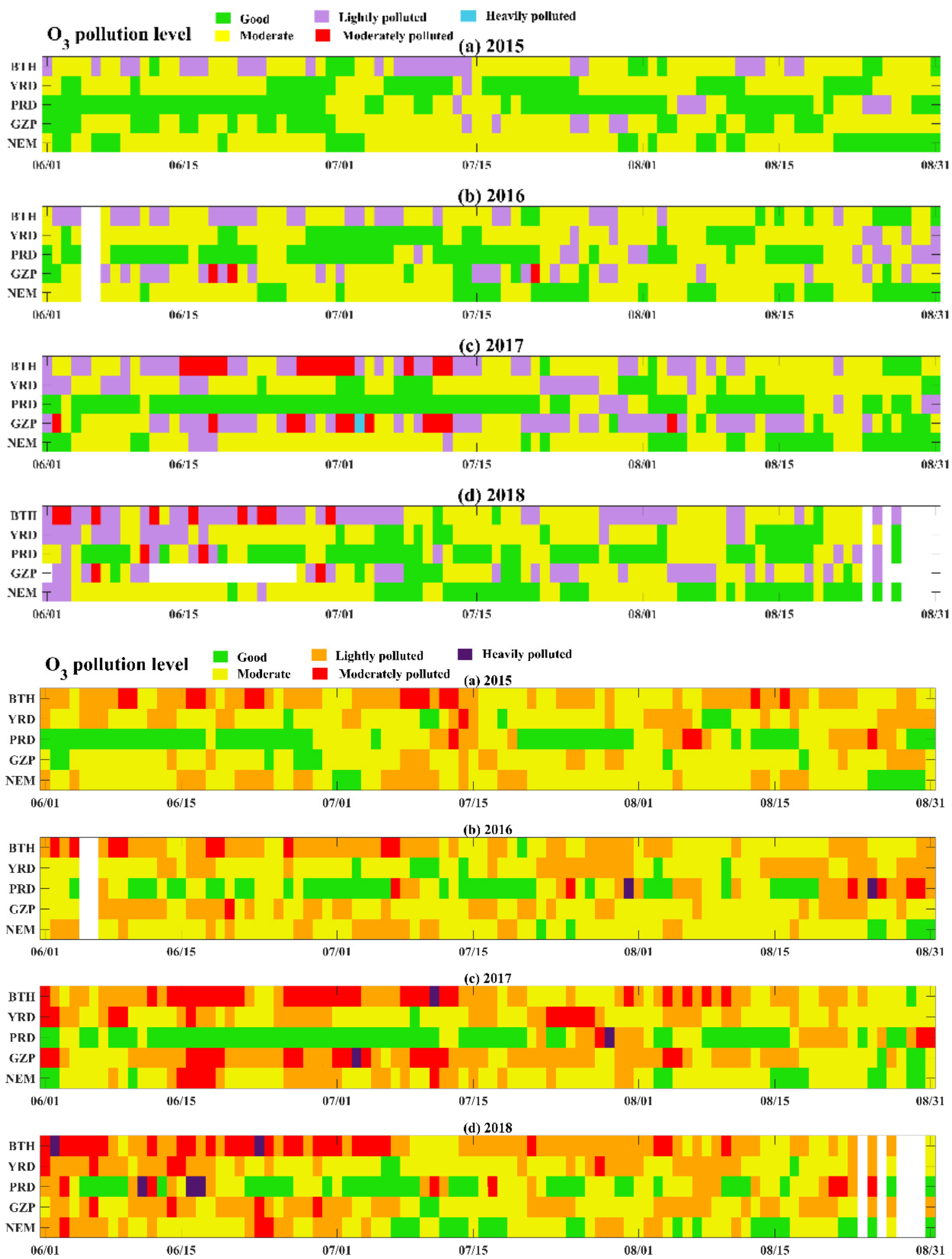

960 **Fig. 2. Time series of MDA8 O_3 pollution levels in key urban clusters.**

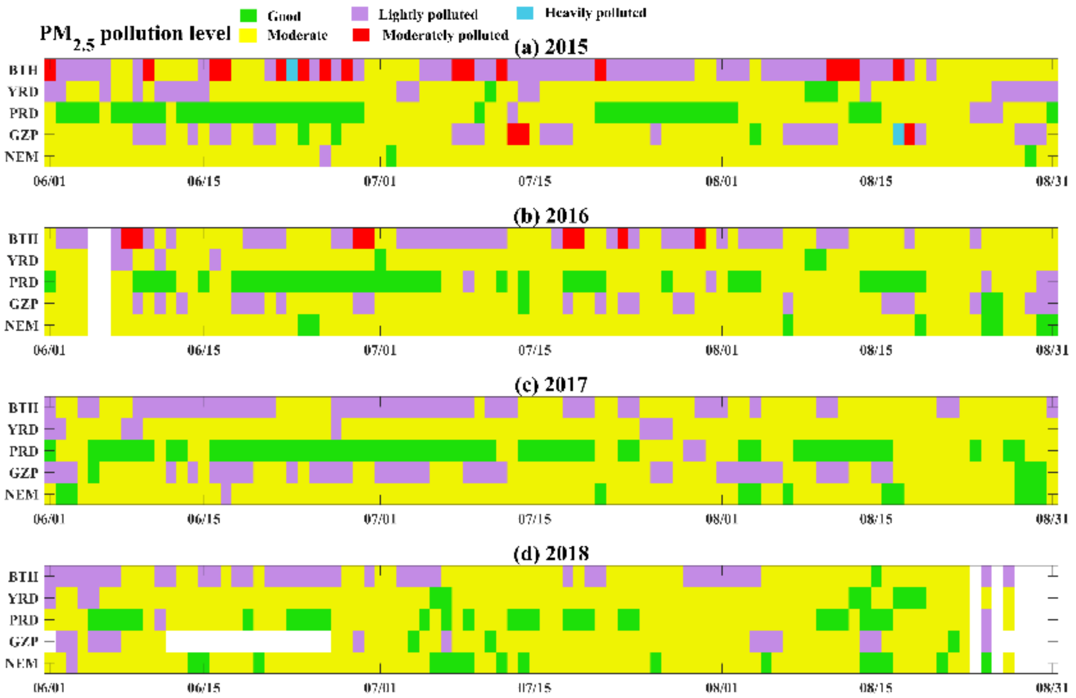

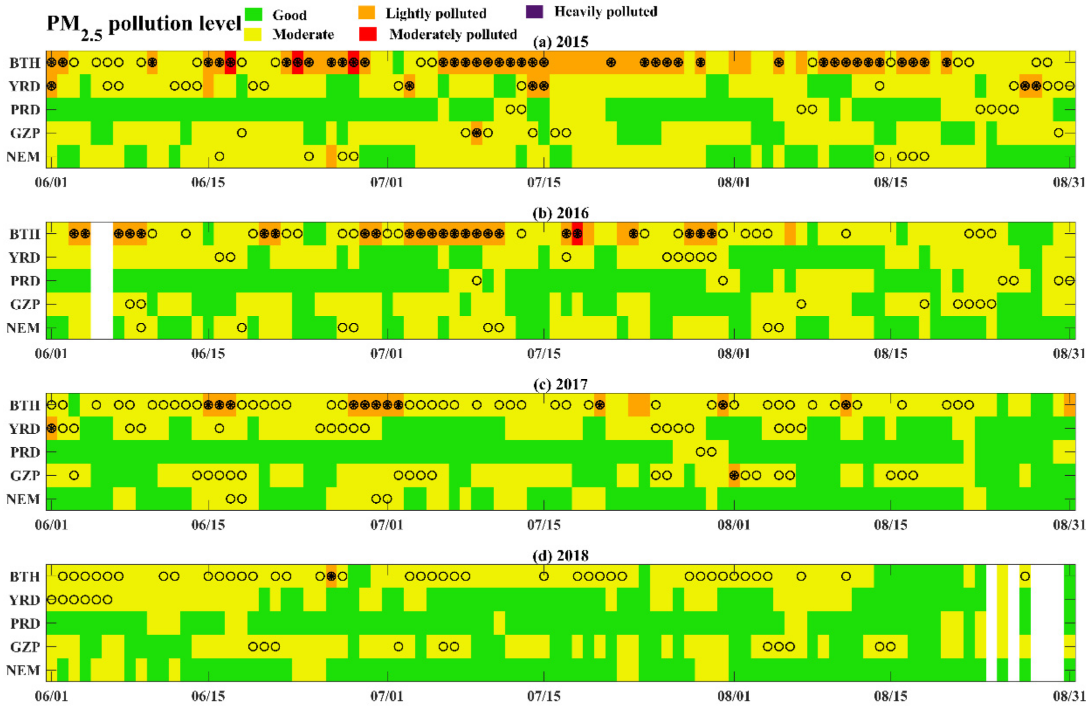

Fig.3. Time series of $PM_{2.5}$ pollution levels in key urban clusters. **The black dots indicate the co-occurred events. The asterisks indicate the co-occurred events under Chinese standard (WHO interim target 1, IT-1), and the circles indicate the co-occurred events under WHO IT-2.**

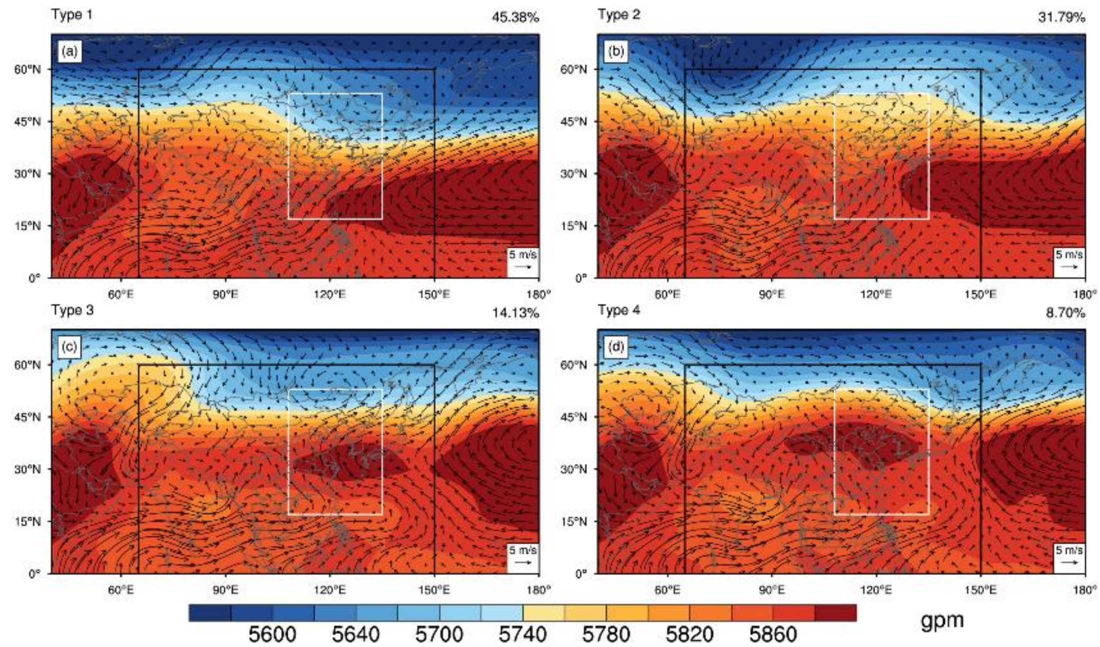

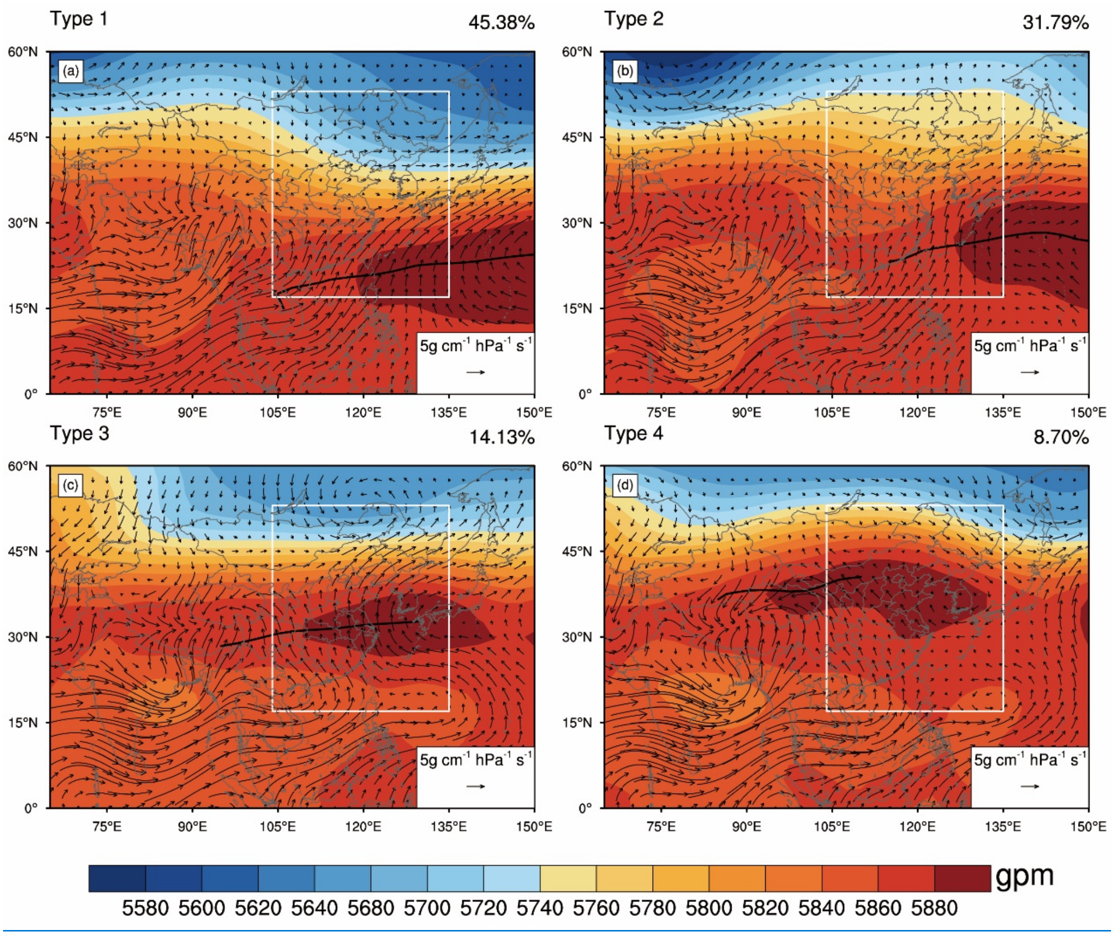

Fig. 4. 850-hPa 850-hPa water vapor flux ($WVF = V * q/g$, q is specific humidity, g is gravitational acceleration, V is horizontal wind; vectors; see scale arrow at the bottom right in units of 5 g cm^{-1}hPa^{-1}s^{-1})~~wind (vectors; see scale arrow at the bottom right in units of 5m/s)~~ and 500-hPa GH (contours; see scale bar at bottom in units of gpm) patterns based on

objective classification (see text for details). ~~Black box area indicates the area for classification and the w~~White box area is for the area of eastern China, the number at the upper right corner of each panel indicates the frequency of the occurrence of each pattern type,~~.~~ and the black line of each panel presents the ridge axis of the WPSH.

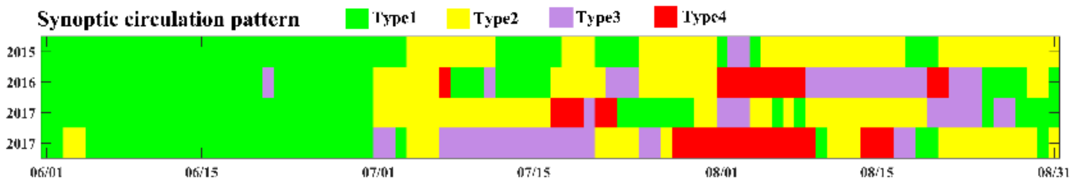

Fig. 5. Time series of synoptic circulation pattern.

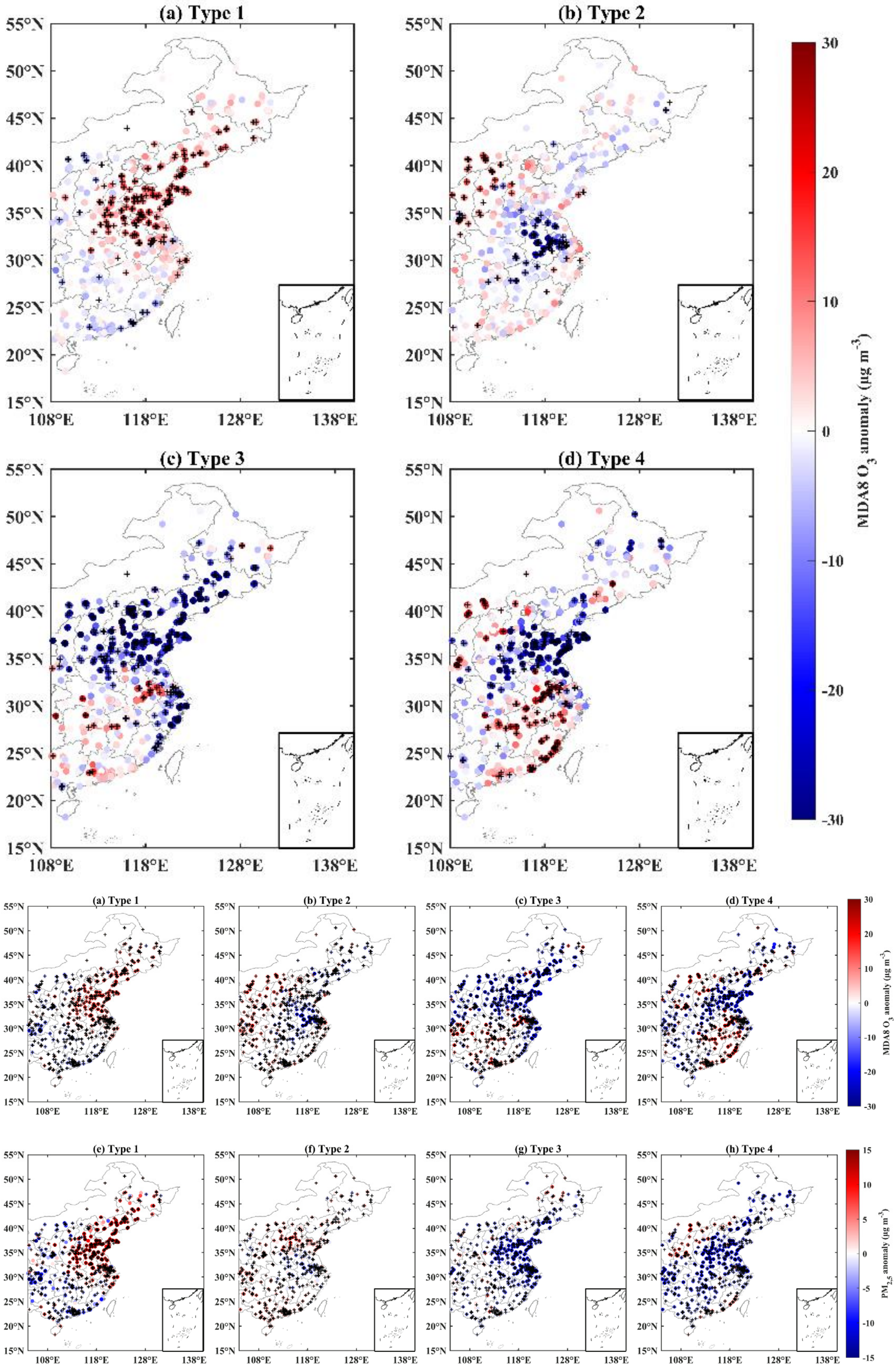

Fig. 6. The MDA8 O_3 (a-d) and $PM_{2.5}$ (e-h) anomaly under four SWPs, where the sites marked with a '+' indicates the Analysis of Variance passes the significance level of 0.05.

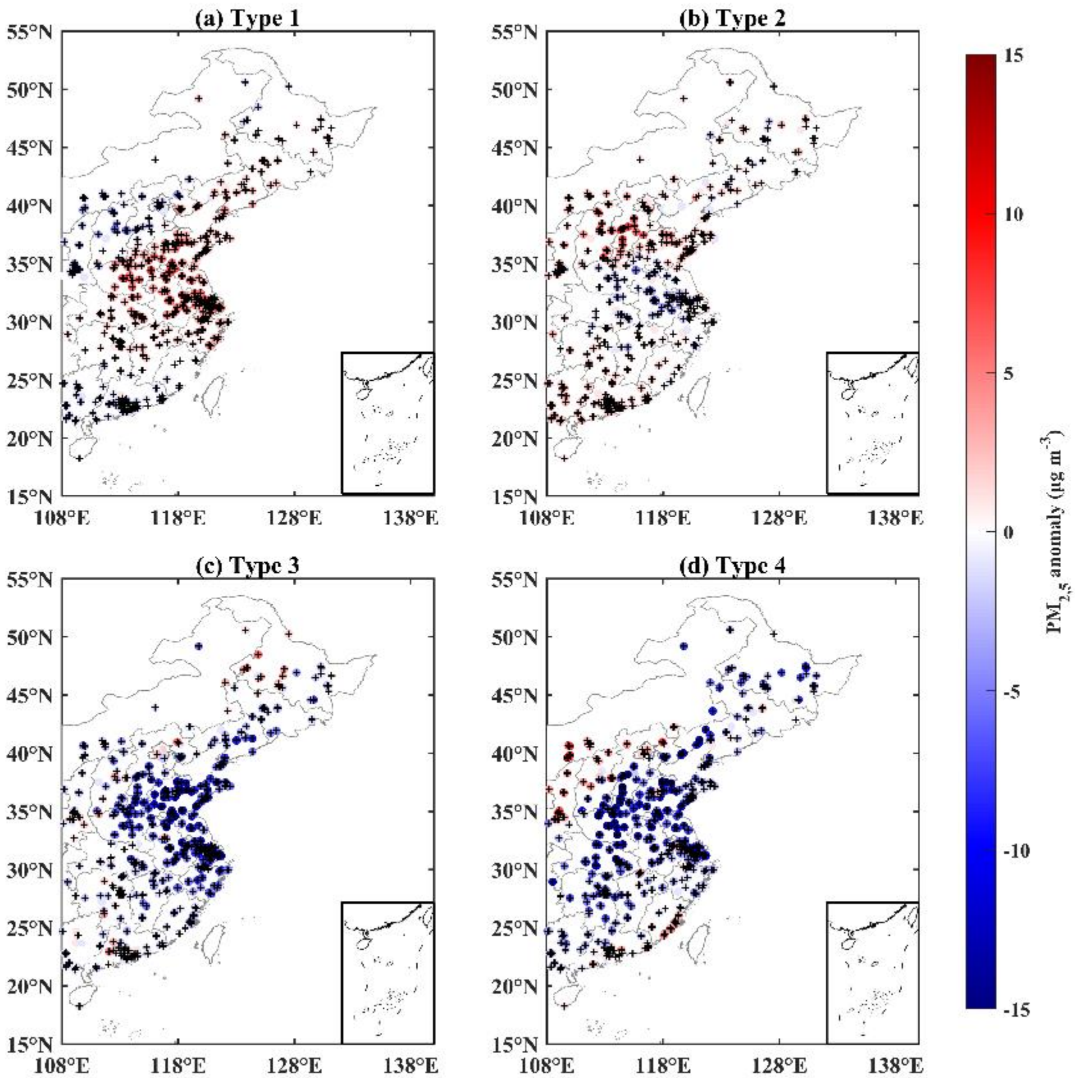

Fig. 7. The $PM_{2.5}$ anomaly under four SWPs, where the sites marked with a '+' indicates the Analysis of Variance passes the significance level of 0.05.

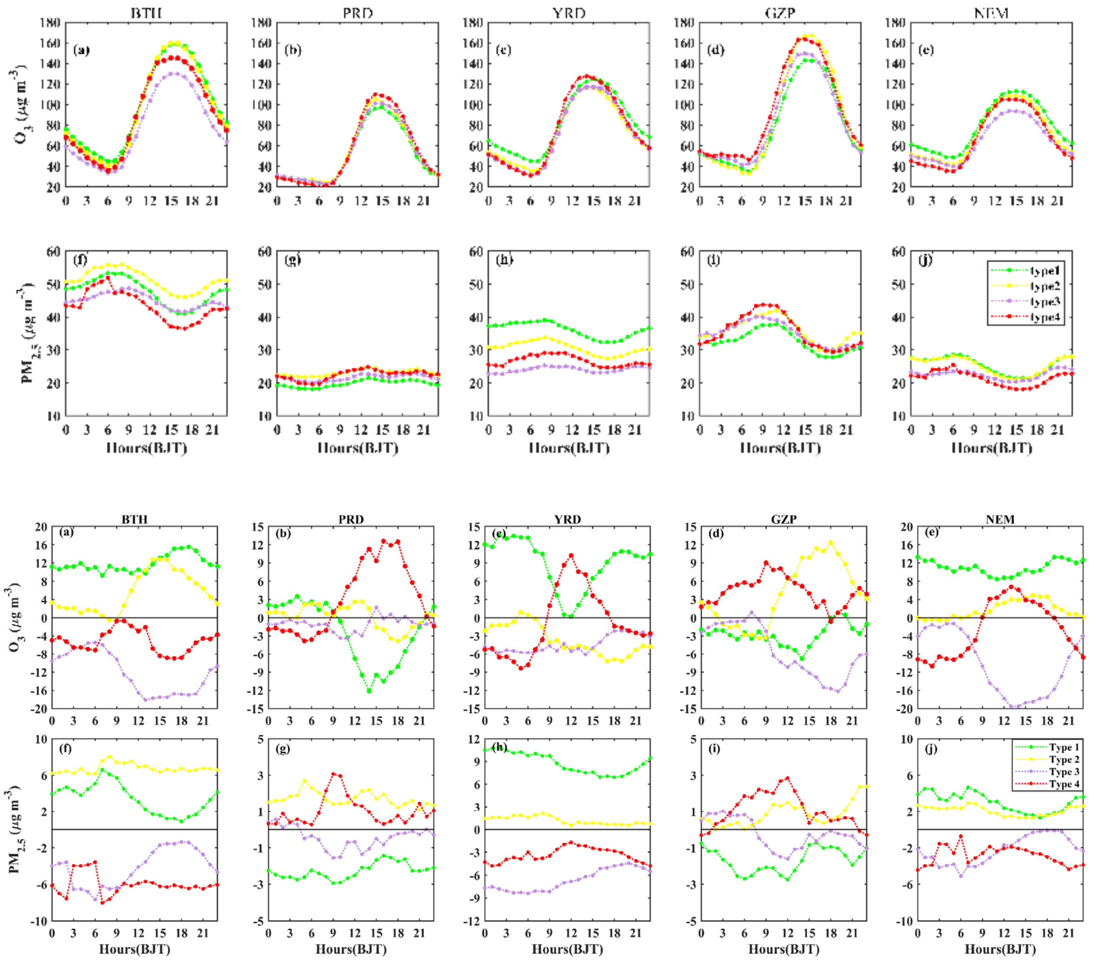

Fig. 87. Daily variation of O_3 and $PM_{2.5}$ anomalies under four SWPs in key urban clusters.

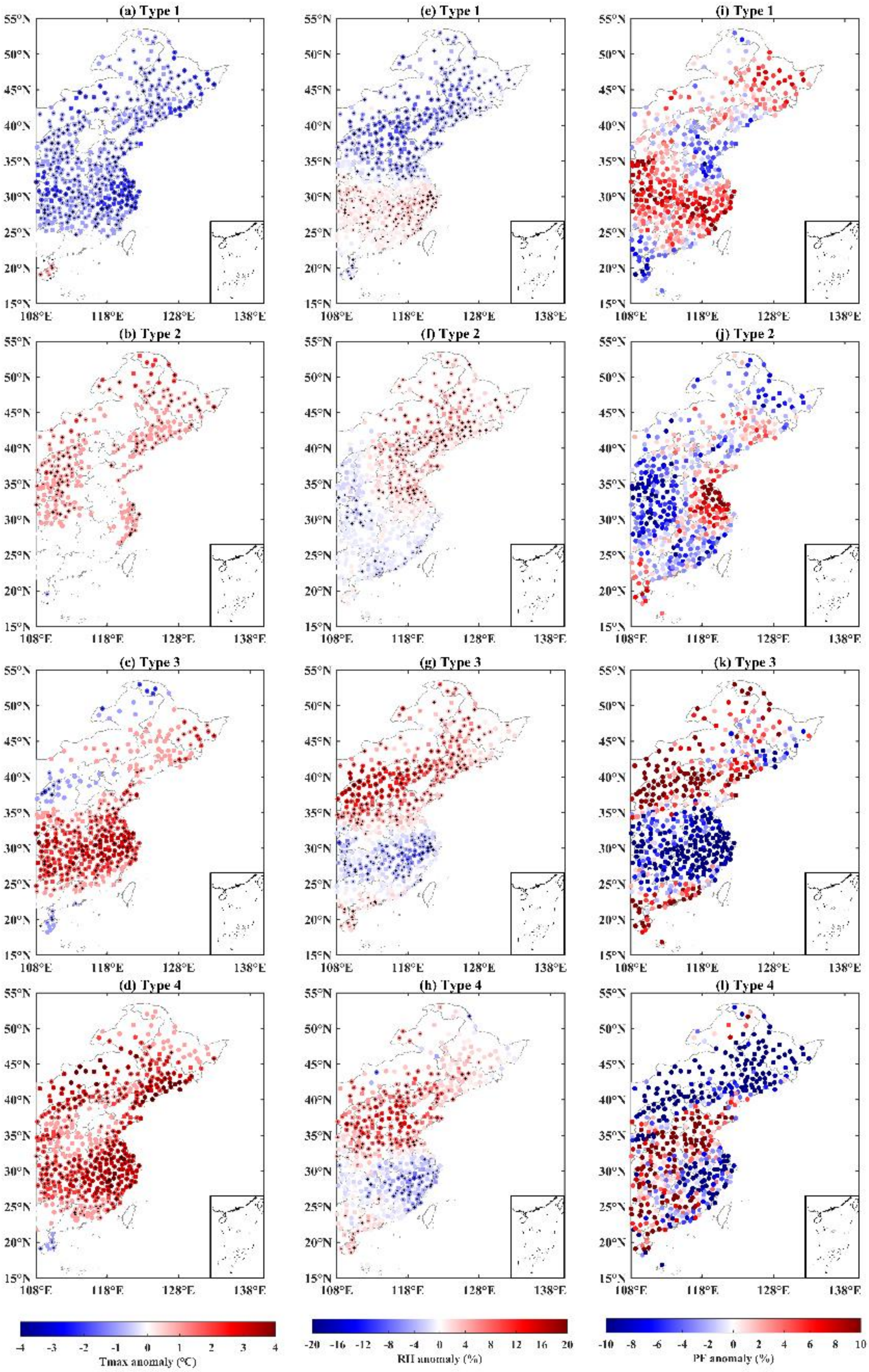

(a) Type 1
(b) Type 2
(c) Type 3
(d) Type 4
(e) Type 1
(f) Type 2
(g) Type 3
(h) Type 4
(i) Type 1
(j) Type 2
(k) Type 3
(l) Type 4
55°N
50°N
45°N
40°N
35°N
30°N
25°N
20°N
15°N
108°E
118°E
128°E
138°E
-4 -3 -2 -1 0 1 2 3 4
Tmax anomaly (°C)
-20 -16 -12 -8 -4 0 4 8 12 16 20
RH anomaly (%)
-10 -8 -6 -4 -2 0 2 4 6 8 10
PF anomaly (%)

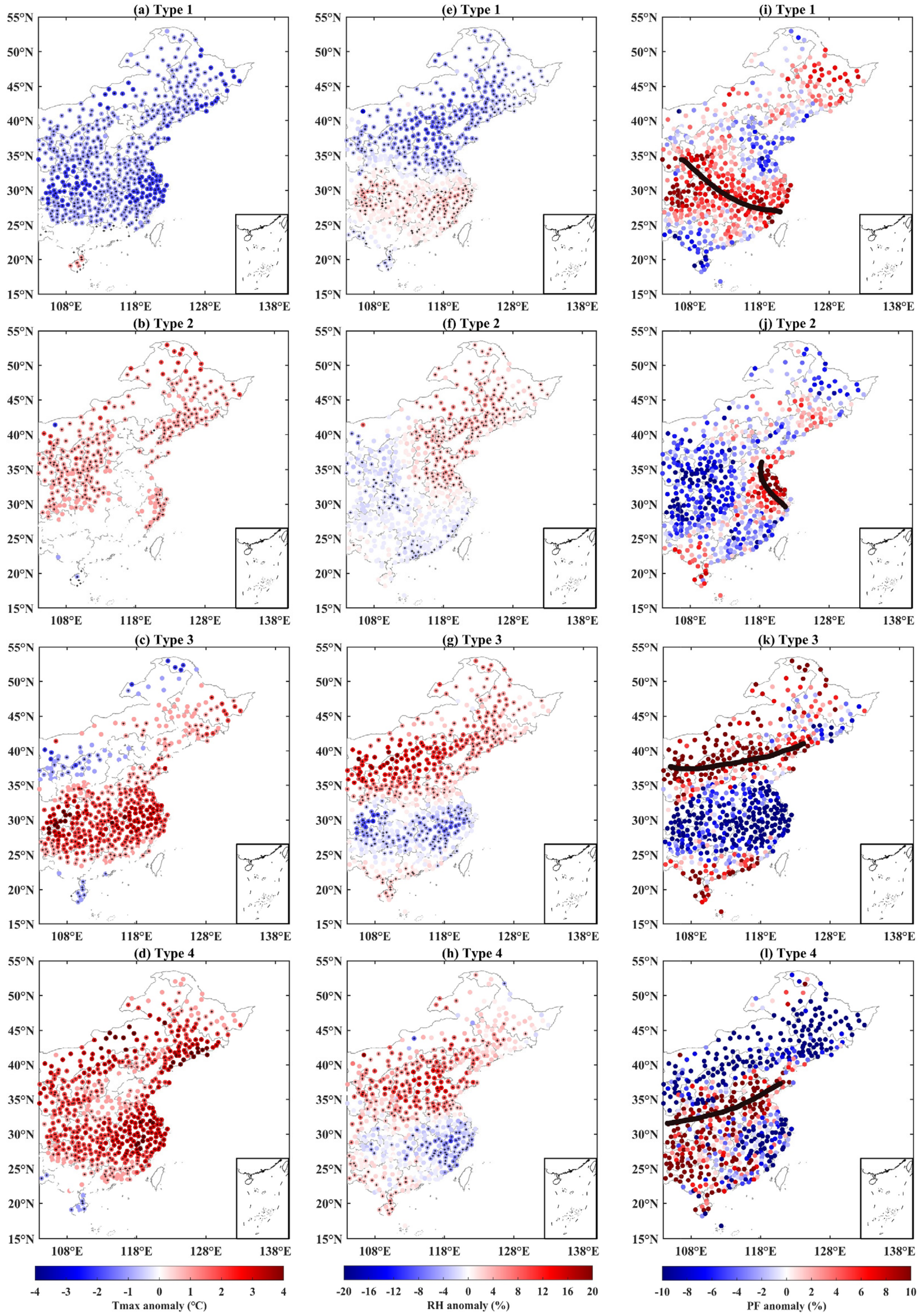

Fig. ~~9~~8. Same as Fig. 6 but for Tmax (a–d), RH (e–h), and PF (i–l). The black solid line presents the rain belt of each SWP.~~The anomaly of Tmax (a–d), RH (e–h), and PF (i–l) under four SWPs, where the sites marked with a '+' indicates the Analysis of Variance passes the significance level of 0.05.~~

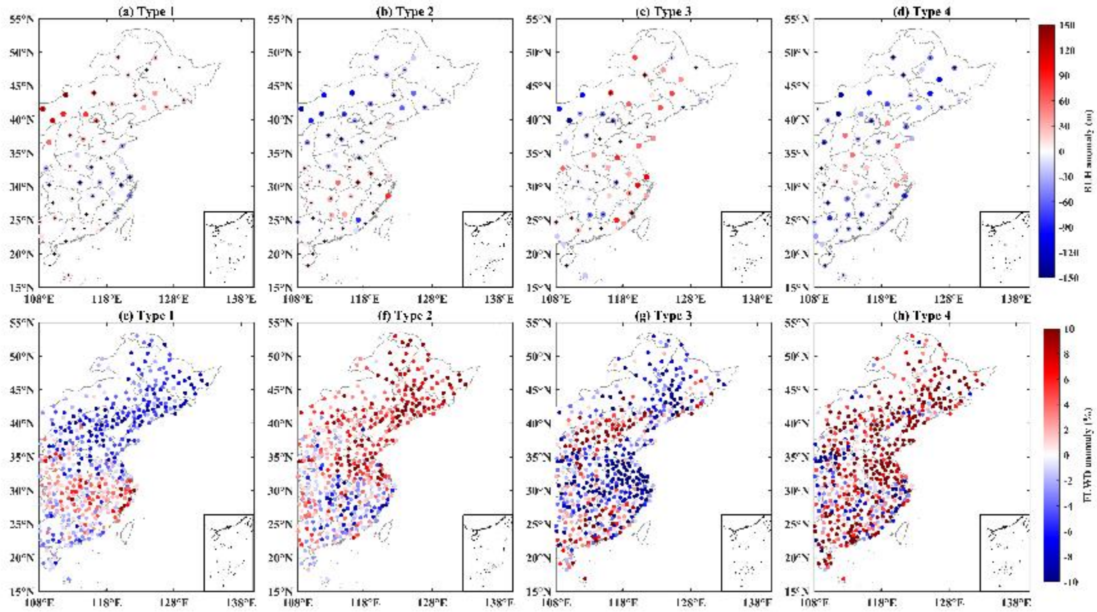

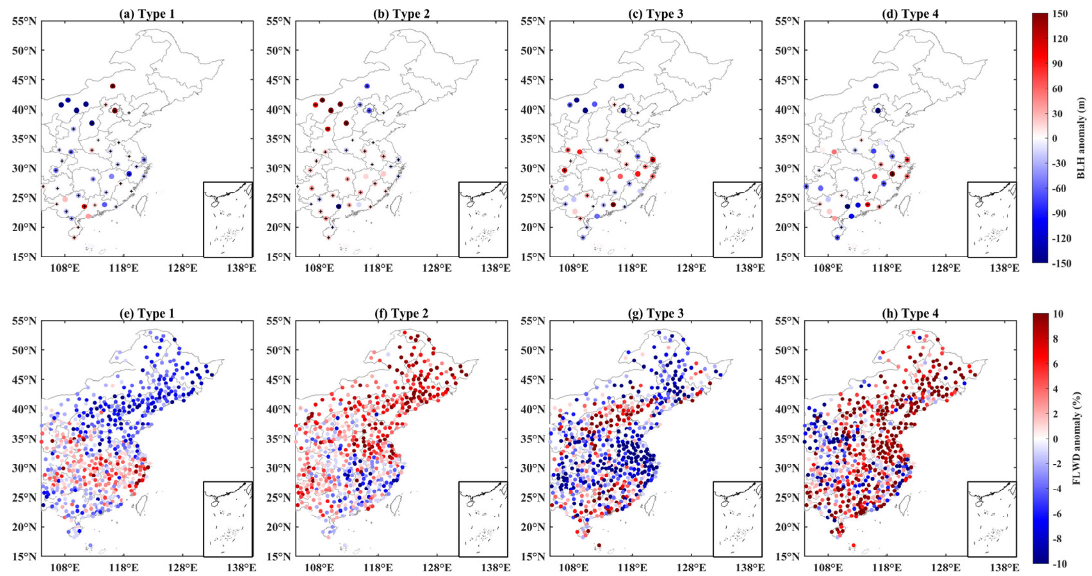

Fig. ~~10~~9. Same as Fig. 6 but for BLH at 14:00 BJT (a–d) and FLWD (e–h).~~The anomaly and significance of difference of BLH (a–d) and FLWD (e–h) under four SWPs, where the sites marked with a '+' indicates the Analysis of Variance passes the significance level of 0.05.~~

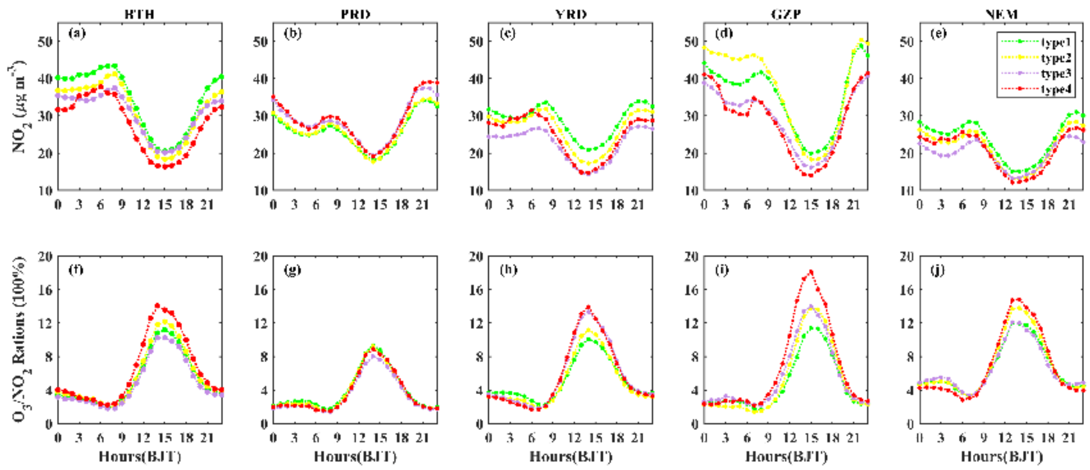

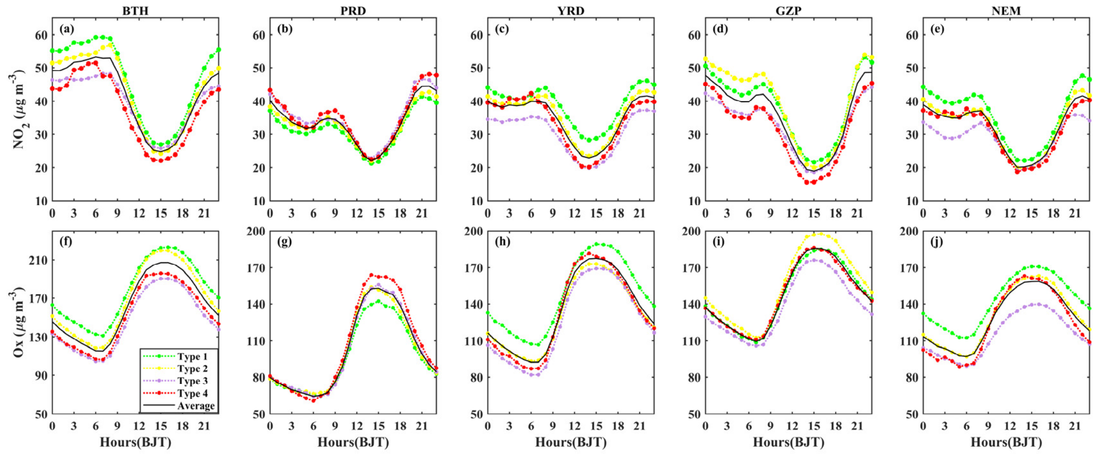

Fig. ~~11~~10. Daily variation of NO_2 (a-e) and Ox (f-j) under four SWPs in key urban clusters.~~NO_2 and O_3/NO_2 daily variation under four SWPs in key urban clusters.~~

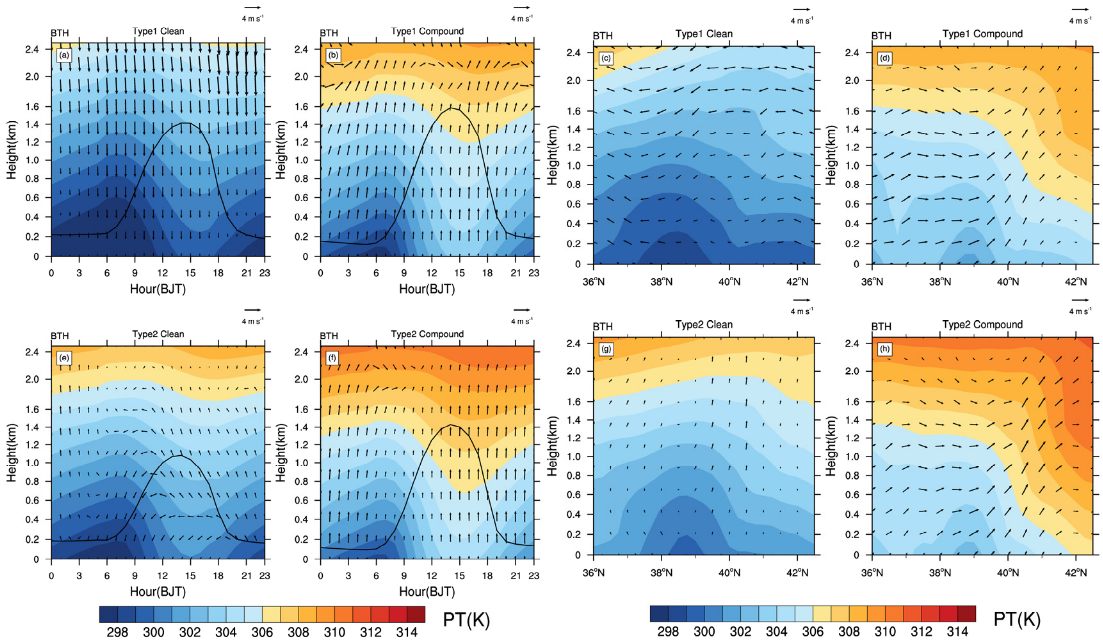

Fig. 11. The daily variation of horizonal wind, potential temperature (PT) and BLH of boundary layer in the BTH under clean and compound pollution period of Type 1 and Type 2 (a, b, e, f). The vertical cross-section of u-wind, w-wind and PT for the same situation of BTH (c, d, g, h). The w-wind is multiplied by 100 when used. The data has been derived from ERA5 reanalysis.

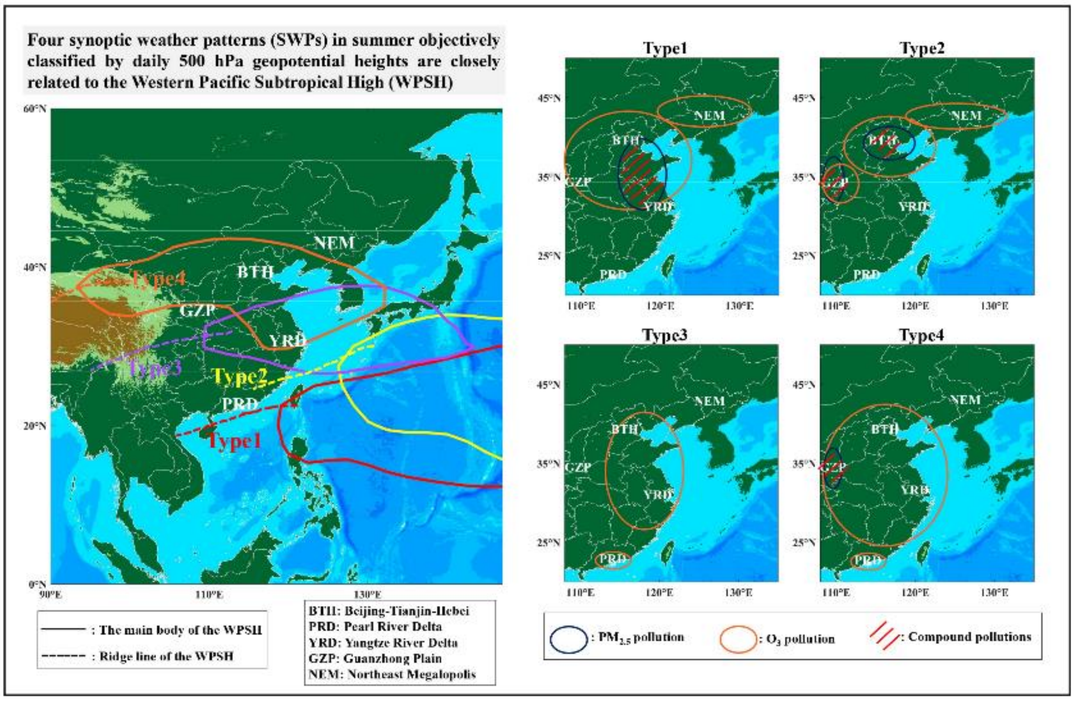

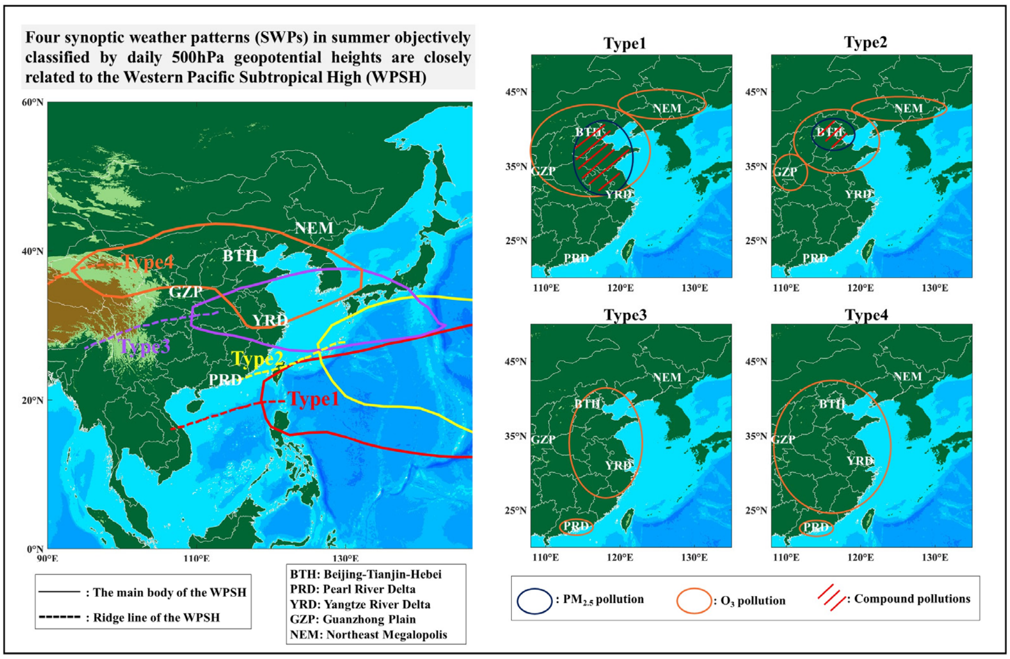

Fig. 12. Schematic diagrams describing the relationships between the WPSH, four SWPs and summertime O_3 and $PM_{2.5}$ pollution in various regions.